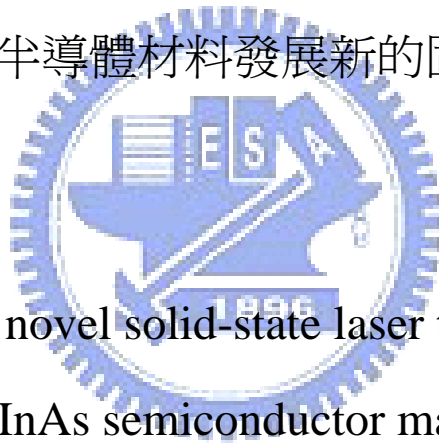# 國 立 交 通 大 學

電子物理研究所

博士論文

以鋁鎵銦砷半導體材料發展新的固態雷射技術

Investigation of novel solid-state laser technologies with

AlGaInAs semiconductor materials

學生：黃仕璋

指導教授：陳永富 教授

中華民國九十八年七月

Investigation of novel solid-state laser technologies with AlGaInAs semiconductor materials

研究生:黃仕璋   Student : Shih-Chang Huang

指導教授:陳永富   Advisor : Yu-Fung Chen

國立交通大學

電子物研究所

博士論文

A Thesis Submitted to Institute of Electrophysics

College of science

National Chiao Tung University

In Partial Fulfillment of the Requirements

For the Degree of Ph.D of Science

In Electrophysics June 2009

Hsinchu, Taiwan, Republic of China

中華民國九十八年七月

以鋁鎵銦砷半導體材料發展新的固態雷射技術

學生:黃仕璋   指導老師:陳永富 教授

國立交通大學電子物理學系博士班

摘要

本論文是探討以 AlGaInAs 半導體材料發展新的固態雷射技術。以週期性結構的量子井半導體材料作為增益介質以及半導體飽和吸收體。除了第一章的簡介和末章的未來工作，主要內容分為三章：第二章主要集中在以光激發砷化鋁鎵銦(AlGaInAs)半導體量子井材料，以主動式 Q 開關固態雷射作為光源，產生 $1.06\,\mu\mathrm{m}$ 雷射激發半導體雷射產生 $1.36\,\mu\mathrm{m}$ 和 $1.57\,\mu\mathrm{m}$，應用在光通訊以及人眼安全。除此之外，還以不同的激發機制(in-well pumping)達到功率優化的目的。第三章主要是以砷化鋁鎵銦(AlGaInAs)半導體量子井材料作為被動式 $1.06\,\mu\mathrm{m}$,$1.34\,\mu\mathrm{m}$ Q 開關雷射中的被動元件,也就是半導體飽和吸收體 以產生高峰值功率(kW)的雷射脈衝。第四章主要是以砷化鋁鎵銦(AlGaInAs)半導體量子井材料作為被動式 $1.34\,\mu\mathrm{m}$ 鎖模雷射中的被動元件,以產生短脈寬(~ps)的雷射脈衝。
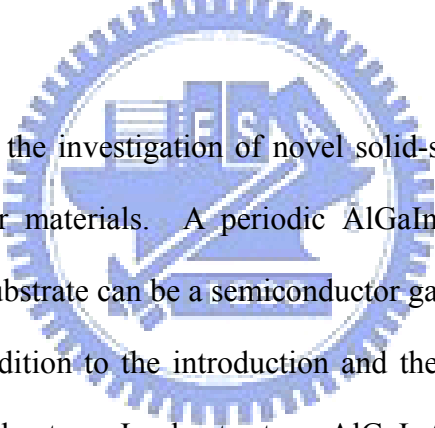
Investigation of novel solid-state laser technologies with AlGaInAs semiconductor materials

Student : Shin Cheng Huang   Advisor: Prof. Yung-Fu Chen

Insitute and Department of Electrophysics
National Chiao Tung University

Abstract

The author demonstrates the investigation of novel solid-state laser technologies with AlGaInAs semiconductor materials. A periodic AlGaInAs quantum well / barrier based on Fe-doped InP substrate can be a semiconductor gain chip and a semiconductor saturable absorber. In addition to the introduction and the future work, the main text were divided into three chapter. In chapter two, AlGaInAs saturable absorber with a periodic QW/barrier structure that can be used to achieve an efficient high-peak-power and high average- power passively 1.06 and 1.34μm Q-switched lasers. In chapter three, AlGaInAs QWs grown on the Fe-doped InP substrate was designed to be a saturable absorber for self-starting continuous-mode-locked Nd:YVO$_4$ laser at 1342 nm. In addition to be a saturable absorber, the periodic quantum well / barrier structure also can be a gain medium in solid-state laser. We demonstrated an AlGaInAs QW/barrier structure grown on an Fe-doped InP transparent substrate was developed to be a gain medium in a room-temperature high-peak-power nanosecond laser at 1.36 and 1.57μm for optical communication and eye-safe applications.

誌　　謝

Table of Content

Chapter One .

Introduction of solid-state laser technology

Chapter Two

Semiconductor gain medium for pulsed laser

Chapter Three

Semiconductor saturable absorber (SESA) for Q-switched laser

Chapter Four

Semiconductor saturable absorber (SESA) for mode-locked laser

Figure of list

Chapter One

Introduction of solid-state technology

1.1 Diode pumped solid-state laser (DPSSL)

The solid state laser uses a solid crystalline material as the lasing medium and is usually optically pumped. Generally speaking, the gain medium of a solid state laser consist of a glass or crystalline host medium which is doped some rare-earth element such as neodymium-doped (Nd:YVO$_4$, Nd:YAG), ytteribium-doped(Yb:YAG), and erbium doped (Er:YAG or Er-doped glass laser). In beginning of 1980s, the progress in the growth technology of semiconductor heterostructures allowed to develop the high-power diode laser. A solid gain medium pumped with a laser diode (LD) is so called diode-pumped solid-state (DPSS) lasers. The diode-pumped Nd:YAG lasers have operated at greater than 10 percent electric to optical efficiency in a single spatial mode. Furthermore, the high spectral power brightness of these lasers has allowed frequency extension by harmonic generation in nonlinear crystals, which has led to green and blue sources of coherent radiation. Diode laser pumping has also been used with ions other than neodymium to produce wavelengths from 946 to 2010 nanometers.

   In addition, Q-switched operation with kilowatt peak powers and mode-locked operation with picosecond pulse widths have been demonstrated in DPSS lasers. The progress in diode pumped solid-state lasers promises all solid-state lasers for high average power levels and at a price that is competitive with flash-lamp pumped laser systems. Thus, the solid-state lasers have become the preferred candidates for a wide range of applications in science and technology including spectroscopy, atmospheric monitoring, micromachining, and precision metrology.

In solid-state laser physics, the lasing wavelength is determined by the doping and the host crystal properties. The limitation of discrete atomic levels is main drawback of crystalline gain medium. One area that demands particular attention is the wavelength spectrum near 1.3–1.6 μm, especially the "eye-safe" spectrum region (from 1.5μm-1.6μm). Extremely short and high-peak-power pulses of lasers at the eye-safe wavelength region are practically valuable for applications such as telemetry and range finders. The common gain medium to generate 1.3μm wavelength are Nd-doped crystals , and the methods for generating eye-safe lasers include the solid-state lasers with Er^{3+}-doped or Cr^{4+}-doped media and the stimulated Raman scattering (SRS) or optical parametric oscillators (OPO) pumped by Nd-doped lasers. In addition, the bandgap engineering and range of semiconductor materials systems provide potential spectral coverage from the near ultraviolet to the mid-infrared. This is a novel class of diode-pumped laser with a few micrometers pump absorption length. Hence, solid-state laser can be more compact by use of semiconductor materials.

The gain medium of semiconductor laser is direct-bandgap compound semiconductor materials. Different type semiconductor such as heterojunction, quantum well, edge emitting and surface emitting are widely applied in industry and scientific research. Besides, the optically pumped vertical-external cavity surface emitting laser (OP-VECSEL) overcomes the power limitation of vertical cavity surface emitting laser (VCSEL) and the beam quality of edge emitting laser(EEL). Thus, the OP-VECSEL technology has in fact become one of promising candidates to overcome the limitations of conventional semiconductor lasers. Moreover, the external cavity configuration allows other interesting application such as broadband laser absorption spectroscopy, single frequency operation, passive mode locking with a saturable absorber resulting in pico-second to femto-second pulse operation and

generating blue and green lights with intra-cavity frequency-doubling

Saturable absorber (SA) is the key element for pulse generation of solid-state laser. The passive saturable absorbers based on saturable optical absorption are of great interest due to their applications for Q switching and mode locking of near-infrared solid-state lasers to obtain short pulses of high peak power. The use of such laser pulses offers rich possibilities in material processing, optical telecommunication, range finding, industrial process control, atmospheric pollutions monitoring, medical diagnostics of diseases, laser surgery, and in scientific areas such as nonlinear optics and laser spectroscopy.

It is necessary for saturable absorber to possess low saturation intensity in conjunction with ultrafast relaxation time (or low saturation energy density together with slow absorption recovery time), high contrast of bleaching, high optical damage threshold, as well as good heat conduction and weak temperature dependence of the refractive index. Generally speaking, the ion-doped saturable absorbers (such as Cr^{4+}:YAG) exhibit long recovery time and larger modulation depth for Q-switching operation. On the other hand, the absorption recovery times of semiconductor-based saturable absorbers are adequate both to Q-switched and to mode-locked lasers. The development of semiconductor saturable absorber mirror (SESAMs) is a novel family of optical devices that allow for very simple, self-starting, passive mode-locking of ultrafast solid-state and semiconductor lasers.   This breakthrough device allowed the first demonstration of a passively mode-locked Nd:YLF laser - without Q-switching in 1992.

1.2 Guide to main text

The most important content in each chapter was sketchily pointed out here.

In chapter two, we give an overview of optically-pumped semiconductor

lasers. And we have demonstrated the periodic AlGaInAs QW/barrier structure grown on an Fe-doped InP transparent substrate was developed to be a gain medium in a room-temperature high-peak-power nanosecond laser at 1.36 μm and 1.57μm. In addition, for power scaling up, we also have demonstrated an optically pumped high-peak-power AlGaInAs/InP eye-safe laser by in-well pumping scheme. The conversion efficiency is enhanced over three times compared with barrier pumping scheme.

In chapter three, we demonstrate, for the first time to our knowledge, an AlGaInAs saturable absorber with a periodic QW/barrier structure that can be used to achieve an efficient high-peak-power and high average- power passively Q-switched lasers. The damage to the semiconductor saturable absorber can be ingeniously avoided by the periodic QW/barrier structure. Besides, compared with InGaAsP/InP QWs, AlGaInAs/InP QWs has larger conduction band offset which prevents carrier leakage at high temperature.

In chapter four, we have designed AlGaInAs QWs grown on the Fe-doped InP substrate to be a saturable absorber for self-starting continuous-mode-locked Nd:YVO$_4$ laser at 1342 nm. Compare with other semiconductor saturable absorber (GaInNAs QWs and InAs/GaAs QD), there is no need to anneal the AlGaInAs QWs to tune the PL wavelength and the optical characteristics of AlGaInAs QWs is more uniform than InAs/GaAs QDs. The present result confirms that the AlGaInAs QWs structures can be utilized to be saturable absorbers for the passively mode-locked lasers in the spectral region near 1.3 μm.

In chapter five, we give an overall conclusion of the entire work carried out in this thesis. Furthermore, we discuss the works and some interesting topics that we are going to do in the future.

Chapter Two

Semiconductor gain medium for pulsed laser

2.1 Introduction to Optically-pumped semiconductor lasers (OPSL)

In 1997, M. Kuznetsov, F.Hakimi and A. Mooradian demonstrated for the first time a new high-power semiconductor laser technology, the optically-pumped semiconductor (OPS) vertical-external-cavity surface emitting laser (VECSEL) [1-2]. Optically-pumped semiconductor vertical-external surface emitting lasers (OP-VECSELs) has become one of promising candidates to overcome the limitations of conventional semiconductor laser. The OP-VECSELs combine the approaches of diode-pumped solid-states lasers and semiconductor quantum well vertical cavity surface emitting lasers (VCESL) and draw on the advantages of both. The OP-VECSELs can generate a multi-watt, near-diffraction-limited output beam with good efficiency in wavelength regions which are not covered by solid-state laser gain materials. Figure 2.1.1 shows the schematic of an optically pumped semiconductor disk laser [3-5].
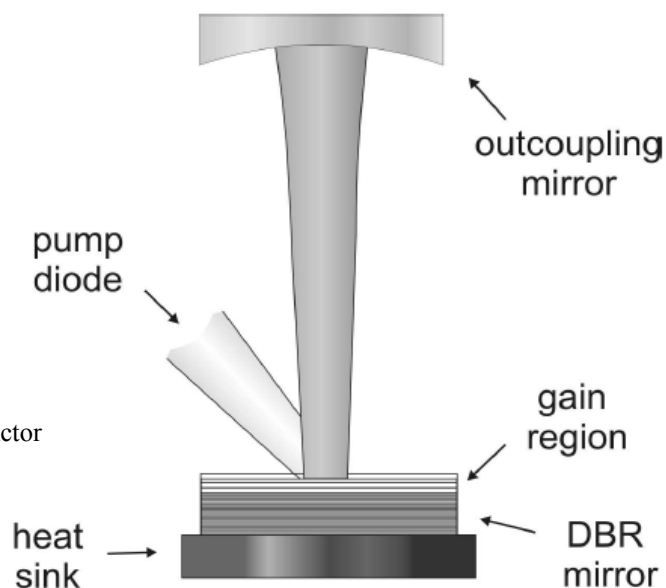
Fig.2.1.1: Schematic of an optically- pumped semiconductor disk laser.

A VECSEL resembles the semiconductor quantum well active layers and a mirror structure contains a distribute Bragg reflectors (DBRs) and an external mirror. Semiconductor disc lasers are power-scalable because the active region is cooled by a one dimensional heat flow and the associated thermal gradient it's along the axis of the optical cavity, minimizing the problems associated with thermal lensing and depolarization.

The layer structure of OP-VECSEL gain chip is shown in Fig2.1.2. In Fig2.1.2 a Bragg mirror, typically 25-30 periods, is grown next to the substrate [4-7].   The final layer in the design of the VECSEL is the capping layer. Its role is to prevent carrier diffusion from the quantum wells and also reduce oxidation of the VECSEL's surface. The capping layer is made from semiconductor material which has a higher energy gap than that of the barrier region.
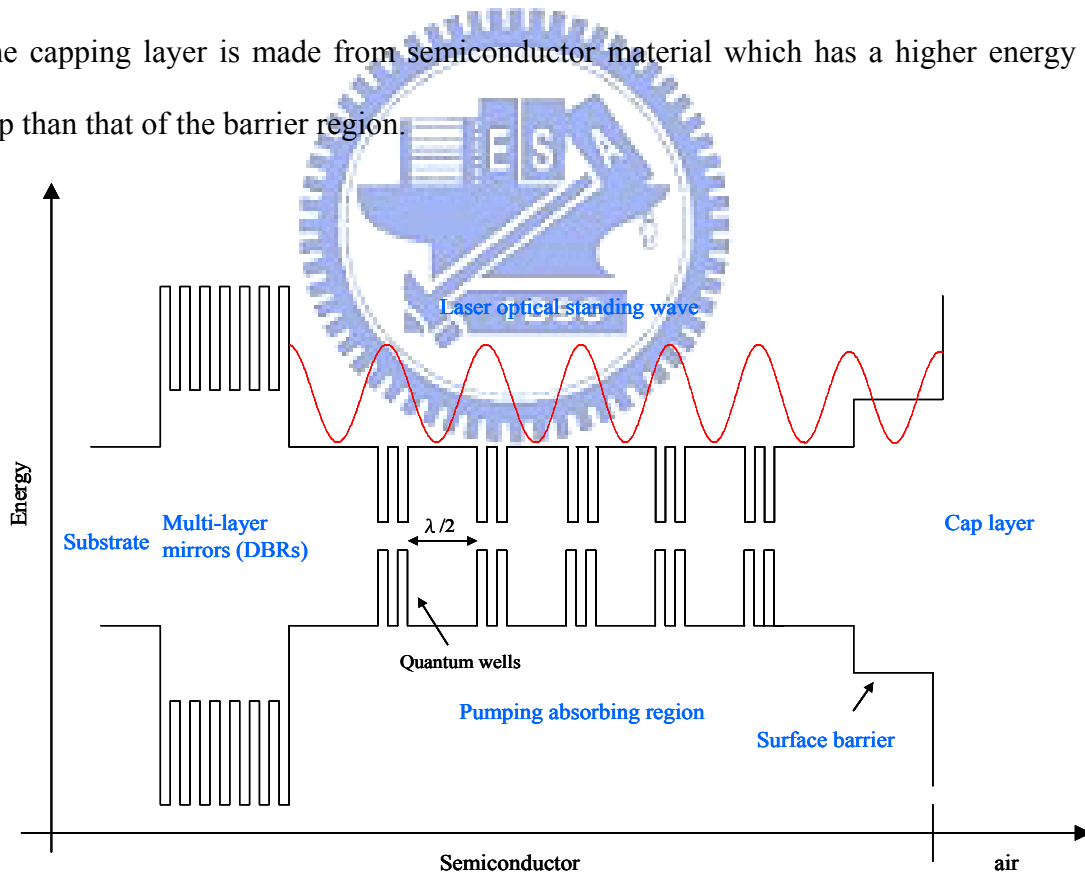
Fig.2.1.2 Bandgap diagram and operation principle of the OP-VECSEL

This acts as a barrier for those electrons with high energies, which can escape the well confinement.   The additional benefit from this layer is that it can be grown to desired thicknesses.   This can enhance the available gain from the laser by forming a

6

resonant structure in the small micro-cavity between the DBR and air surface. The most important feature of the RPG structure is that the position of the quantum-well active regions is arranged periodically such that they coincide with antinodes of a vertical standing wave pattern at the lasing wavelength. The spacer thickness determines the resonant wavelength at which the interaction of the optical field with the gain distribution is maximized. This structure has several advantages. First, since the gain medium only exists at the peaks of the standing-wave optical field, the spatial overlap integral between optical field and the gain elements is enhanced in the vertical direction (normal to the quantum well planes) at the resonant wavelength determined by the spatial periodicity of the gain medium. Hence, the gain in this structure is both anisotropic and wavelength selective. Second, charge carriers generated or injected tend to remain within the quantum wells and cannot at accumulate in the spacer regions, thus eliminating the possibility of longitudinal spatial hole burning. Moreover, loss of carriers through spontaneous emission is considerably reduced because the spacer medium around the nodes of the optical field contains no free carriers; this should result in a lower threshold and improved overall power efficiency.

Compared with optical pumping of semiconductor lasers, electrical pumping, in general, is the preferred approach. Electrically pumped VECSELs have a gain structure similar to that of a VCSEL, where a ring electrode around the active area injects carriers into that region. Current injection i.e. non-uniform current injection, current crowding, localize Joule heating, and free carrier absorption with attendant optical loss and excess heat deposition, are the major hurdles in the development of such large diameter devices. Non-uniform injection particularly favors higher-order transverse modes and reduces the transverse single mode wall-plug efficiency [8].

Optically pumping is particularly advantageous for high power operation, on

account of the controlled and uniform distribution of pump power over large active region and the absence of free carrier absorption, with attendant optical loss and excess heat deposition in the undoped active structure. Since optical pumping occurs via interband transition of the bulk barrier material, the pump absorption band is broad and imposes on practical constraint on the wavelength stability of the pump laser. The pumping absorption band is broad and absorption coefficient of the barrier material is typically $\sim 0.8 \mu\,\mathrm{m}^{-1}$ such that pump radiation can be absorbed efficiently on a single or double pass of a very thin active region. Due to the very short absorption length of the semiconductor gain structure (at least for spacer pumping), the beam quality of the pump light is not very important. In general, for barrier pumping the carriers that are created by optical pumping in the barrier are trapped subsequently in the quantum wells. The gain bandwidth, differential gain, peak gain wavelength and quantum efficiency depend sensitively on carrier concentration and temperature. The active region is therefore affected by the pump power level, pumping spot-size, and thermal coupling to the heat sink more strongly than is the gain medium of a dielectric disc laser. An external laser cavity enforces output in a low divergence, circular, near diffraction-limited beam of high beam quality. With this external cavity configuration allows some interesting applications such as broadband laser absorption spectroscopy, single frequency operation, passive mode-locking with a saturable absorber resulting in pico-second to femto-second pulse operation and generating blue and green lights with intra-cavity frequency-doubling [9-17]. A summary of the main features, including advantages and disadvantages, of OPS- VECSELs is shown in Table 2.1.1 below.

Advantages	(1) Customized emission wavelength (2) Bandgap engineering of the multi-QW semiconductors allows the design of laser medium with the desired laser properties. (3) Broad pump bandwidth simplifies optical pumping with diodes (4) Very short pump absorption length leads to efficient pump absorption (5) No need for material doping or electric contacting (6) Wide potential tuning range (7) External cavity allows control of the output transverse mode and enables the incorporation of intra-cavity elements to control the laser spectral properties.
Disadvantages	(1)Intense localized heat is created in the semiconductor amounting to thermal roll over and limited powers. Thermal management techniques can be used to delay the arrival of roll-over losses. (2)External cavity can make the overall size of the laser large in comparison to other semiconductor lasers.

Table 2.1.1. Summary of advantage and disadvantage of OPSL

Table 2.1.2 shows the recent development of optically-pumped semiconductor laser [18-27]. Much work on the development of OP-VECSELs has used the high gain, compressively strained InGaAs/GaAs quantum well system. GaAs-based substrate optically pumped vertical external cavity semiconductor lasers (VECSEL) with high contrast GaAs/AlAs reflectors have operated in two wavelength regions: around 850nm using lattice-matched GaAs/AlGaAs quantum wells and around 1000nm using strained InGaAs/GaAs quantum wells [28-31]. For telecommunication application i.e. in the 1.3-1.55μm wavelength region, the natural material system is the InP-based. Unlike for GaAs-based semiconductor laser operating in 0.78-1.0μm short-wavelength range, the main obstacle for long-wavelength InP-based with low refractive index contrast semiconductor laser is the difficult realization of high-reflective Bragg mirrors (DBR) for 1.3-1.55μm long-wavelength region [32-36]. Moreover, this high thickness, combined with poor

thermal conductivity of these materials and the high temperature sensitivity of the active layers lattice matched to InP, leads to poor thermal properties of semiconductor lasers.

Gain	λ_{lasing}	$\lambda_{pumping}$	Max Power	Reference
GaN-based				
InGaN/GaN	391nm	335nm		APL 2003
GaAs-based				
AlGaInP	668-678nm	532nm	390mW	Opt Express 2005
AlGaAs	830-860nm	660nm	523mW	IEEE PTL 2003
AlGaAs	850nm	808nm	135mW	APL 2004
InGaAs	1000nm	808nm	8W (CW) at RT	APL 2003
InGaAs	1060nm	808nm	10W(CW) at RT	APL 2006
GaInNAs	1320nm	810nm	0.612W at 5°C	Electronic Lett 2004
InP-based				
InGaAsP	1550nm	980nm	45mW	Opt Comm 2004
InGaAsP	1538-1545nm	1250nm	780mW	IEEE PTL 2004
GaSb-based				
AlGaAsSb	2.3 μm	830nm	8.5mW	Cryst Growth 2004
AlGaAsSb	2.33 μm	1064nm	0.6W at -18°C	IEEE PTL 2004

Table 2.1.2 The recent development of optically-pumped semiconductor laser

2.2 Motivation and background

2.2.1. AlGaInAs quantum well 1.36μm laser

High-peak-power all-solid-state laser sources in the 1.3–1.6 μm spectral region are of particular interest in remote sensing, eye-safe optical ranging, fiber sensing, and communication [1–4]. Diode-pumped solid-state lasers (DPSSLs) that have the advantages of relatively compact size, high power, excellent beam quality, long lifetime, and low heat production have been widely used for various applications, including industry, pure science, medical diagnostics, and entertainment [5]. Nevertheless, the spectral range of diode-pumped solid-state laser systems is limited by the properties of existing doped crystals and glasses. Recently, the optically pumped vertical-external-cavity surface-emitting semiconductor lasers (VECSELs) have been proposed as a novel class of all-solid-state lasers with potential spectral coverage from the near ultraviolet to the mid-infrared [6,7].

Typically, a VECSEL device consists of a highly reflecting distributed Bragg reflector (DBR) and a resonant periodic gain (RPG) structure that comprises a series of barriers to provide the pump absorption, quantum wells (QWs) to provide gain, and layers to prevent oxidation. Although InP-based material could offer a gain region with a smaller lattice mismatch for 1.3 μm wavelength, the small contrast of refractive indices hinders the performance of the DBRs. As a consequence, until now the InP-based material has never been used as a VECSEL device at 1.3 μm. To reach a wavelength near 1.3 μm, GaInNAs/GaAs QWs have been developed as a gain medium[8] and a 0.6 W cw output power has been demonstrated [9]. Even so, there has been no experimental demonstration of room-temperature high-peak-power 1.3 μm laser sources with semiconductor QWs as gain media in an external cavity.

In this chapter, we report, for the first time to our knowledge, a room-temperature high-peak-power nanosecond semiconductor QW laser at 1.36 μm,

using a diode-pumped actively Q-switched Nd:GdVO$_4$ 1.06 μm laser as a pump source.   With an average pump power of 1.85 W, an average output power of 340mW at a pulse repetition rate of 40 kHz was obtained corresponding to an optical-to-optical conversion efficiency of 18.4%.   At a pulse repetition rate of 10 kHz, the peak output power was found to be up to 1.2 kW at a peak pump power of 7.9 kW

2.2.2. AlGaInAs quantum well 1.57μm laser

High-peak-power nanosecond pulsed lasers operating with emission at the eye-safe wavelength region (1.5–1.6 μm) are of great interest because of their potential applications, such as laser radar, active imaging, and remote sensing [10–12]. The methods for generating eye-safe lasers include the solid-state lasers with Er^{3+}-doped or Cr^{4+}-doped media [13–16] and the stimulated Raman scattering (SRS) [17–20] or optical parametric oscillators (OPO) [21–23] pumped by Nd-doped lasers. The advent of diode-pumped solid-state lasers (DPSSLs) [24–27] with high peak powers and excellent brightness leads to a renaissance of interest in wavelength conversions with the SRS or OPO process

   Another practical approach for eye-safe laser sources is based on semiconductor quantum-well (QW) materials including InGaAsP and AlGaInAs systems [28–31]. Recently, a high-peak-power AlGaInAs laser at 1.36 μm was designed with a diode-pumped actively Q-switched Nd:YAG laser as a pump source [32]. Nevertheless, there has been no experimental demonstration of high-peak-power optically pumped AlGaInAs eye-safe laser.

   In this chapter, a high-peak-power nanosecond AlGaInAs eye-safe 1.57-μm laser driven by a diode-pumped actively Q-switched Nd:GdVO4 laser is presented for the first time to our knowledge.   An average output power of 135 mW with a pulse

width of 30 ns at a pulse repetition rate of 30 kHz was obtained with an average

power of 1.5 W to pump an AlGaInAs QW/barrier structure grown on a Fe-doped InP

transparent substrate. The maximum peak power was up to 290 W at a pulse

repetition rate of 20 kHz.
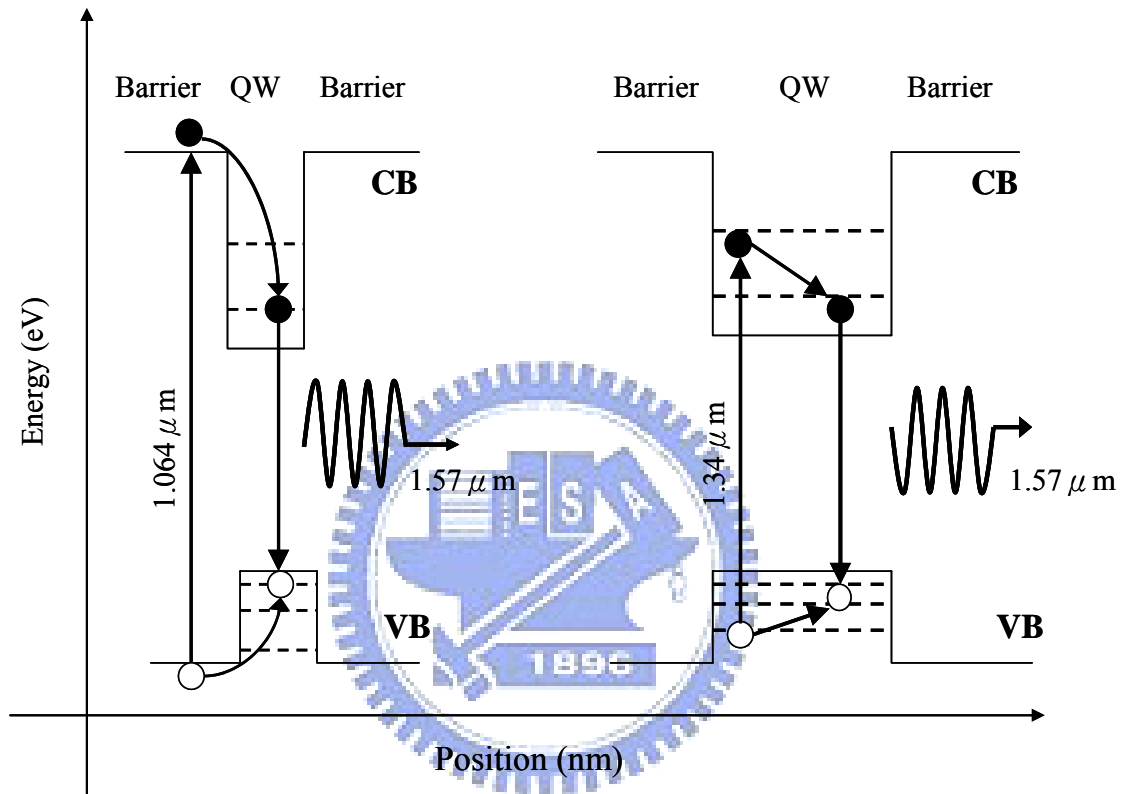
Fig.2.2.1 Schematic of barrier pumping (left) and in-well pumping (right)

On the other hand, the quantum defect, the energy difference between a pump

and a laser photon, is the main source of heat generation in active region, the in-well

pumping scheme has potential for high optical efficiency because of smaller quantum

defect [33-39].   The quantum defect and the thermal load can be reduced by

pumping the quantum well directly.   Fig 2.2.1 shows a schematic diagram of

barrier pumping and in-well pumping.   Optical transition in barrier pumping:

electron-hole pairs are generated in the barrier region and recombine via photon

emission from the quantum well ground state levels in the conduction band.   On the

contrary, optical transitions for quantum well pumping: electron-hole pairs are generated inside the quantum well with energies slightly above the ground state energy. In contrast to barrier-pumping scheme, the quantum defect is considerably reduced by in-well pumping.

However, a problem arising for in-well pumping is the short absorption length, since the quantum wells are only a few nanometers thick. Higher numbers of quantum wells lead to longer total absorption lengths, but also result in a higher laser threshold. To increase the pump efficiency, a resonant absorption scheme was introduced. Another approach to increase the absorption length is a multi-pass pump setup, which is a well-known concept for dielectric solid state thin disk lasers [40-50]. Multi-pass pumping can also be combined with resonant absorption for further improvement of the absorption efficiency. A decreased thermal shift of the output wavelength for in-well pumping indicates a significantly reduced thermal load compared to barrier pumping. Several reports of an in-well pumping laser have been demonstrated with wavelength in the range of 800 nm to 2.35μm except to 1.55μm.

In this chapter, we have demonstrated an efficient high-peak-power AlGaInAs eye-safe laser at 1570 nm. The quantum defect and the thermal load are significantly reduced by pumping the quantum well directly.   The overall conversion efficiency is enhanced over three times compared with the barrier pumping method. With a pump peak power of 3.7 kW, an output peak power of 0.52 kW is generated at a pulse repetition rate of 20kHz.

2.3. AlGaInAs quantum well 1.36μm laser

2.3.1 Device fabrication and laser structure

The present gain medium is an AlGaInAs QW/barrier structure grown on an Fe-doped InP substrate by metal-organic chemical-vapor deposition (MOCVD). It is worthwhile to mention that the AlGaInAs material system has a larger conduction band offset than the most widely used InGaAsP system [1–4]. This larger conduction band offset has been confirmed to yield better electron confinement in the conduction band and higher temperature stability. The AlGaInAs material has been used as a surface-emitting optical amplifier pumped by a laser diode [5]. However, until now there has been no experimental realization involving the VECSEL with AlGaInAs. Here the gain region consists of 30 groups of two QWs with the luminescence wavelength around 1365 nm, spaced at half-wavelength intervals by AlGaInAs barrier layers with the bandgap wavelength around 1070 nm. The barrier layers are used not only to absorb the pump light but also to locate the QW groups in the antinodes of the optical field standing wave. An InP window layer was deposited on the gain structure to avoid surface recombination and oxidation. The back side of the substrate was mechanically polished after growth. Both sides of the gain chip were antireflection (AR) coated to reduce back-reflections and coupled-cavity effects. The total residual reflectivity of the AR-coated sample is approximately 5%. Figure 4.3.1 shows the transmittance spectrum at room temperature for the AR-coated AlGaInAs/InP gain chip. It can be seen that the strong absorption of the barrier layers leads to low transmittance near 1070 nm. The total absorption efficiency of the barrier layers at 1064 nm was found to be approximately 95%. On the other hand, an abrupt change in transmittance near 1365 nm comes from the absorption of the AlGaInAs QWs. The room-temperature spontaneous-emission spectrum, obtained by pulse excitation at 1064 nm, is shown in

the inset of Fig2.3.1.   As expected, the emission is quite broad, with a peak around

1365 nm, and has a long tail extending to shorter wavelengths.
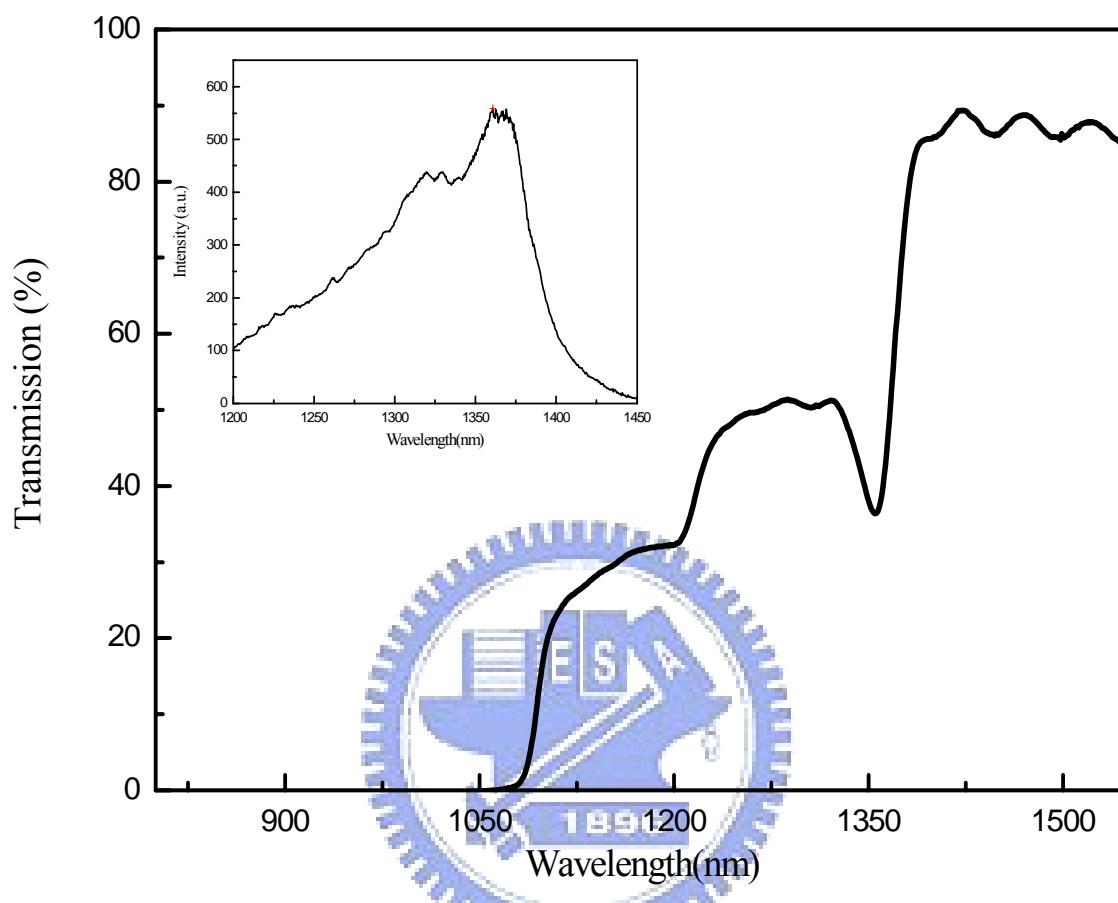
Fig 2.3.1: The transmittance spectrum at room-temperature for AR-coated AlGaInAs/InP
gain chip   Inset : Room-temperature spontaneous-emission spectrum by 0.8W pulse
excitation at 1064nm.

Figure 2.3.2 shows the experimental configuration of the room-temperature

high-peak-power AlGaInAs QWs laser at 1365 nm.   The pump source is a

diode-pumped acousto-optically Q-switched Nd:GdVO$_4$ 1064 nm laser to provide

12-90 ns pulses at repetition rates between 10 and 100 kHz.   The pump spot diameter

is controlled to be 380±20 μm for efficient spatial overlap with the fundamental

transverse mode.   The gain chip was mounted on a copper heat sink, but no active

cooling was applied. The laser resonator is a concave–plano cavity.   The input

mirror was a 500 mm radius-of-curvature concave mirror with AR coating on the

entrance face at 1064 nm *(R<0.2%)*, high-reflection coating at 1365 nm *(R>99.8%)*, and high-transmission coating at 1064 nm on the other surface *(T>90%)*. The reflectivity of the flat output coupler is 94% at 1365 nm. The overall laser cavity length is approximately 10 mm.
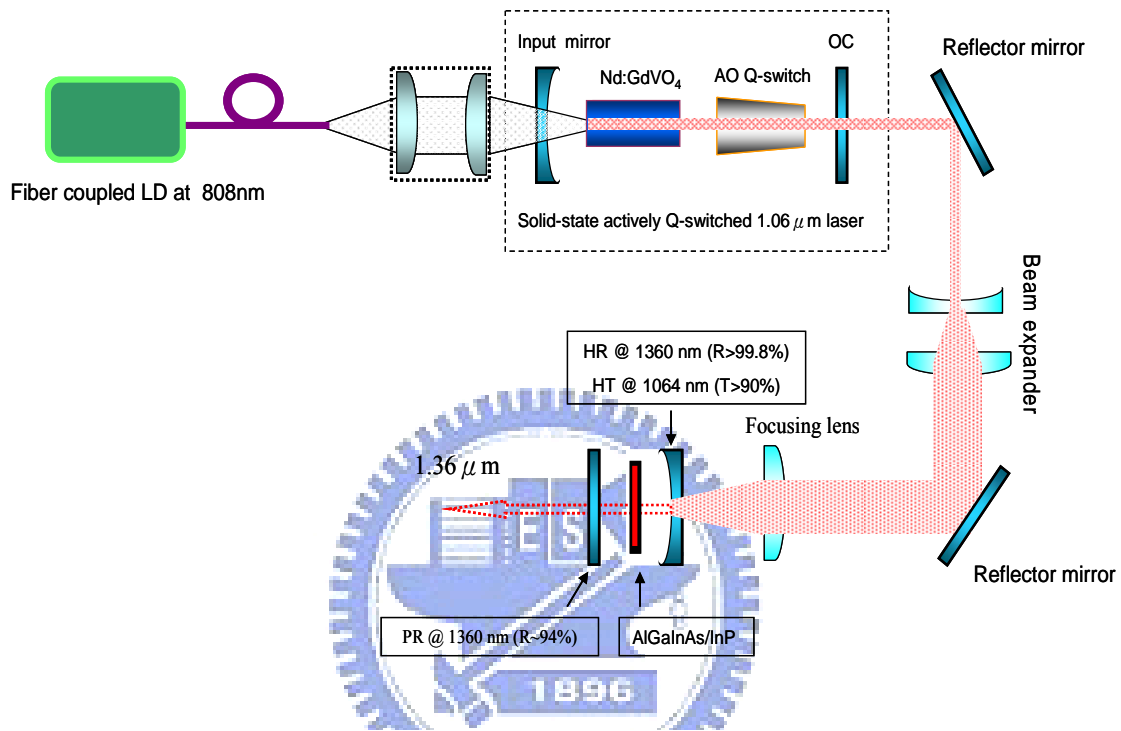
Fig. 2.3.2. Experiment configuration of 1.36μm optically pumped semiconductor laser.

2.3.2 Experimental result

Figure 2.3.3 shows the performance of the optically pumped AlGaInAs laser at pump repetition rates of 10, 40, and 100 kHz. The pump pulse widths for repetition rates of 10, 40, and 100 kHz are approximately 12, 35, and 75 ns, respectively. The cavity decay time is approximately 0.11 ns. The beam quality factor was determined by a Gaussian fit to the laser beam waist, and the divergence angle and was found to be less than 1.5. At a repetition of 40 kHz, the average output power could be up to 340 mW; the output power saturation beyond the average pump power of 1.8 W was due to the thermally induced gain degradation. At a repetition of 10 kHz, the absorption efficiency of the gain chip for the pump power higher than 0.8 W was found to be

significantly reduced because of pump-saturation effects of the barrier layers.   As a consequence, maximum average output power at a repetition rate of 10 kHz was saturated at around 120 mW.   With the experimental data on a pump pulse energy of 80 μJ, a pump pulse width of 15 ns, and a pump area of 0.113 mm^2, the pump saturation intensity was estimated to be 4.7 MW/cm^2.   This value was 2–3 orders of magnitude higher than conventional solid-state laser crystals because of its shorter fluorescence decay time [6].   However, the lower conversion efficiency at the 100 kHz repetition rate might be due to the longer pump pulse duration that enhanced the local heating effect.   The maximum output power at 100 kHz was found to be nearly the same as the result obtained at 10 kHz.   In other words, management of the thermal effects is necessary to scale up the average output power.
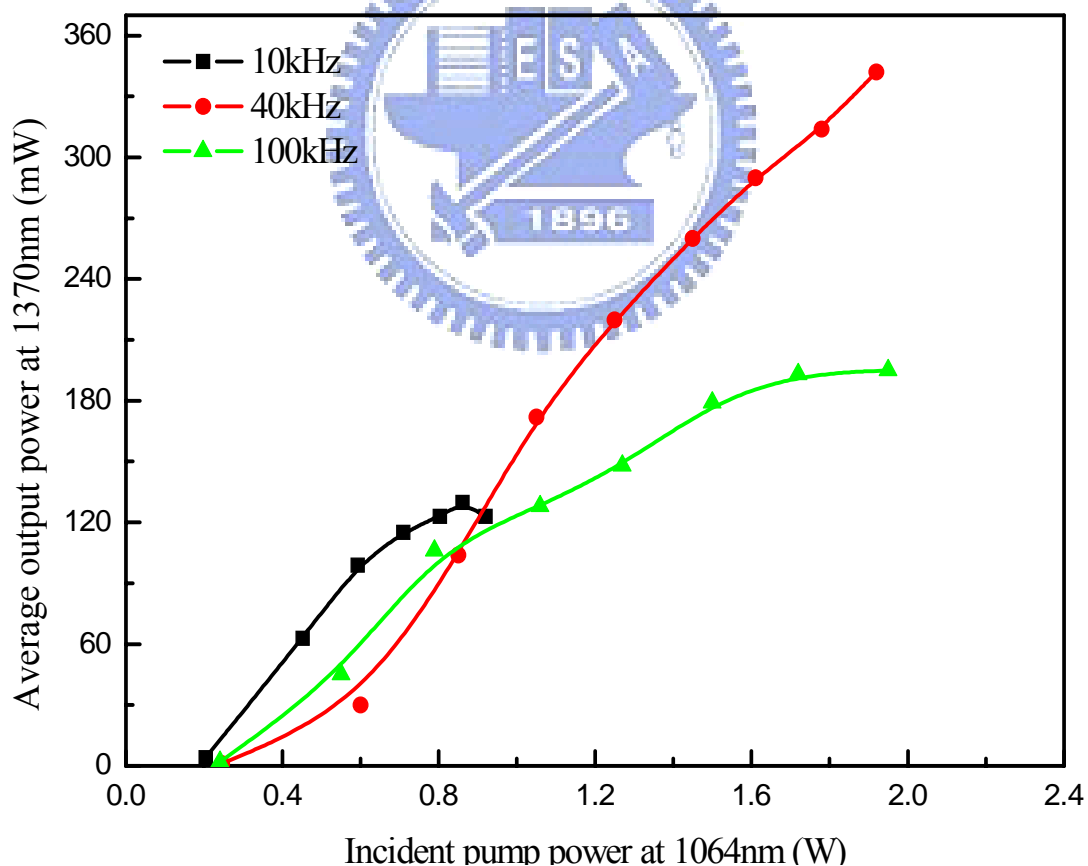
Fig 2.3.3 Experimental results for the optically pumped AlGaInAs laser at pump repetition rates of 10, 40, and 100 kHz.

Figure 2.3.4 shows a typical oscilloscope trace of a train of output and pump

pulses and expanded shapes of a single pulse.   It can be seen that the output pulses tracked the pump pulses for each pumping case.   Figure 2.3.5 shows the peak output power as a function of peak pump power.   The peak output power was up to 1.2 kW at a peak pump power of 7.9 kW, and the slope efficiency was approximately 15.2%. The typical lasing spectrum shown in the inset of Fig. 2.3.5 was obtained with 1.2W of average pump power at a repetition rate of 40 kHz.   The lasing spectrum was composed of dense longitudinal modes, and its bandwidth was up to 20 nm for an average pump power greater than 500 mW.   The wide spectral range indicates the potential for achieving ultra-short pulses in mode-locked operation.
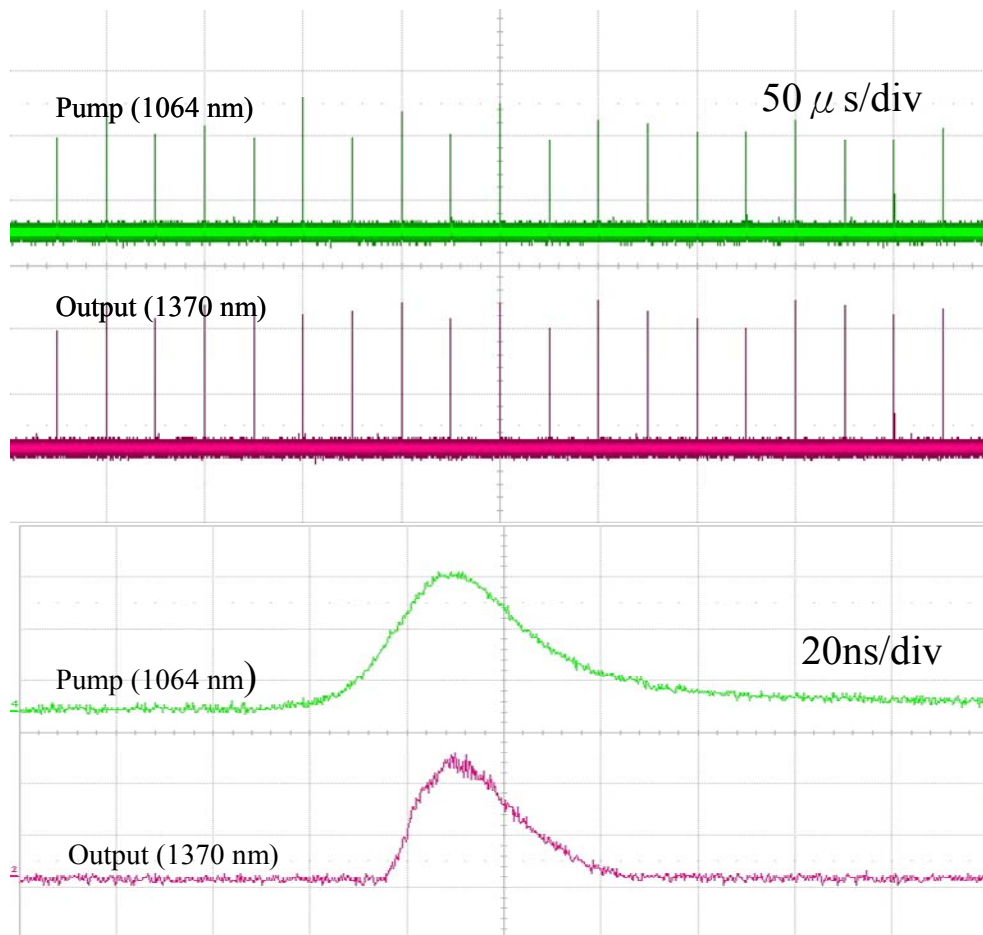
Fig. 2.3.4 (Color online) (a) Typical oscilloscope trace of a train of pump and output pulses
and (b) expanded shapes of a single pulse.
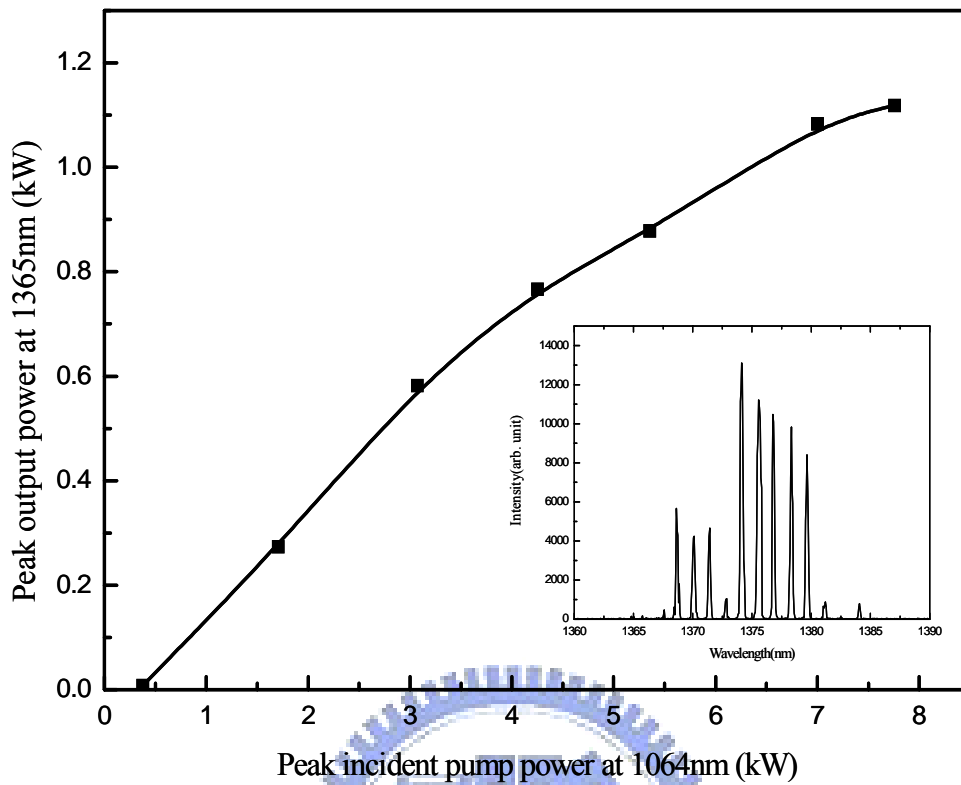
Fig. 2.3.5. Experimental results for the peak output power as a function of peak pump power. Inset, typical lasing spectrum obtained with 1.2W of average pump power at a repetition rate of 40 kHz

2.3.3 Conclusion

In summary, an AlGaInAs QW/barrier structure grown on an Fe-doped InP transparent substrate was developed to be a gain medium in a room-temperature high-peak-power nanosecond laser at 1365 nm. Using an actively Q-switched 1064 nm laser to pump the gain chip, an average output power of 340 mW was obtained at a pulse repetition rate of 40 kHz and an average pump power of 1.9 W. At a pulse repetition rate of 10kHz, the peak output power was found to be up to 1.2 kW at a peak pump power of 7.9 kW

2.4. AlGaInAs quantum well 1.57μm laser (barrier pumping)

2.4.1 Laser structure and device fabrication

Figure 2.4.1 shows the experimental configuration of the high peak-power AlGaInAs QWs 1570-nm laser pumped by a diode actively Q-switched Nd:GdVO$_4$ laser.   The pump source provides 20–60 ns pulses at repetition rates between 20 and 60 kHz. The pump spot diameter was controlled to be 480±20 μm for efficient spatial overlap with the fundamental transverse mode.
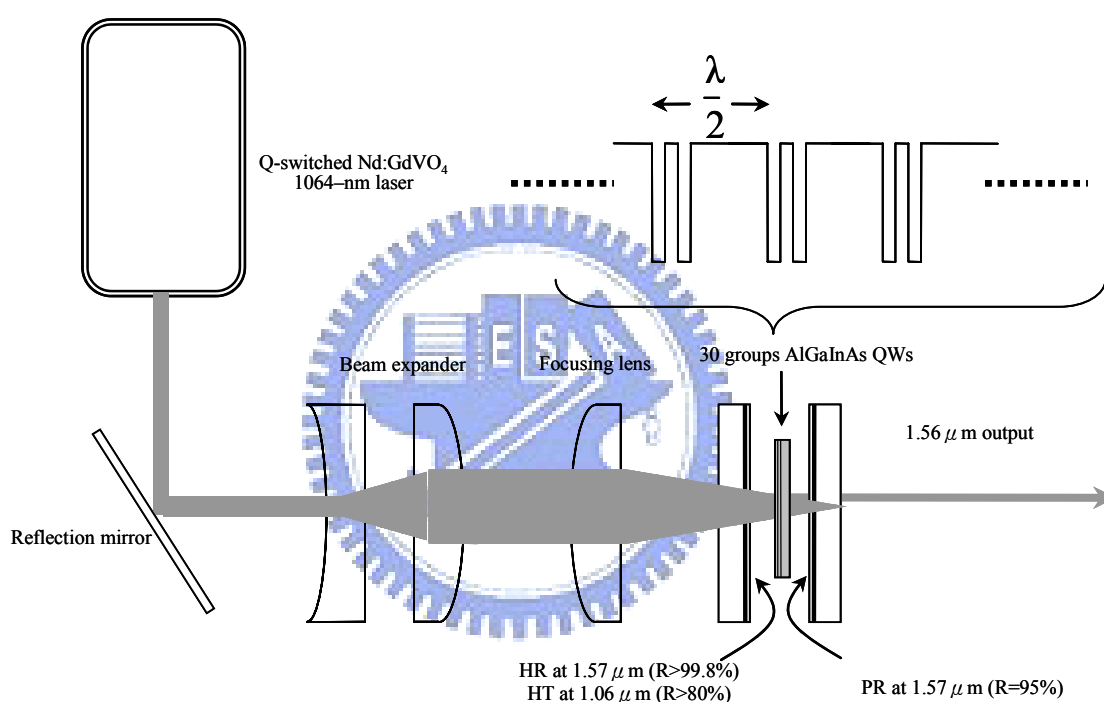
Fig. 2.4.1 Experimental configuration of the high-peak-power AlGaInAs QWs 1570-nm laser pumped by a Q-switched Nd:GdVO$_4$ laser; HR: high reflection, HT: high transmission, PR: partial reflection.

The laser resonator is a linear flat–flat cavity that was stabilized by the thermally induced lens in the gain medium. This concept was found nearly simultaneously by Zayhowski and Mooradian [1] and by Dixon et al. [2].   A linear flat–flat cavity is an attractive design because it reduces complexity and makes the system compact and rugged.   When the average pump power is between 0.5 and 1.5 W, the mode-to-pump ratio is experimentally found to be in the range of 1.0–1.5.   The input mirror was a flat mirror with antireflection coating on the entrance face at 1064 nm (*R*

<0.2%), high-reflection coating at 1570 nm ($R > 99.8\%$), and high-transmission coating at 1064 nm on the other surface ($T > 90\%$).   The reflectivity of the flat output coupler is 95% at 1570 nm. The overall laser cavity length is approximately 10 mm.

The present gain medium is an AlGaInAs QW/barrier structure grown on a Fe-doped InP substrate by metal-organic chemical-vapor deposition (MOCVD). Note that the conventional S-doped InP substrate has large absorption in the 1.0–2.0 μm spectral region, while the Fe-doped InP substrate is chosen because of its transparency at the lasing wavelength.   The gain region is made up of thirty groups of two 8-nm-thick 1570-nm AlGaInAs QWs with 10-nm-thick barriers.   Each QW group is spaced at a half-wavelength interval by an AlGaInAs barrier layer with the band-gap wavelength approximately 1064 nm to absorb the pump light as well as to locate the QWs in the antinodes of the optical standing wave.   An InP window layer was deposited on the gain structure to avoid surface recombination and oxidation.   The backside of the substrate was mechanically polished after growth.   The both sides of the gain chip were antireflection-coated (AR-coated) to reduce back reflections and the couple-cavity effects.   For simplicity, we used a single layer of coating on the gain medium.   As a result, the total residual reflectivity of the AR-coated sample is approximately 5%.

Figure 2.4.2 depicts the room-temperature spontaneous emission spectrum obtained by pulse excitation at 1064 nm. It can be seen that the emission is quite broad with a peak at around 1570 nm and has a long tail extending to shorter wavelength. In the laser experiment, the semiconductor chip was simply mounted on a water-cooled copper block and the water temperature was feedback maintained.
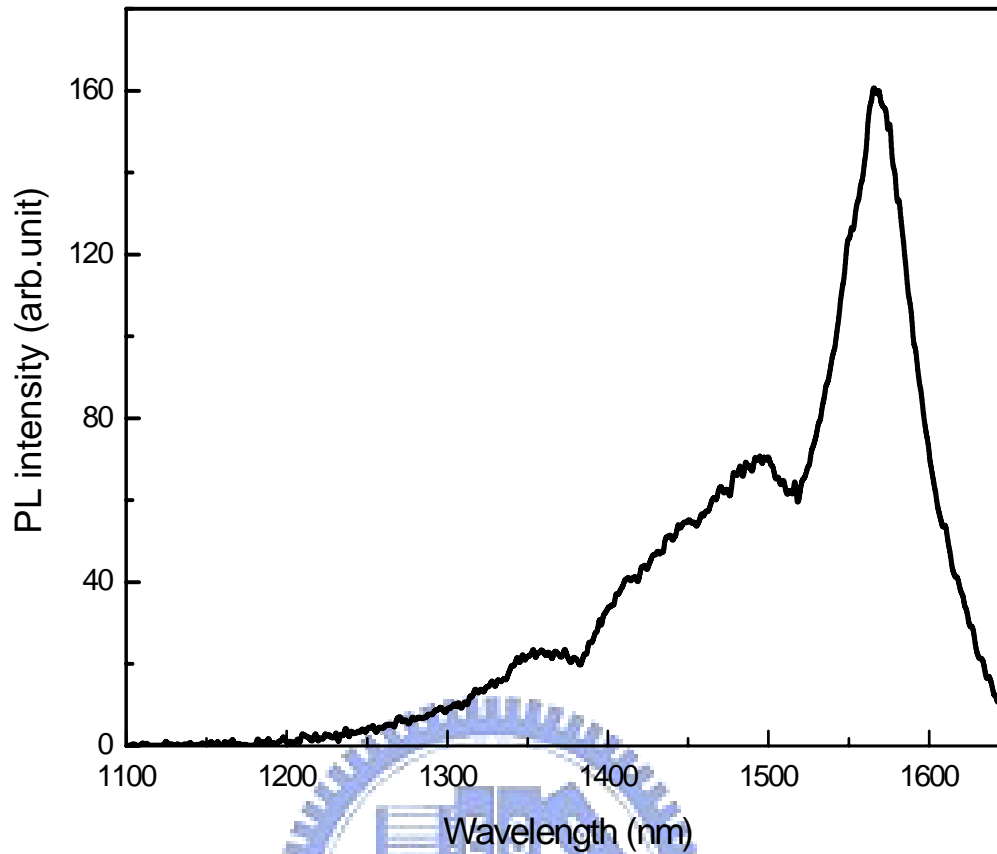
Fig.2.4.2. Room-temperature spontaneous emission spectrum of the AlGaInAs QWs pumped by a

Q-switched Nd:GdVO4 1064-nm laser

2.4.2 Experimental results and discussion

Figure 2.4.3 shows the performance of the optically pumped AlGaInAs laser operated

at the water temperature of 10°C at four repetition rates of 20, 30, 40, and 60 kHz.

The pump pulse widths for the repetition rates of 20, 30, 40, and 60 kHz are

approximately 20, 25, 30, and 40 ns, respectively. The transverse mode was measured

to be the fundamental mode over the complete output power range. The beam quality

factor was determined by a Gaussian fit to the laser beam waist and the divergence

angle, and was found to be less than 1.3 indicating fundamental transverse-mode

operation. Spectral information of the laser was monitored by an optical spectrum

analyzer (Advantest Q8381A). The spectrum analyzer with a diffraction

monochromator can be used for high-speed measurement of pulse light with a

resolution of 0.1 nm. It was found that the bandwidth of the lasing spectrum initially

increases linearly with the pump power but varies slowly at the higher pump power. The lasing spectrum has the highest peak approximately at 1570 nm with maximum bandwidth up to 18 nm. The typical lasing spectrum shown in the inset of Fig. 2.4.3 was obtained with 1.0 W of average pump power at repetition rate of 30 kHz. The lasing spectra generally comprised dense longitudinal modes and their bandwidth were up to 20 nm at the average pump power greater than 200 mW. The temporal shapes for pump and output pulses were recorded by a LeCroy digital oscilloscope (Wave pro 7100, 10 G samples/s, 1 GHz bandwidth).
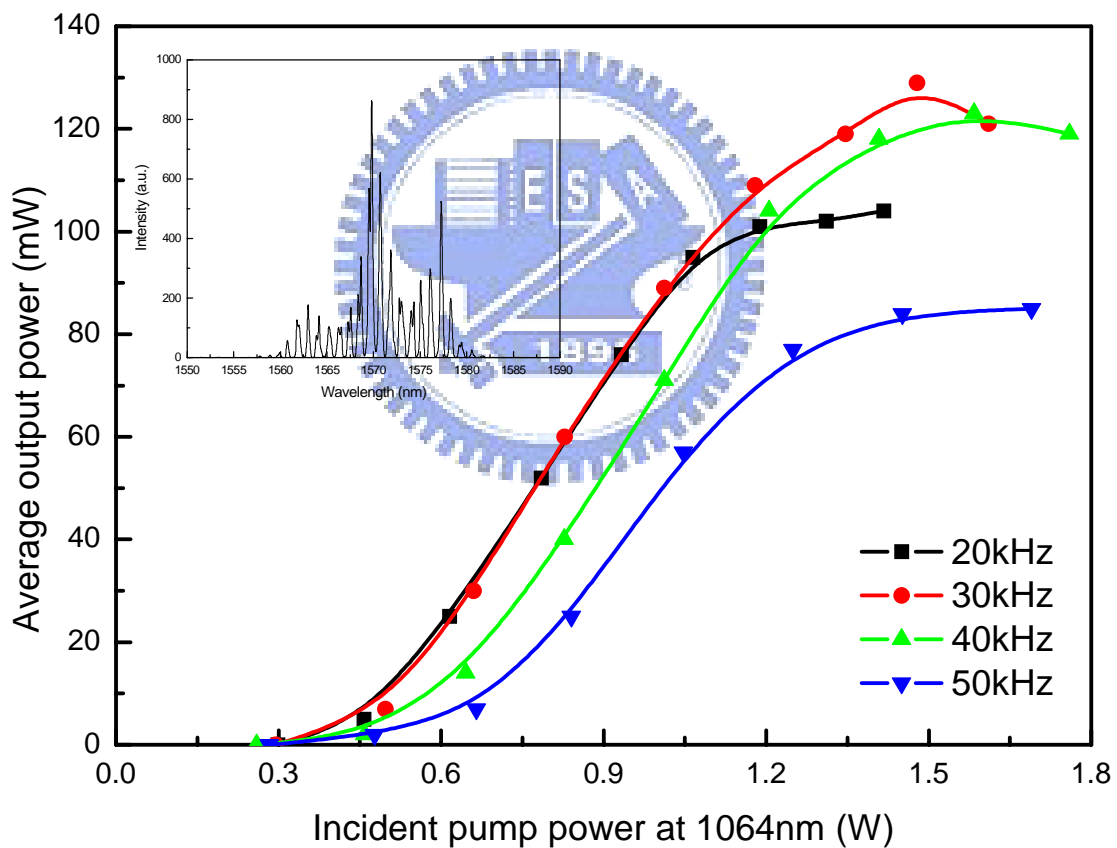
Fig. 2.4.3 Experimental results for the optically pumped AlGaInAs 1570-nm laser operated at the water temperature of 10°C at pump repetition rates of 20, 30, 40, and 60 kHz. *Inset* shows typical lasing spectrum obtained with 1.0 W of average pump power at a repetition rate of 30 kHz

Typical oscilloscope traces of pump and output pulses are shown in Fig. 2.4.4.With the finest alignment, the pulse-to-pulse amplitude fluctuation was found to be within ±10%, which is mainly attributed to the instability of the pump beam. As shown in Fig. 2.4.3, the average output power at a repetition rate of 30 kHz initially increases with the pump power and begins to saturate at 135 mW at an average pump power greater than 1.25W. Similarly, the conversion efficiency at a repetition rate of 20 kHz is reduced significantly at the average pump power greater than 1.0W and the maximum average output power is saturated at approximately 115mW. The reduction of the conversion efficiency at higher pump powers mainly comes from the gain-saturation effect.
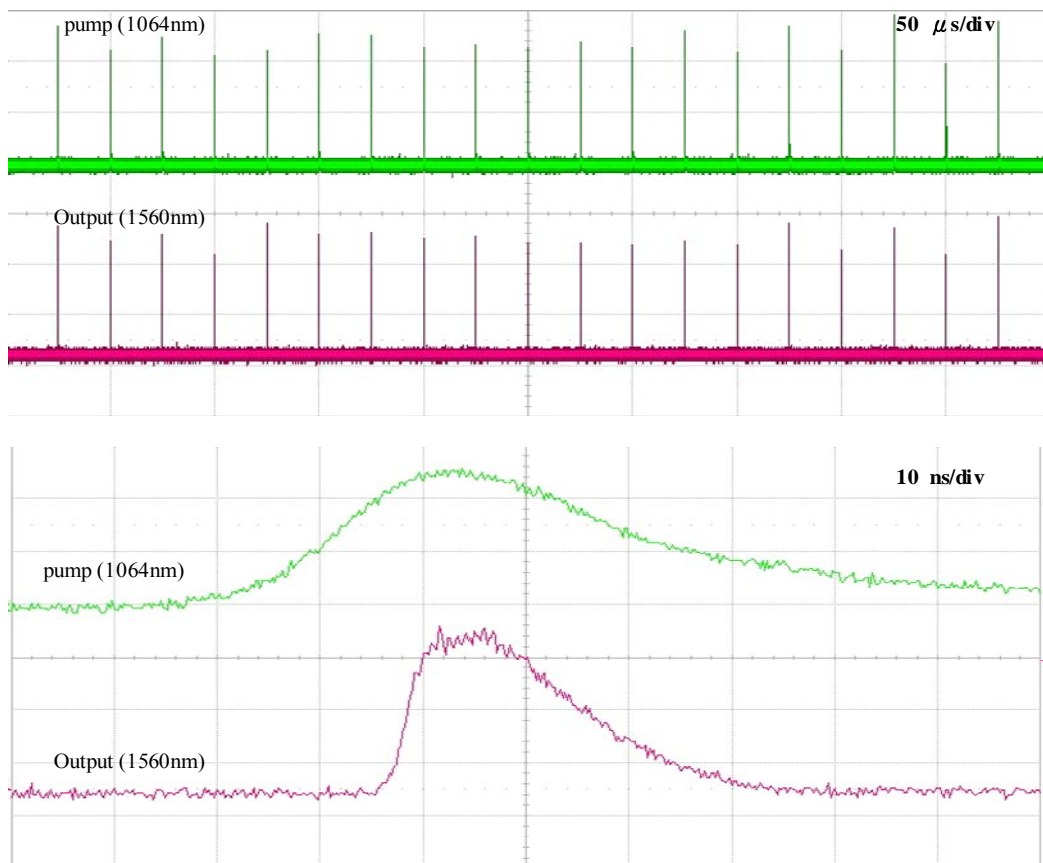
Figure 2.4.4 (a) Typical oscilloscope trace of a train of pump and output pulse and (b) expanded shapes of a single pulse

Figure 2.4.5 shows the output peak power as a function of pump peak power at a repetition rate of 20 kHz. The maximum output peak power is found to be 290 W at a pump peak power of 2.3 kW. With the transmission of the output coupler of 5%, the maximum intra-cavity lasing power can be calculated to be 5.8 kW. We use the formula $A = \pi(\omega_L)^2$ to calculate the lasing mode area, where ω_L is the lasing mode size. Using $\omega_L = 250$ μm, the lasing mode area and the saturation intensity of the gain chip can be found to be 0.002 cm^2 and 2.9 MW/cm^2, respectively. This value was two orders of magnitude higher compared to conventional solid-state laser crystals because of its shorter fluorescence decay time. To confirm the gain-saturation effect we used a pulsed semiconductor laser at 1.57 μm to measure the transmittance versus the excitation intensity with the z-scan method. The excitation pulse energy and pulse width were 3 μJ and 50 ns, respectively. The pump radius was varied from 0.01 to 0.1 cm. As a consequence, the excitation fluence was in the range of 0.1–10 mJ/cm^2 and was comparable to the fluence in the present laser cavity.
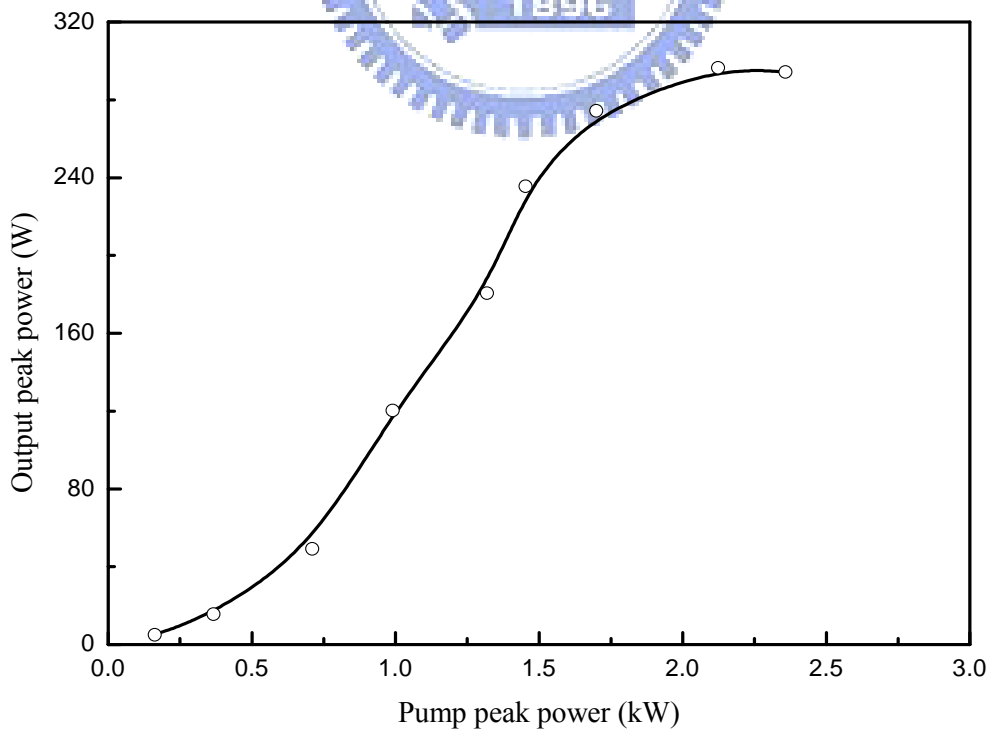
Fig. 2.4.5 Experimental results for the peak output power as a function of peak pump power at a repetition rate of 20 kHz

As shown in Fig. 2.4.6, the transmittance of the gain material exceeds 85% at the excitation intensity higher than 3.0 MW/cm^2.   Therefore, the number of QWs in the gain chip needs to increase to overcome the gain-saturation effect for scaling up the output peak power. On the other hand, the lower conversion efficiency at 60 kHz is speculated to arise from the longer pump pulse width at this repetition rate leading to the heavier heating effect.   We examined the dependence of lasing efficiencies on the water temperature to investigate the influence of the thermal effect.
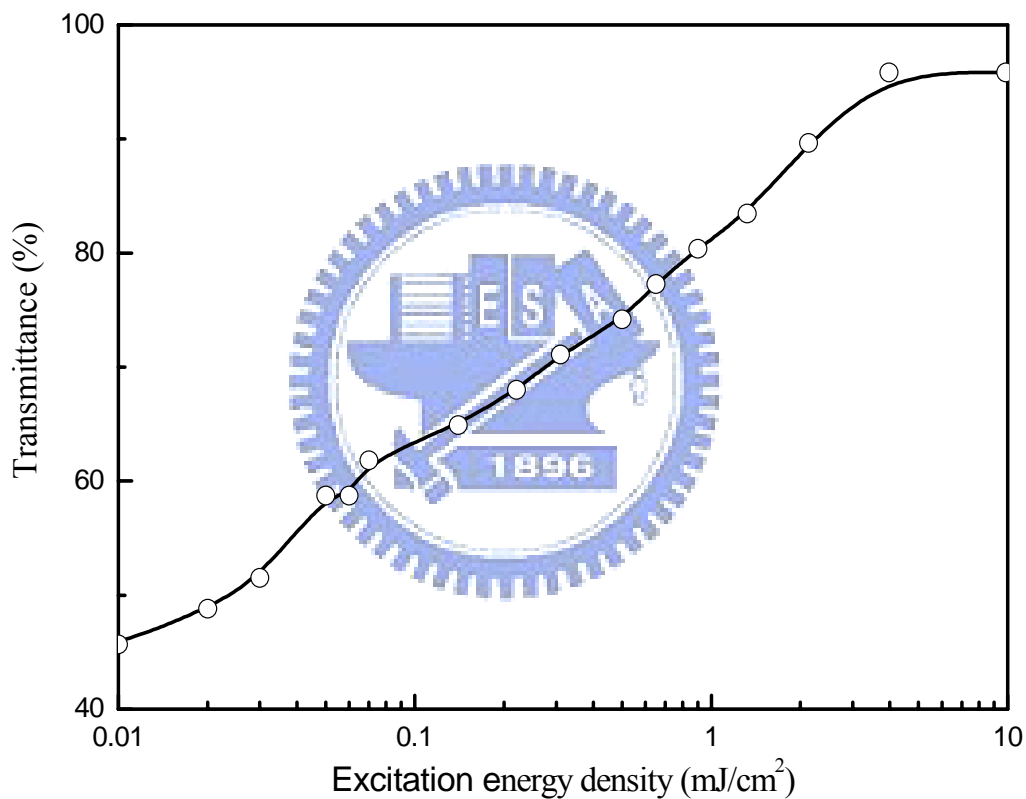
Fig. 2.4.6 Experimental results for the transmittance of the gain chip versus the excitation intensity at 1.57 μm

Figure 2.4.7 depicts the input–output characteristics for the water temperatures of 10, 15, 20, and 25°C at a repetition rate of 30 kHz.   Increasing temperature can be seen to lead to a certain reduction in the lasing efficiency.   Compared with the experimental results shown in Fig. 2.4.3 it can be found that the maximum output power at 20°C at a repetition rate of 30 kHz is almost comparable with that at 10°C at

a repetition rate of 60 kHz. As a result, we estimate the overall temperature of the gain chip at 60 kHz to be approximately 10° higher than that at 30 kHz. However, further investigation is required to analyze the influence of the heating dynamics on the conversion efficiency. Finally, it is worthwhile mentioning that even though the present slope efficiency is not better than the methods based on the nonlinear wavelength conversion, the present pump threshold is generally lower than of the approaches with SRS and OPO processes. Furthermore, there is some room for optimizing the output performance. One promising way for improving the slope efficiency is to reduce the quantum defect by using a pump laser with longer wavelength and gain chip and with a proper absorption barrier.
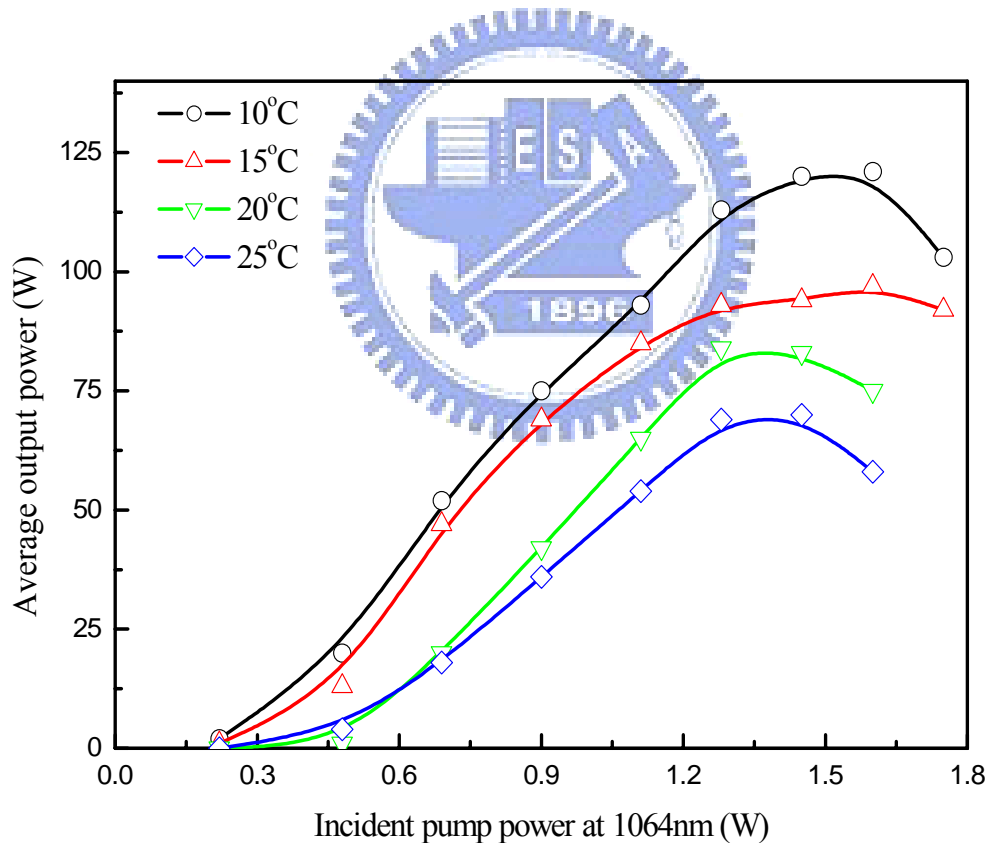
Fig. 2.4.7 Input–output characteristics for the water temperatures of 10, 15, 20, and 25°C at a repetition rate of 30 kHz

2.4.3 Conclusion

We have reported a high-repetition-rate high-peak-power AlGaInAs 1.57-μm TEM00 laser driven by a diode-end pumped actively Q-switched Nd:GdVO$_4$ 1.06-μm laser. The active region comprised 30 groups of two AlGaInAs quantum wells grown on a Fe-doped InP substrate and each group was spaced at half-wavelength intervals by barrier layers.   With an average pump power of 1.25 W, an average output power of 135 mW was produced at a repetition rate of 30 kHz. The maximum peak power was up to 290 W at a peak pump power of 2.3 kW and a pulse repetition rate of 20 kHz.

2.5. AlGaInAs quantum well 1.57μm laser (in-well pumping)

2.5.1 Experimental setup

Figure 2.5.1 shows the experimental configuration for the AlGaInAs QWs 1555-nm laser pumped by a diode-pumped actively Q-switched Nd:YVO$_4$ laser at 1342 nm. The pump source provides 20~110-ns pulse width between 20 kHz and 100 kHz. For comparison, a 1064-nm Q-switched laser was used in barrier-pumping scheme. The pump spot radius was controlled to be 70-100 μm by a focusing lens to maintain the spatial overlapping between lasing mode and pump mode.
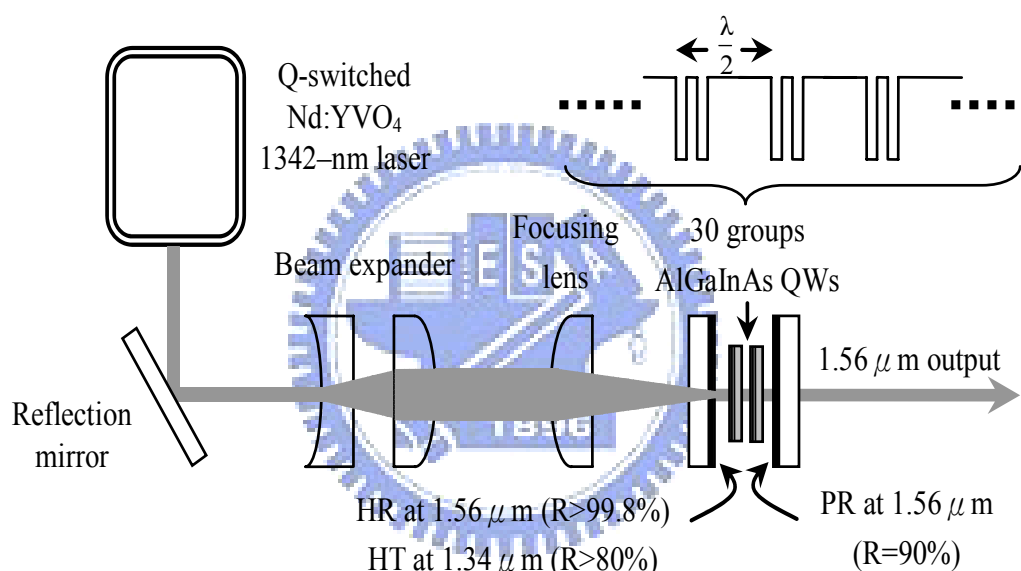
Fig. 2.5.1. The schematic of the AlGaInAs/InP eye-safe laser at 1555 nm. The pump source is an actively Q-switched Nd:YVO$_4$ laser at 1342 nm. HR: high reflection; HT: high transmission; PR: partial reflection

To simplify the cavity structure, the resonator is designed to be a flat-flat cavity stabilized by thermal lens effect of gain medium [1-2]. For the pump power between 0.4 W and 1.7 W, the mode to pump size was experimentally measured to be 0.6-0.9. The front mirror of resonator is a flat mirror coated with anti-reflection coating at pumping wavelength (R<0.2%) on the entrance surface, and with high-reflection coating at 1555 nm (R>90%) as well as high-transmission coating at pumping wavelength (T>80%) on the other surface. The output coupler is a flat mirror with

partial refection of 90% at 1555nm. The overall laser cavity length is approximately 5 mm.

However, a problem for in-well pumping scheme is the low pump absorption efficiency, which limits the efficiency of the laser. Due to the shorter effective thickness of quantum well, the active gain region has lower absorption at pump wavelength. In order to increase the absorption efficiency, double chips were further used in the serial experiments. The advantage of directly using multiple chips is that could reduce the difficulty of fabrication of gain medium with more quantum wells [3-6]. The experimental result shows that the absorption efficiency was increased from 45% to 65% when double chips were employed.

2.5.2 Experimental results and discussion

Figure 2.5.2 shows the comparison of average output power of single gain chip with in-well and barrier pumping. The maximum values shown in the two curves were measured for the comparable incident pumping power. It can be seen that employing the 1342-nm laser as a pump source exhibits good performance in conversion efficiency. This significant improvement result is contributed from the heat reduction by lowering the quantum defect which is diminished from 32% to 14%. However, since the absorption efficiency of gain medium at 1342 nm is lower than at 1064 nm, the available pump power is restricted. Double gain chips, accordingly, were investigated to improve the absorption efficiency.
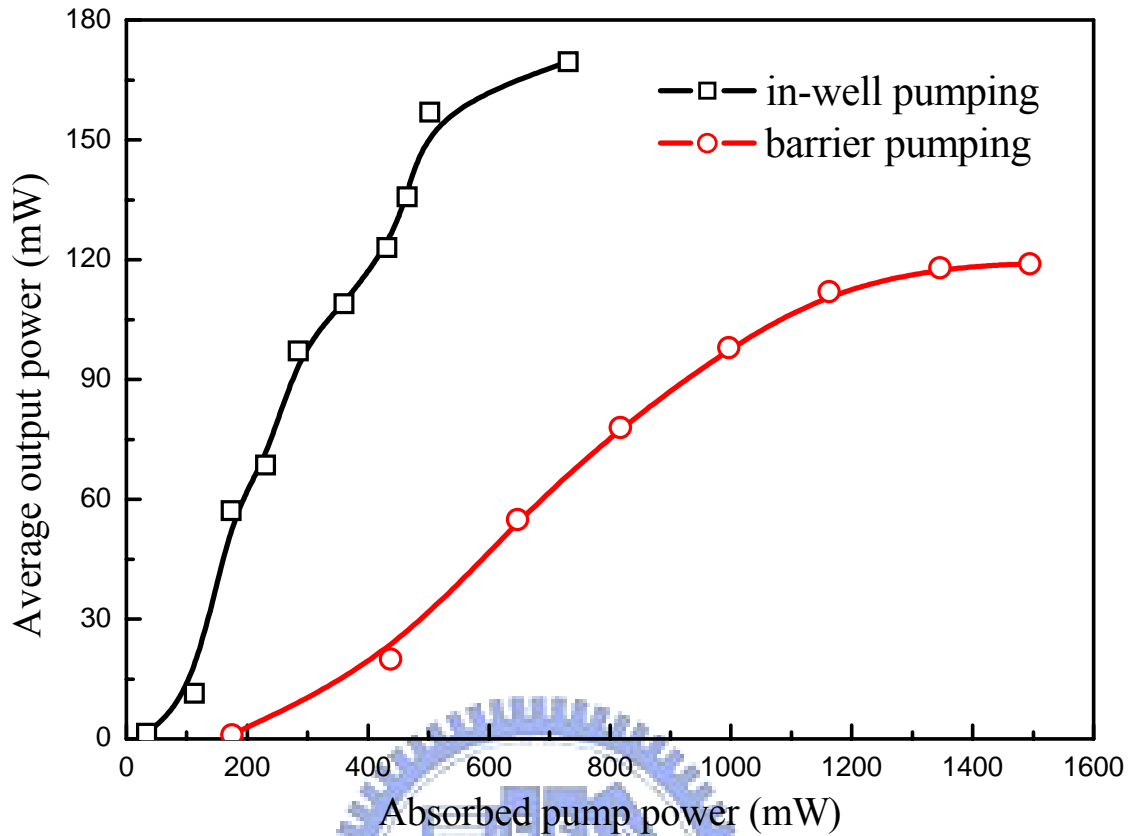
Fig. 2.5.2. The performance of AlGaInAs 1555-nm laser in the scheme of barrier (line with empty-square) and in-well pumping (line empty-circle), respectively. The in-well pumping scheme exhibits good performance in conversion efficiency.

Figure 2.5.3(a) shows the performance of the optically pumped AlGaInAs eye-safe laser with double gain chips operated at 12 °C for different pump repetition rate from 20 kHz to 100 kHz in 20 kHz interval. The corresponding average pump pulse width ranges from 20 ns to 110 ns with increasing repetition rate. In the process of increasing the repetition rate for the given cavity and absorbed pump power, the number of pump pulses increased per second, but the corresponding peak power of a single pulse decreased. In the beginning of lower repetition rate, the instantaneous high peak power resulted in a rapid temperature rise and the conversion efficiency decreased. As a result, the average output power increased with increasing the repetition rate due to decreasing the peak power. Further increasing the repetition rate, the duty cycle of pump pulses increased and resulted in an average temperature rise as

well as decrease of conversion efficiency. Therefore, there was an optimum repetition rate for obtaining the maximum average output power. This conclusion is coincident to the result of the experiment and the published research [7]. However, the difference from the published research is that the heating effect was enormously reduced in this experiment. From the experimental result shown in figure 2.5.3 (a), the optimum repetition rate was between 40 kHz and 60 kHz.
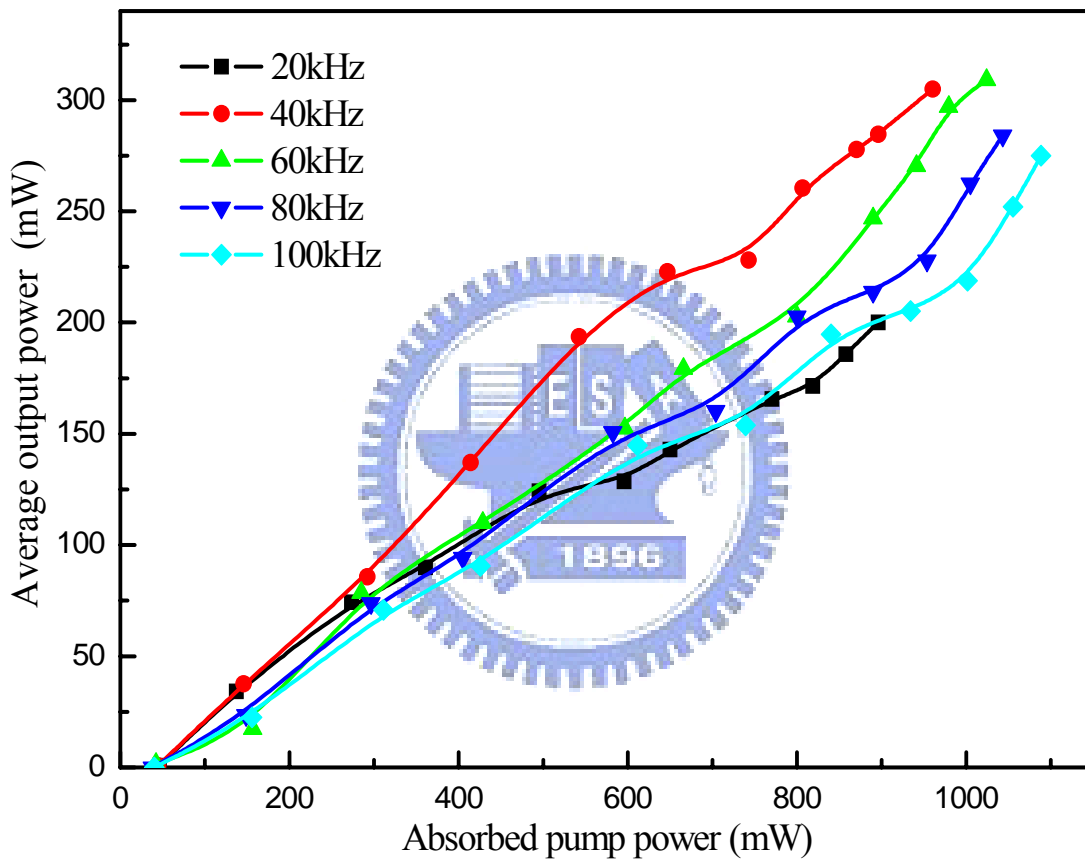
Fig. 2.5.3 (a) Experimental results for the optically pumped AlGaInAs eye-safe laser operated at 12 °C for several pulse repetition rates. The repetition rate for optimum performance of conversion efficiency was between 40 kHz and 60 kHz.

Figure 2.5.3(b) shows the typical lasing spectrum for the operation of 40-kHz repetition rate with average pump power of 0.65 W. The spectral bandwidth was approximately 17 nm.
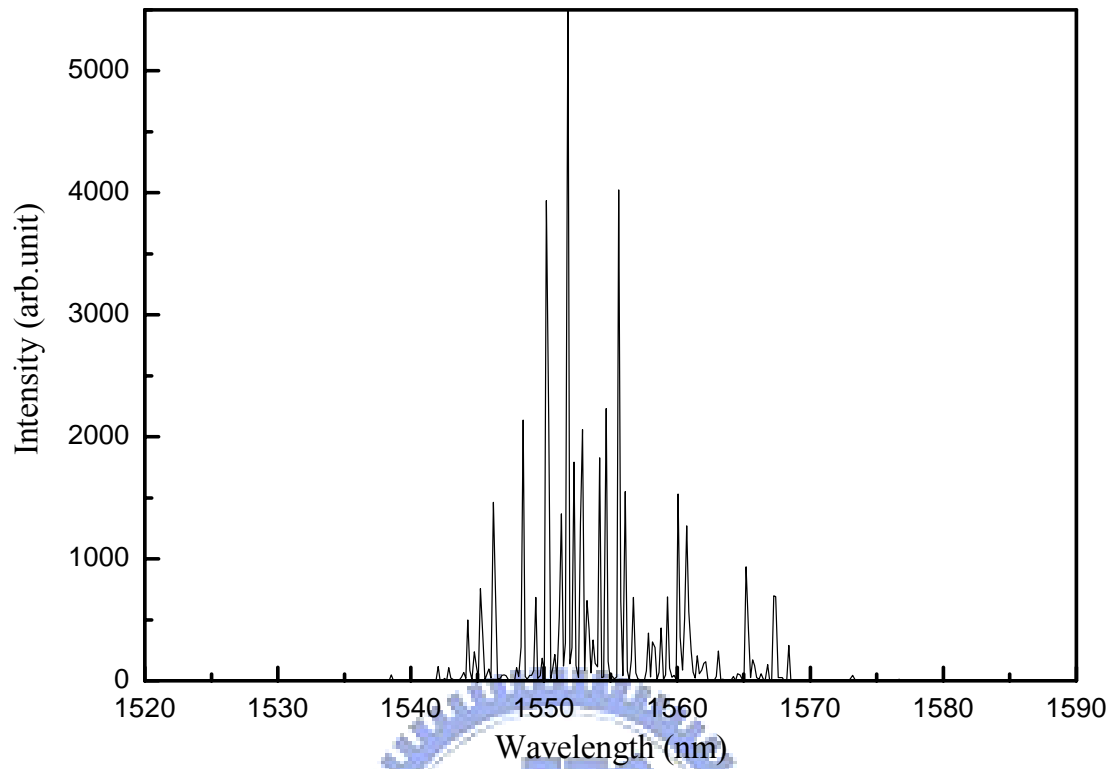
Fig. 2.5.3 (b) Typical lasing spectrum at repetition rate of 40 kHz and average pump
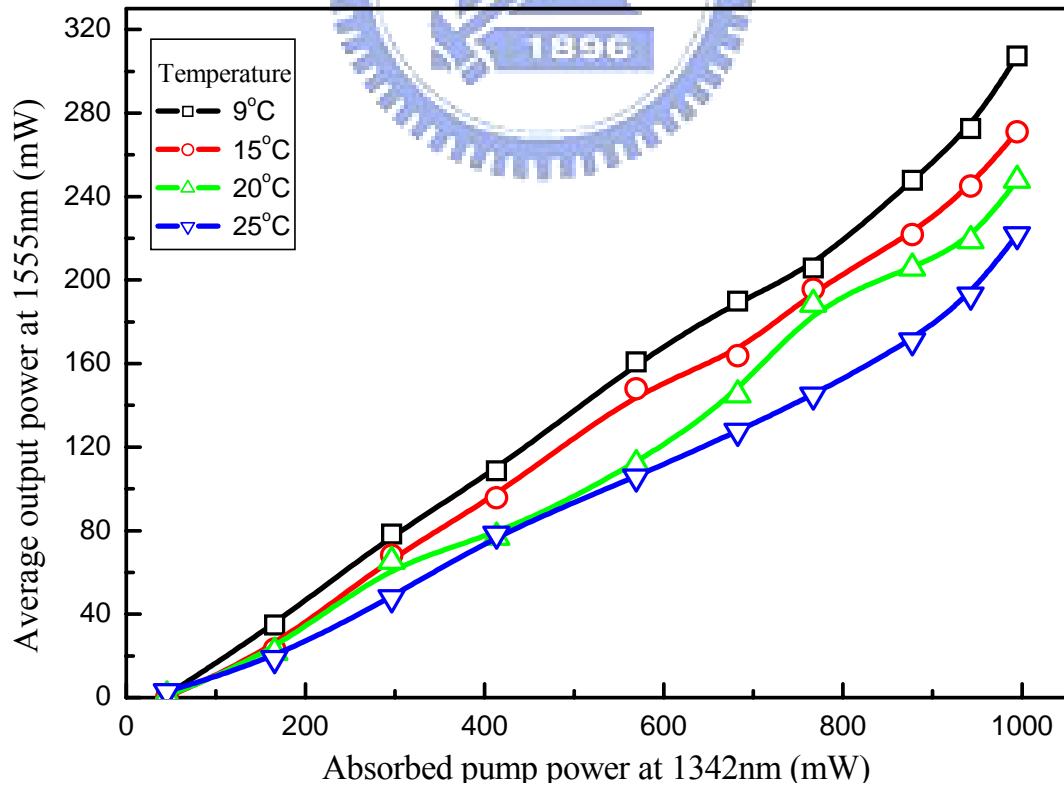
Fig. 2.5.4. The output characteristic was measured for the operation of different temperature.

The result shows the influence of thermal effect on conversion efficiency.

In order to further realize the influence of thermal effect, the average output power versus pump power was measured for different operating temperature, 9°C, 15°C, 20°C, and 25°C, at 50 kHz repetition rate and the result was shown in figure 6. Increase of temperature leads to the reduction of conversion efficiency and this result demonstrates the reduction of quantum defect is a practical way to improve optical conversion efficiency. The optical conversion efficiency could be up to 30% under the operating temperature of 9°C. Compared with pumped by 1064-nm laser, the optical conversion efficiency exceeds 3 times and over 20% of enhancement was obtained. For the operation at the temperature of 9 °C, the output peak power at 1555 nm versus the absorbed pump power at pulse repetition rate of 20 kHz was measured and shown in figure 2.5.5.
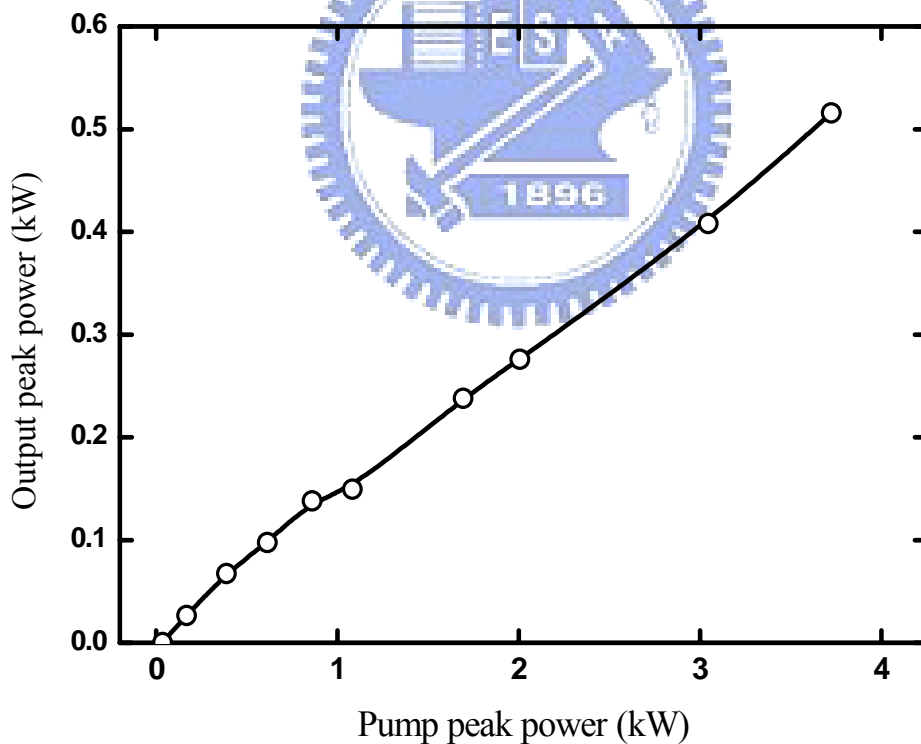
Fig. 2.5.5. The output peak power of AlGaInAs eye-safe laser at repetition rate of 20 kHz. At the pump peak power of 3.7 kW, the output peak power is up to 0.52 kW.

At the pump peak power of 3.7 kW, the output peak power up to 0.52 kW was generated. Experimental result shows that the output beam possesses an excellent beam quality. The half divergence angle of output beam was measured by using knife-edge method to be approximately 0.01 rad. Consequently, the M square value was estimated to be smaller than 1.3.

2.5.3 Conclusion

We have demonstrated an optically pumped high-peak-power AlGaInAs/InP eye-safe laser by using a pump method with lower quantum defect. The pump source is an actively Q-switched 1342-nm laser. With lower quantum defect, the thermal effect in gain medium decreases and results in improvement of optical conversion efficiency. The conversion efficiency is enhanced over three times compared with conventional pumping method. Double gain chips were used to increase the absorption efficiency of pump laser and a high peak output power of 0.52 kW was generated at a pulse repetition rate of 20 kHz and peak pump power of 3.7 kW.
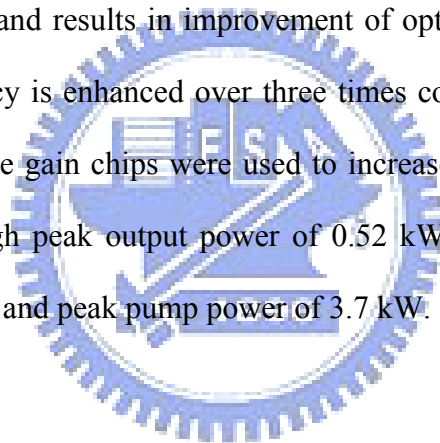
2.6. Summary

In this chapter, we give an overview of optically-pumped semiconductor lasers. The optically-pumped semiconductor lasers (OPSLs) combine the approaches of diode-pumped solid-states lasers and semiconductor quantum well vertical cavity surface emitting lasers (VCESL) and draw on the advantages of both. The OPSLs can generate a multi-watt, near-diffraction-limited output beam with good efficiency in wavelength regions which are not covered by solid-state laser gain materials.

We have demonstrated the periodic AlGaInAs QW/barrier structure grown on an Fe-doped InP transparent substrate was developed to be a gain medium in a room-temperature high-peak-power nanosecond laser at 1.36 μm and 1.57μm. The maximum peak power was achieved 1.2kW and 290 W at 1.36 μm and 1.57μm, respectively.

In addition, for power scaling up, we also have demonstrated an optically pumped high-peak-power AlGaInAs/InP eye-safe laser by in-well pumping scheme. The conversion efficiency is enhanced over three times compared with barrier pumping scheme. Double gain chips were used to increase the absorption efficiency of pump laser and maximum output power and peak power was up to 300mW and 0.52kW.

Chapter Three

Semiconductor saturable absorber

3.1 Introduction of Q-switched laser

Q-switching is a method to generate laser pulses with short duration and high peak power. In this method, the fast giant pulse is generated by allowing the pumping process to build up a population inversion and gain inside the cavity without oscillations. The Q-switching element has to be needed to introduce the losses inside the laser cavity and alter the quality factor Q of the cavity to low values for a period of time. Thus allowing storage of energy inside the gain medium and the population inversion in the gain medium is increased to levels that are above threshold. When the Q value of the cavity is switched to high values, a short, high peak power laser pulse is generated.

Q switching is carried out either by active or passive methods. Among the active methods are electro-opticak, acousto-optical and mechanical devices. The active Q-switches is driven by external driving sources such as Pockels cell voltage power supply, RF oscillator nad rotating mirror, coupled with polarized optics, and are usually expensive and bulky.

Contrary to active Q-switch method, the passive Q-switch is is a simple optical element which utilizes the nonlinearity of the absorption at the some photo flux. There is no need for external devices with high-voltage drivers and modulators or polarizers. Therefore, it has several advantages: light weight, low cost, design simplicity. It is worthy to note that the passive Q-switching process is a competition between the saturation of the saturable absorber and the gain media. If the gain medium saturates first, no Q-switch pulse will be developed. $Cr^{4+}YAG$ or Cr^{4+}-doped

solids are attractive for passively Q-switching Nd-based lasers, mainly Nd:YAG lasers because of its relatively large absorption cross-section and low saturation fluence of around 1064nm.

On the other hand, with the progressing technology in epitaxial growth, band-gaps of compound semiconductors can be engineered to cover almost the entire range of the spectrum from visible to infrared, so that essentially all-solid-state lasers may be Q switched by employing suitable-compound semiconductors. Semiconductor based Q switched have the advantage that the absorption can be tuned to be so strong that the length of the saturable absorber (SA) can be as short as several micro-meters or even shorter. The cavity length can be few hundred micrometer to be a single longitudinal mode microchip lasers that emit sub-nanosecond pulses with high pulse energies and high peak powers in a diffraction limited output beam. Semiconductor saturable absorber (SESA) or SESAMs have been widely applied in 1.06, 1.34 and 1.56μm with different semiconductor materials.
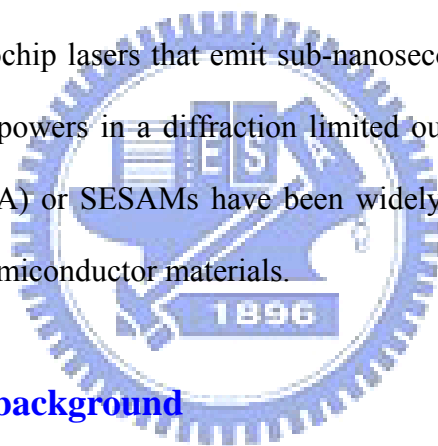
3.2 Motivation and background

3.2.1. Diode-pumped 1.06-μm passively Q-switched laser

Diode-pumped passively Q-switched solid-state lasers that use saturable absorbers have attracted significant attention because of their compactness and simplicity in operation. Numerous saturable absorbers have been developed to replace the dyes used in solid-state lasers, such as Cr^{4+}-doped crystals [1–5] and semiconductor saturable absorber mirrors (SESAMs) [6,7]. Nowadays, Cr^{4+}:YAG crystals are no doubt the most used saturable absorbers in the 0.9–1.2 μm spectral region. Although InGaAs/GaAs quantum wells (QWs) have been utilized as SESAMs, the lattice mismatch leads to the limitation of the modulation depth that is defined as the maximum absorption change between low and high intensities. As a consequence,

the output pulse energies and the conversion efficiencies with InGaAs SESAMs are generally significantly lower than those with Cr^{4+}:YAG crystals. It is, however, commonly inconvenient to apply Cr^{4+}:YAG crystals as saturable absorbers in conventional Nd-doped vanadate crystals because the absorption cross sections of Cr^{4+}:YAG crystals are not large enough for the good Q-switched criterion [3,8–10]. Therefore it is highly desirable to develop a saturable absorber with a large absorption cross section, a large modulation depth, and a high damage threshold.

The quaternary alloy of InGaAsP has been shown to be an important material for optoelectronic device applications [11–13] because it can be grown epitaxially on an InP substrate without lattice mismatch in the 0.84–1.65 μm spectral region. Recently, an InGaAsP multiple QW/barrier structure grown on a transparent InP substrate has been successfully used as a semiconductor saturable absorber (SESA) in a 1.3 μm laser with a Q-switching efficiency (ratio of the Q-switched output power to the cw power at the maximum pump power) of 27.6% [14]. Compared with InGaAsP materials, the AlGaInAs quaternary alloy with a larger conduction band offset can provide a better electron confinement covering the same wavelength region [15,16]. Although AlGaInAs/InP QWs have been used to fabricate high-performance uncooled 1.3 μm lasers [17,18], they have not yet been applied to be the saturable absorbers in passively Q-switched solid-state lasers.

In this chapter we demonstrate, for the first time to our knowledge, an AlGaInAs saturable absorber with a periodic QW/barrier structure that can be used to achieve an efficient high-peak-power and high average- power passively Q-switched 1.06 μm laser. With an incident pump power of 13.5 W, an average output power of 3.5 W with a Q-switched pulse width of 0.9 ns at a pulse repetition rate of 110 kHz was obtained. The maximum peak power was greater than 36 kW. As the result of the rather low nonsaturable loss, the overall Q-switching efficiency could be up to 80%.

More important, damage to the absorber can be ingeniously avoided by the periodic QW/barrier structure.

3.2.2. Diode-pumped 1.34-μm passively Q-switched laser

In recent years, the compact, diode-pumped passively Q-switched nanosecond laser sources near 1.3 μm have wide applications in many fields such as optical fiber communication, micro machining, remote sensing, information storage. By inserting the saturable absorber is the most efficient and easy way to realize methods for obtaining short pulses from diode-pumped lasers. Recently, the saturable absorbers including $Co^{2+}:MgAl_{11}O_{19}$ [19], PbS-doped phosphate glasses [20,21] and $V^{3+}:YAG$ [22,23] have been used as the saturable absorber in the passively Q-switched lasers at 1.3 μm.

In addition, the semiconductors have also been utilized as saturable absorber from 0.8~1.6μm spectral region in passively Q-switched and mode-locked lasers. Up to now, the semiconductor saturable absorber mirrors (SESAMs) have been successfully designed for application to practical laser systems. The GaAs and InP based substrate are two main types of materials for the SESAMs. A main advantage of GaAs-based substrate is the availability of high-quality (Al)GaAs/AlAs distributed Bragg reflector(DBRs) with a reasonable refractive index contrast and good thermal properties. The semiconductor saturable absorber for 1.3μm wavelength spectral including InGaAs/GaAs quantum wells (QWs) [24], GaInNAs/GaAs QWs[25,26], InAs/GaAs quantum dots(QDs)[27,28]. The InGaAs QWs for 1.3μm SESAMs have large insertion lose because of the high indium concentration resulting in significantly strained layers on GaAs distributed Bragg reflectors(DBRs). The GaInNAs SESAMs have to be postgrowth annealed to reduce nonradiative defects and to tune the PL wavelength close to the lasing wavelength. The InAs QDs for 1.3μm

SESAMs have lower nonsaturable loss, but the smaller modulation depth of QDs is so difficult to scale up that the pulse energy is lower than QWs.

On the other hand, the quaternary alloy of InGaAsP and AlGaInAs have been shown to be the important materials because they can be grown epitaxially on an InP substrate without lattice mismatch in the 0.84-1.65μm spectral region [29,30]. In spite of lattice match with InP substrate, the overall performance of the DBRs on InP substrates are hindered by the disadvantage of a small contrast between refractive indices. Even though AlGaAsSb/InP and AlGaInAs/InP have been demonstrated to be lattice-matched DBRs at 1.55 μm VCSEL [31,32], it is more difficult for the 1.3 μm wavelength because the choice of DBR becomes tighter. Nevertheless, the DBRs are merely an optional structure for the cavity design of the passive Q-switched lasers. Without the use of DBRs, the semiconductor saturable absorber (SESA) has to be grown on a transparent substrate. The Fe-doped InP material is a particularly useful substrate to grow the SESA for passively Q-switched Nd-doped or Yb-doped solid-state lasers [33], since it is transparent at the lasing spectral region. More importantly, using an external output coupler is beneficial to the flexibility of the cavity design and the optimization of the output coupler. The InGaAsP quantum wells as a saturable absorber in the solid-state laser have been used in the Q-switching and mode-locking operation in 1.3μm and 1.55μm wavelength spectrum [34-36]. Although of InGaAsP/InP QWs has been utilized as SESA, the carrier leakage from the quantum well leads to the limitation of pulse energy and stability under high temperature operation.

Figure 3.2.1 depicts the conduction band offset of AlGaInAs and InGaAsP semiconductor. It can been shown that the reduced carrier leakage results from $Al_xGa_yIn_{1-x-y}As$/InP having a larger conduction band offset at the heterojunctions compared to the smaller conduction band offset of $In_{1-x}Ga_xAs_yP_{1-y}$ / InP, and this is

very significant to prevent carrier leakage at high temperatures [37,38]. Recently, AlGaInAs quantum wells have been successfully used as a semiconductor saturable absorber (SESA) in 1.06μm laser with high damage threshold, low nonsaturable loss and high Q-switched efficiency [39].

$$Al_x Ga_y In_{1-x-y} As \,,\, \frac{\Delta E_c}{\Delta E_v} = \frac{0.72}{0.28} \qquad\qquad In_{1-x} Ga_x As_y P_{1-y} \,,\, \frac{\Delta E_c}{\Delta E_v} = \frac{0.4}{0.6}$$
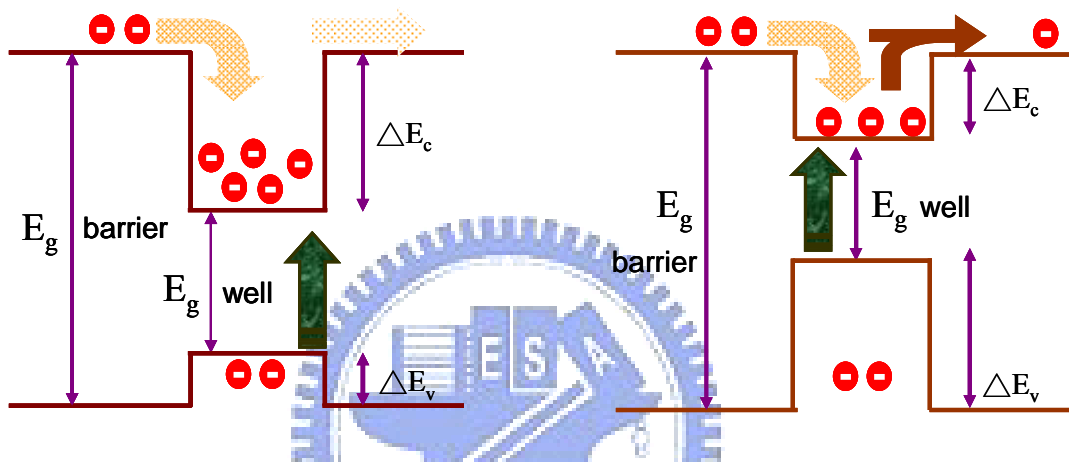
Figure. 3.2.1. Conduction band offset of AlGaInAs and InGaAsP semiconductor

In this chapter , we report , for the first time to our knowledge , the AlGaInAs/InP QW/barrier structure grown on an Fe-doped InP substrate to be a semiconductor saturable absorber(SESA) for a Nd:YVO$_4$ 1.34μm laser .Compared with InGaAsP/InP QWs, AlGaInAs/InP QWs has lower threshold , higher Q-switching efficiency and higher peak power . With an incident pump power of 15W , the fifteen pairs AlGaInAs QWs has an average output power of 1.69W with a peak power of 1.54kW and average pulse energy are 26.4 μJ .

3.3. Diode-pumped 1.06μm passively Q-switched laser

3.3.1 Device fabrication and experiment setup

The present saturable absorber is an AlGaInAs QW/barrier structure grown on a Fe-doped InP substrate by metal-organic chemical-vapor deposition (MOCVD). Instead of the conventional S-doped InP substrate, a Fe-doped InP substrate is used because it is almost transparent for light wavelengths greater than 940 nm. The region of the saturable absorber consists of 30 groups of two QWs with the luminescence wavelength around 1060 nm, spaced at half-wavelength intervals by InAlAs barrier layers with the bandgap wavelength around 805 nm. It is worthwhile to mention that, compared with a conventional SESAM structure, the missing DBR significantly simplifies the structure and thus growth and yield. Since the cavity modes with lower losses always dominate the lasing output, the lasing modes are naturally the modes with the electric field minima along the periodic QWs. Therefore the barrier layers are used not only to confine the carriers but also to locate the QW groups in the region of the nodes of the lasing standing wave.

The backside of the substrate was mechanically polished after growth. Both sides of the SESA were antireflection coated to reduce back reflections. Since the total residual reflectivity of the antireflection-coated sample is approximately 5%, the SESA device has to be aligned accurately in the tilt direction to recapture as much as possible of the reflected light in the cavity mode. The initial transmission of the SESA device at the wavelength of 1064 nm was measured to be approximately 70%. With the z-scan method, the modulation depth was experimentally found to be approximately 27% in a single pass. Furthermore, the total nonsaturable loss introduced by the SESA was found to be lower than 2%. From the numerical simulations of the SESA design, the saturation fluence is estimated to be in the range of 1 mJ/cm^2. The relaxation time of the SESA is of the order of 100 ns.

Figure 3.3.1 depicts the experimental configuration for the passively *Q*-switched 1.06 μ m Nd:YVO$_4$ laser with AlGaInAs/InP QWs used as a saturable absorber.
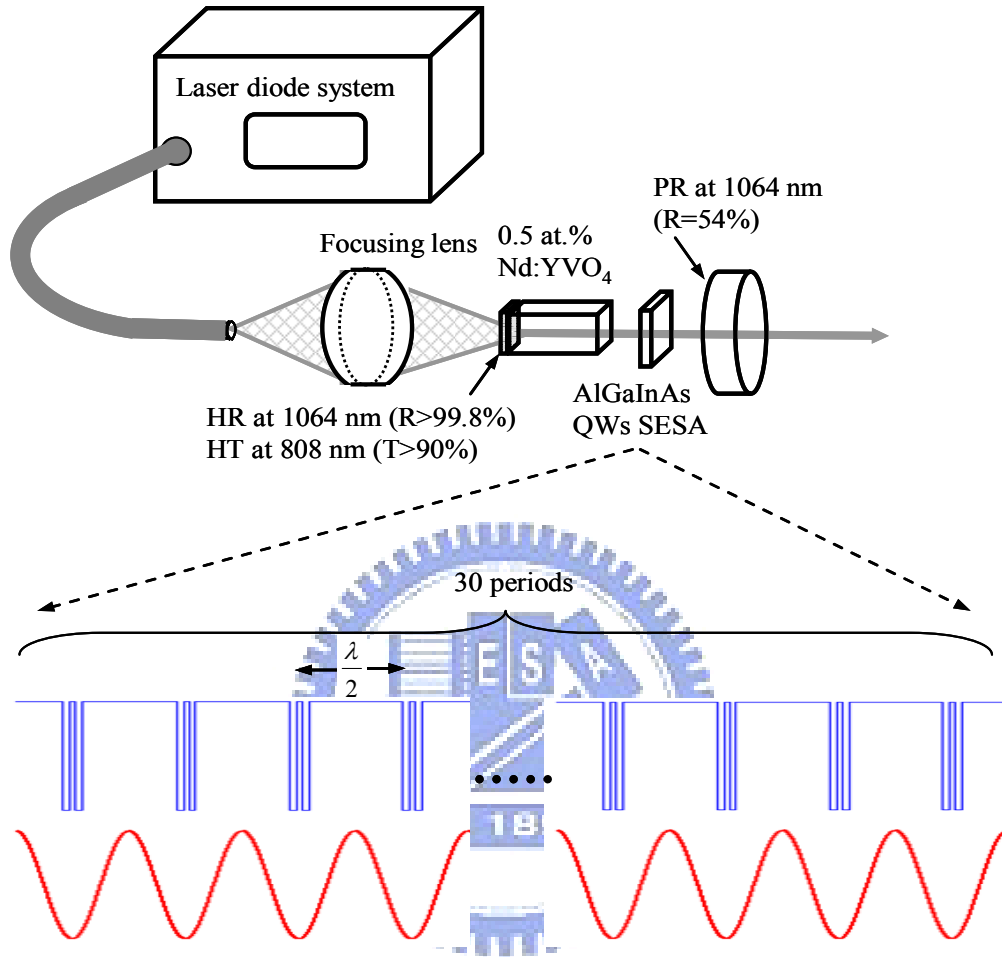
Fig. 3.3.1. An experimental diagram of a diode-pumped passively Q-switched Nd:YVO$_4$ laser using a periodic AlGaInAs QW/barrier structure as a saturable absorber. The lasing modes are naturally to have the electric field minima along the periodic QWs.

The laser crystal is 8 mm long and doped with a 0.5% Nd^{3+} concentration. One side of the Nd:YVO$_4$ was coated so as to be nominally highly reflecting at 1064 nm (*R*>99.8%) and antireflection coated at 809 nm (*T*>90%). The other side was antireflection coated at 1064 nm (*R*<0.2%). The pump source was a 15 W 809 nm fiber-coupled laser diode with a core diameter of 800 _m and a numerical aperture of 0.16. A focusing lens with a 16.5 mm focal length and 85% coupling efficiency was used to reimage the pump beam into the laser crystal. The pump spot radius was

around 350 μm. The reflectivity of the output coupler is 54% at 1064 nm. The overall Nd:YVO$_4$ laser cavity length was approximately 25 mm. The SESA device was positioned in the middle of the cavity to enable the lasing modes spontaneously to have their field nodes near the QWs.

3.3.2 Experimental result and discussion

Figure 3.3.2 shows the average output powers at 1064 nm with respect to the incident pump power in cw and passively Q-switching operations.
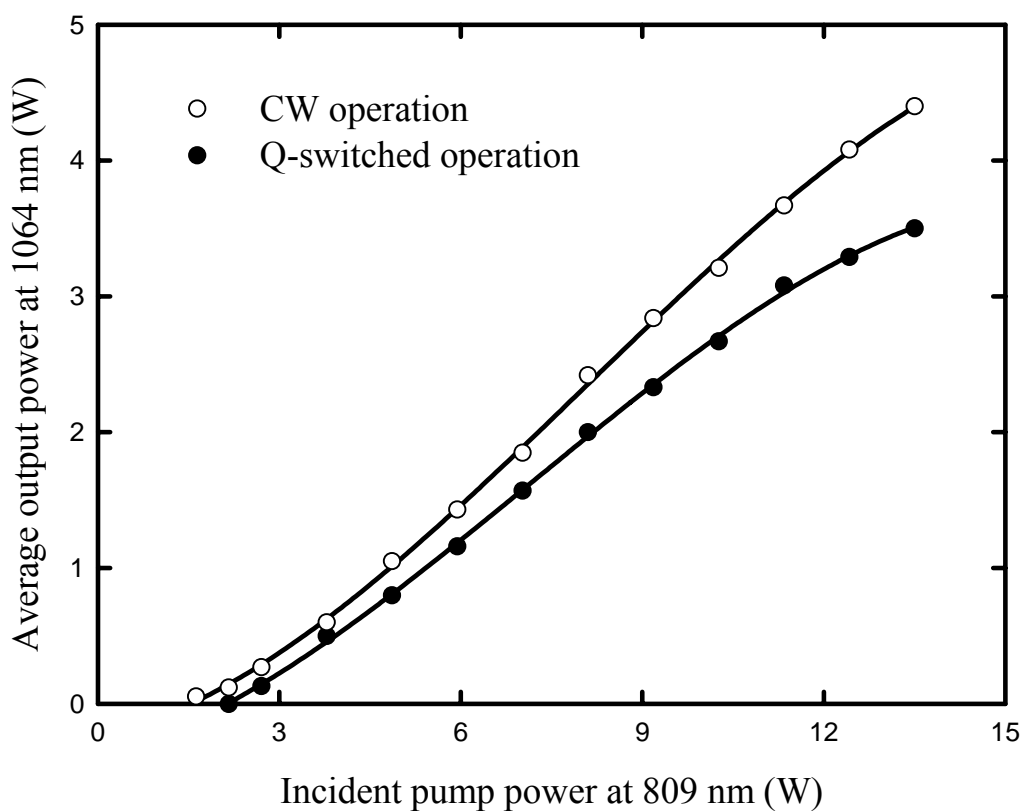
Fig. 3.3.2. Average output powers at 1064 nm with respect to the incident pump power in cw
and passively Q-switching operations.

The cw performance at 1064 nm provides the baseline for evaluating the passively Q-switched efficiency. Without the SESA in the cavity, the cw laser at 1064 nm had an output power of 4.4 W at an incident pump power of 13.5 W. In the passively Q-switching regime, an average output power of 3.5 W was obtained at an incident pump power of 13.5 W. The Q-switching efficiency (ratio of the Q-switched

output power to the cw power at the maximum pump power) was found to be close to 80%. This *Q*-switching efficiency is considerably better than the results obtained with an InGaAs SESAM [1]. The pulse temporal behavior was recorded by a LeCroy digital oscilloscope (Wavepro 7100, 10 G samples/s, 1 GHz bandwidth) with a fast p-i-n photodiode. Figure 3.3.3 shows the pulse repetition rate and the pulse energy versus the incident pump power.   The pulse repetition rate increases monotonically with the pump power up to 110 kHz. On the other hand, the pulse energy increases with the incident pump power little by little, from 22 μJ at the threshold of 3 W to 33μJ at an incident pump power of 13.5 W.   The increase of the pulse energy with increased pump power may come from the thermal effects that induce changes of the mode sizes on the gain medium and the SESA device.
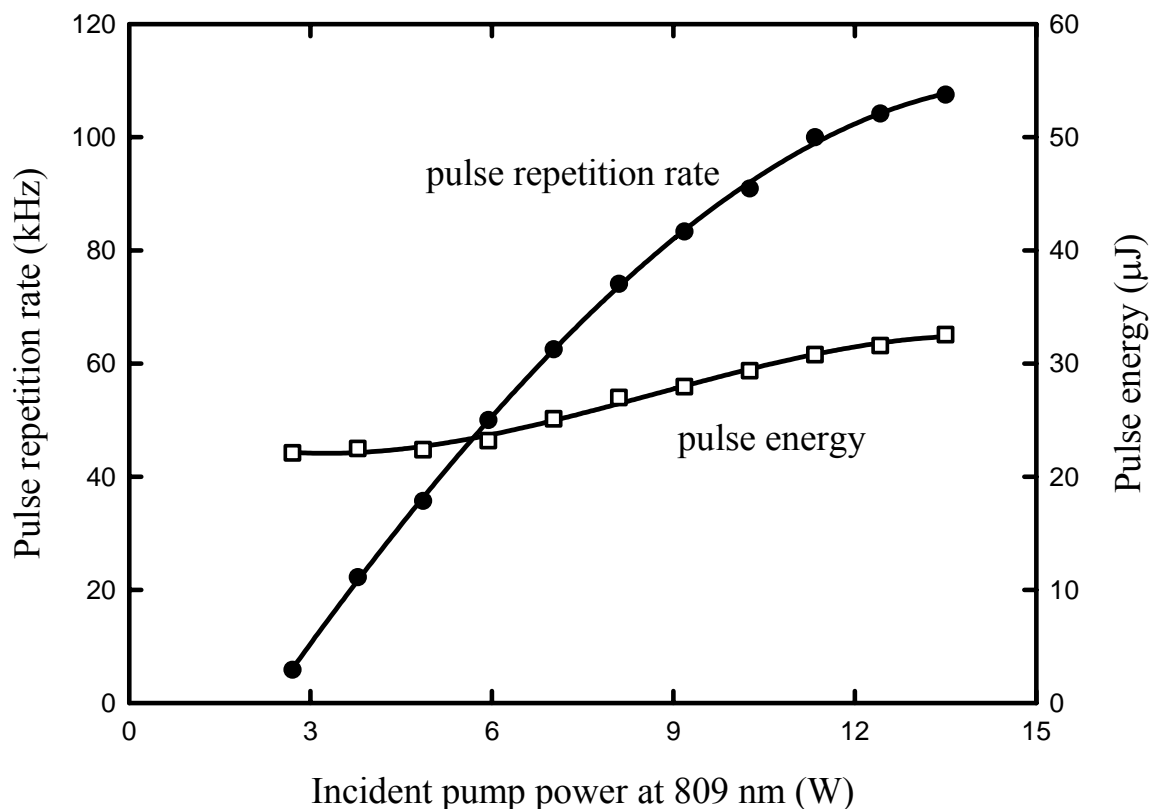
Fig. 3.3.3. Experimental results for the pulse repetition rate and the pulse energy versus incident pump power.

Figure 3.3.4 shows the peak power and the pulse width (FWHM) as a function of

the incident pump power.   A typical oscilloscope trace of a train of output pulses and an expanded shape of a single pulse are shown in Fig. 3.3.5.   Under the optimum alignment condition, the pulse-to-pulse amplitude fluctuation was found to be within ±5%.   As seen in Fig. 3.3.4, the pulse width decreases rather slowly from 1.6 ns at the threshold of 3 W to 0.9 ns at an incident pump power of 13.5 W.   As a consequence, the peak power of the passively Q-switched Nd:YVO4 laser increases from 14 kW at the threshold of 3 W to 36 kW at an incident pump power of 13.5 W. The overall performance can parallel the results obtained with Cr^{4+}:YAG crystals [2,3,4].
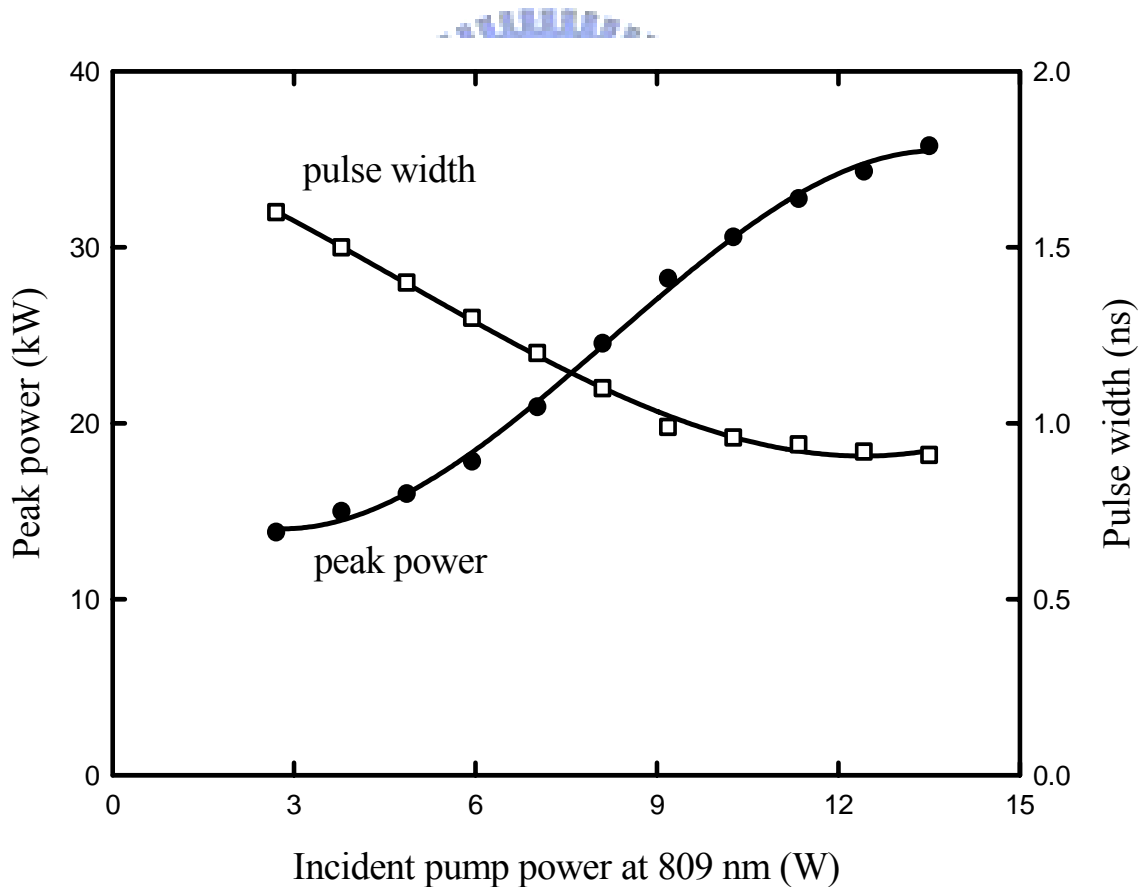
Fig. 3.3.4. Experimental results for the peak power and the pulse width (FWHM) as a function of the incident pump power.
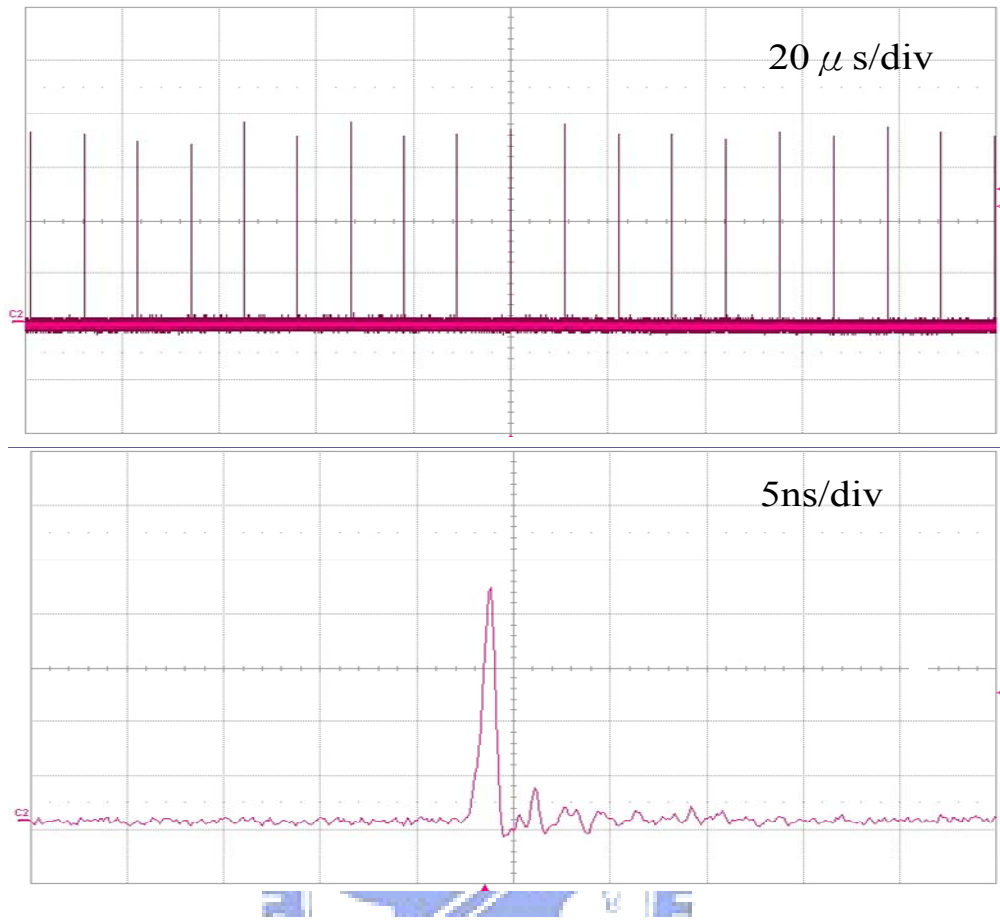
Fig. 3.3.5. (a) typical oscilloscope trace of a train of output pulses and (b) expanded shape of a single pulse.

3.3.3 Conclusion

In summary, a periodic AlGaInAs QW/barrier structure grown on a Fe-doped substrate was used as a saturable absorber for the Q-switching of a high power diode-pumped Nd:YVO$_4$ laser operating at 1064 nm. The barrier layers play a role not only to confine the carriers but also to locate the QW groups in the region of the nodes of the lasing standing wave to avoid damage. Stable Q-switched pulses of 0.9 ns duration with an average output power of 3.5 W and a repetition rate of 110 kHz were obtained at an incident pump power of 13.5 W. The remarkable performance confirms the prospect of using AlGaInAs QWs as saturable absorbers in solid-state lasers.

3.4. Diode-pumped 1.34μm passively Q-switched laser

3.4.1 Device fabrication and experiment setup

This AlGaInAs QW/barrier structure grown on an Fe-doped InP substrate by metal-organic chemical-vapor deposition (MOCVD). The saturable absorber region includes fifteen (15) groups of two QWs with bandgap wavelength around 1.34μm, spaced at half-wavelength intervals by AlGaInAs barrier layers with the band-gap wavelength around 1.06μm. It is important that the barriers layers with strong absorbance at 1.06μm are designed not only to confine the carriers but also to locate the QW groups in the region of nodes of the lasing standing wave. It is worthwhile to mention that the AlGaInAs material system has larger conduction band offset than the most widely used InGaAsP system and this larger conduction band offset has been confirmed to yield better electron confinement in the conduction band and higher temperature stability. The backside of the substrate was mechanically polished after growth. Both sides of the SESA were antireflection (AR) coated to reduced back reflections and couple-cavity effects.

Fugure3.4.1 shows the transmission spectrum of the AR-coated AlGaInAs/InP and InGaAsP/InP saturable absorbers at room temperature. It can be seen that the strong absorption of the barrier layers leads to low transmission near 1.06μm. The initial transmissions at 1.06μm and 1.34μm for AlGaInAs/InP are 0.06 and 0.67 respectively. The modulation depth of the AlGaInAs/InP semiconductor saturable absorber (SESA) is experimentally estimated to be approximately 28% in a single pass, so in total 56% for a cavity roundtrip. With the numerical stimulations of the SESA design, the saturation fluence is estimated to be in the range of 32μJ/cm^2.The recovery time and optical damage threshold of the SESA are approximately 30~50ns and 500~600MW/cm^2, respectively.
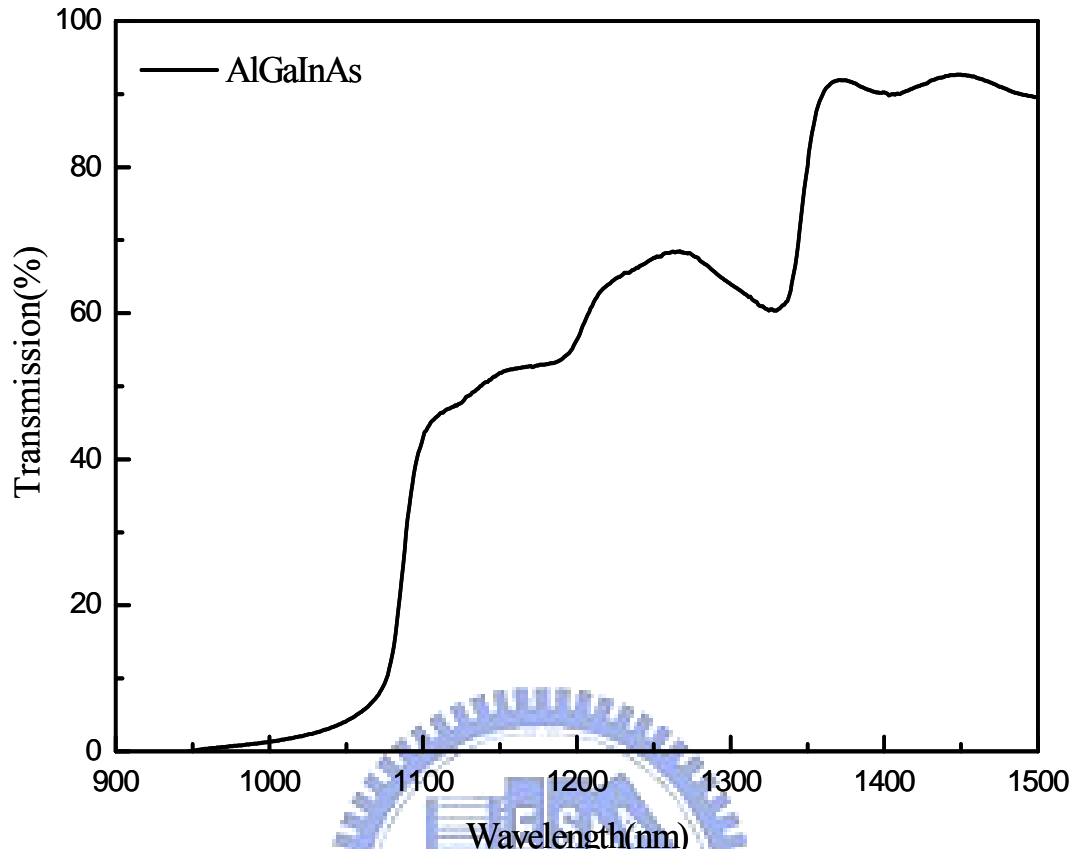
Fig3.4.1 The transmittance spectrum at room temperature for the AR-coated AlGaInAs saturable absorber

Figure3.4.2 depicts the experimental configuration for the passively Q-switched 1.34-μm Nd:YVO$_4$ laser by use of AlGaInAs/InP QWs as a saturable absorber.   The active medium was a 0.5% 3x3x7mm long Nd:YVO$_4$ crystal.   Both sides of the laser crystal were coated of antireflection at 1.34-μm(R<0.2%).   The pump source was a 15W 808nm fiber-coupled laser diode with a core diameter of 600μm and a numerical aperture of 0.16.   A focusing lens with a 16.5mm focal length and 90% coupling efficiency was used to re-image the pump beam into the laser crystal.   The pump spot radius was around 320μm.   The input mirror was a 500mm radius-of-curvature concave mirror with antireflection coating at the diode wavelength on the entrance face(R<0.2%), high-reflection coating (HR) at the lasing wavelength(R>99.8%) and a high-transmission coating at the diode wavelength on the other surface(T>90%). Note that the laser crystal was placed near the input mirror (<1mm) for the spatial

51

overlap of the transverse mode structure and pump power distribution.   The AlGaInAs/InP QWs SESA was mounted on a copper heat sink with active water cooling.   The reflectivity of the output coupler is 94% at 1342nm.   The overall Nd:YVO$_4$ laser cavity was approximately 30mm.   The cavity losses introduced by the pump mirror and output coupler are approximately 0.48 and 0.0065 for wavelength at 1.06μm and 1.34μm.   The total non-saturable loss introduced by the SESA is lower than 0.3.   Without the SESA in the cavity, the cavity loss can be introduced by resonator mirrors at 1.34 μm under cw operation.   However, the gain of Nd:YVO$_4$ at 1.06 μm is so larger than at 1.34 μm that we use the AlGaInAs SESA to give the extra gain suppression at 1.06μm for the Q-switching operation at 1.34μm.
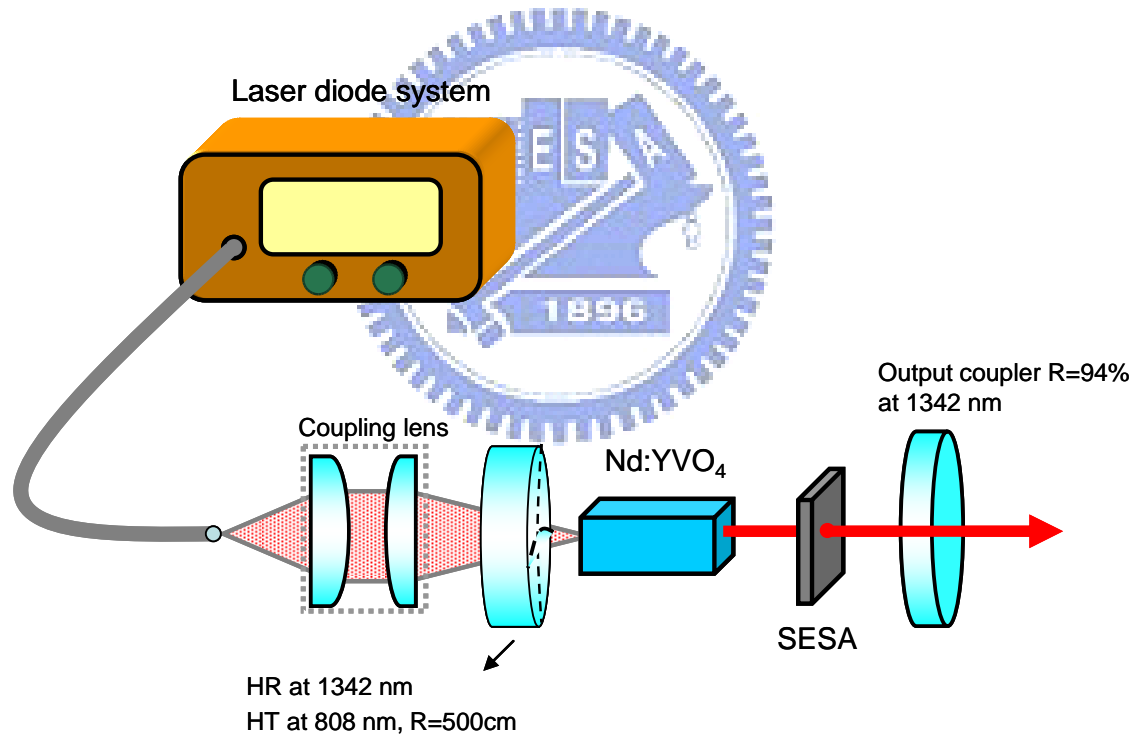
Fig.3.4.2 An experimental setup of a diode-pumped 1.34μm passively Q-switched Nd:YVO$_4$ laser.

3.4.2 Experimental results and discussions

Figure 3.4.3 shows the average output powers at 1342 nm with respect to the incident pump power in cw and passively *Q*-switching operations.   Without the SESA in the cavity, the cw laser at 1342 nm had a slope efficiency of 30.7% and an output power

of 3.95Wat an incident pump power of 14W.   In the passively *Q*-switching regime with AlGaInAs saturable absorber an average output power of 1.53Wwas obtained at an incident pump power of 14W.   The *Q*-switching efficiency (ratio of the *Q*-switched output power to the cw power at the maximum pump power) was found to be 45%.   This *Q*-switching efficiency is considerably higher than that obtained with an InGaAsP SESA and the threshold is also lower than that of InGaAsP SESA.
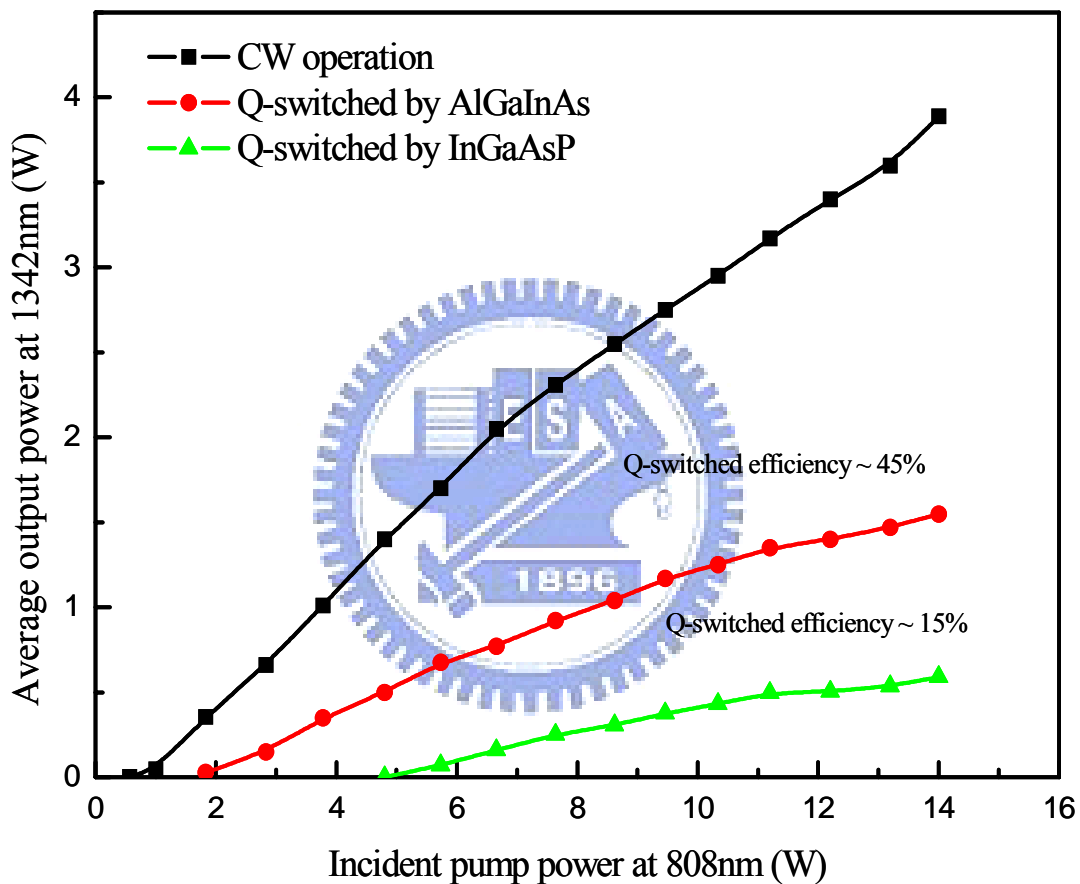
Fig.3.4.3 Average output power at 1342 nm with respect to the incident pump power in cw and Q-switching operation

However, the pulse trains of InGaAsP would become unstable above 8W of incident pump power in CW operation. In order to compare the AlGaInAs and InGaAsP quantum well saturable absorber, we took the pulse operation with 200/800μs for analysis of pulse energy and pulse peak power. Figure3.4.4 shows the pulse energy versus the incident pump power. The pulse energy increases with the pump power from 23 to 31μJ.   Obviously, the pulse energy of AlGaInAs SESA is

larger than that of InGaAsP SESA.
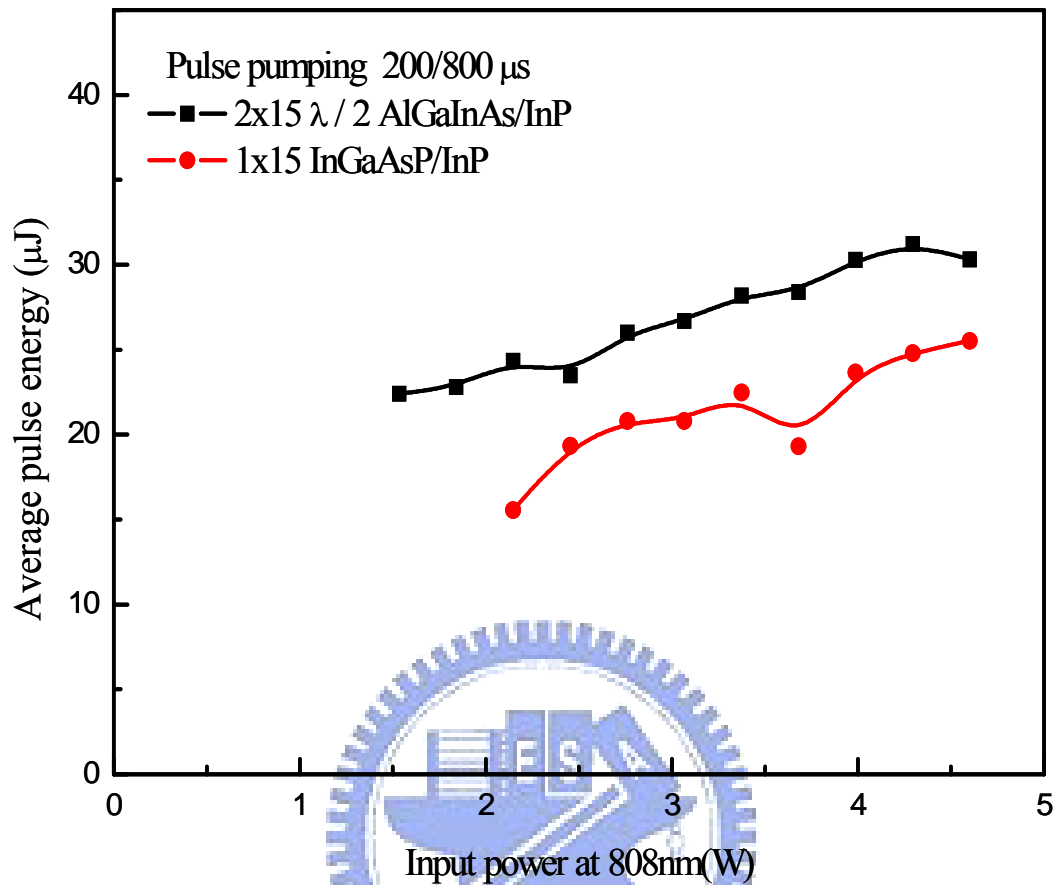
Fig.3.4.4 Experimental result for the pulse energy with respect to the pump power under pulse

It was believed that the higher conduction band offset of AlGaInAs can prevent carrier leakage at high temperatures and therefore have higher temperature stability than InGaAsP. Figure 2.4.5 shows the peak output power with respect to the incident pump power under pulse pumping operation. The pulse with of the AlGaInAs and InGaAsP were both from 17 ns to 23ns such that the peak power can be achieved to 1.0-1.6 kW. The pulse temporal behavior was recorded by a LeCroy digital oscilloscope (Wavepro 7100, 10 G samples/sec, 1 GHz bandwidth) with a fast p-i-n photo diode.   A typical oscilloscope trace of a train of output pulses and an expanded shape of a single pulse are shown in Fig. 2.4.6. Under the optimum alignment condition of AlGaInAs saturable absorber, the pulse-to-pulse amplitude fluctuation was found to be within ±5%. The pulse width was measured to be 19 ns.
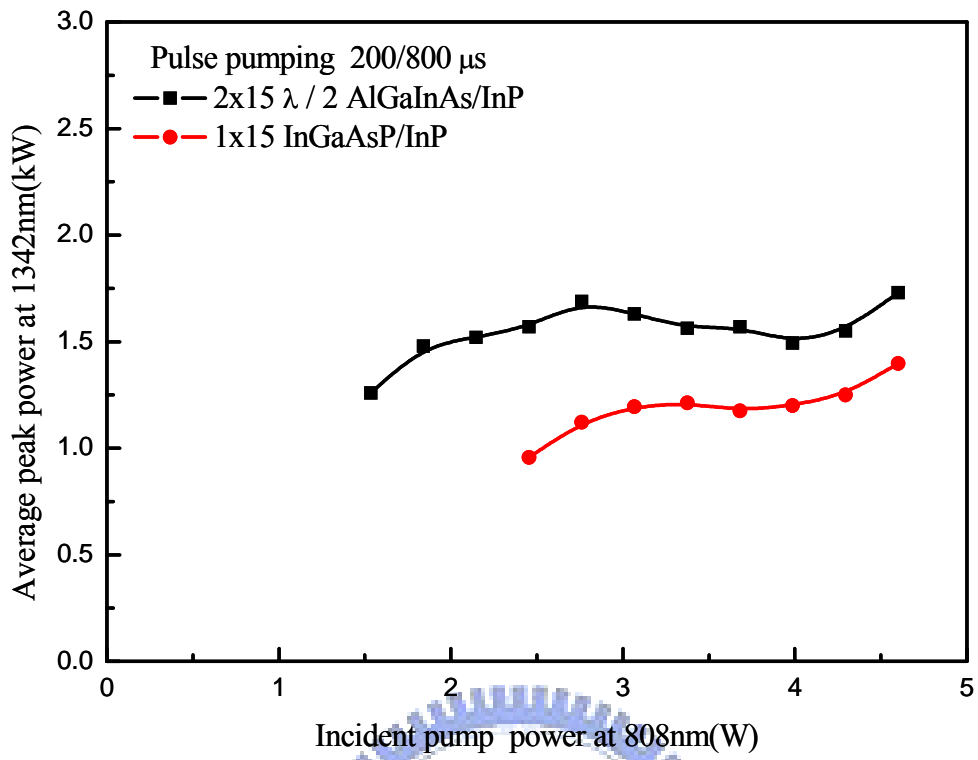
Fig3.4.5 Experiment result for peak power with respect to pump power under pulse pumping
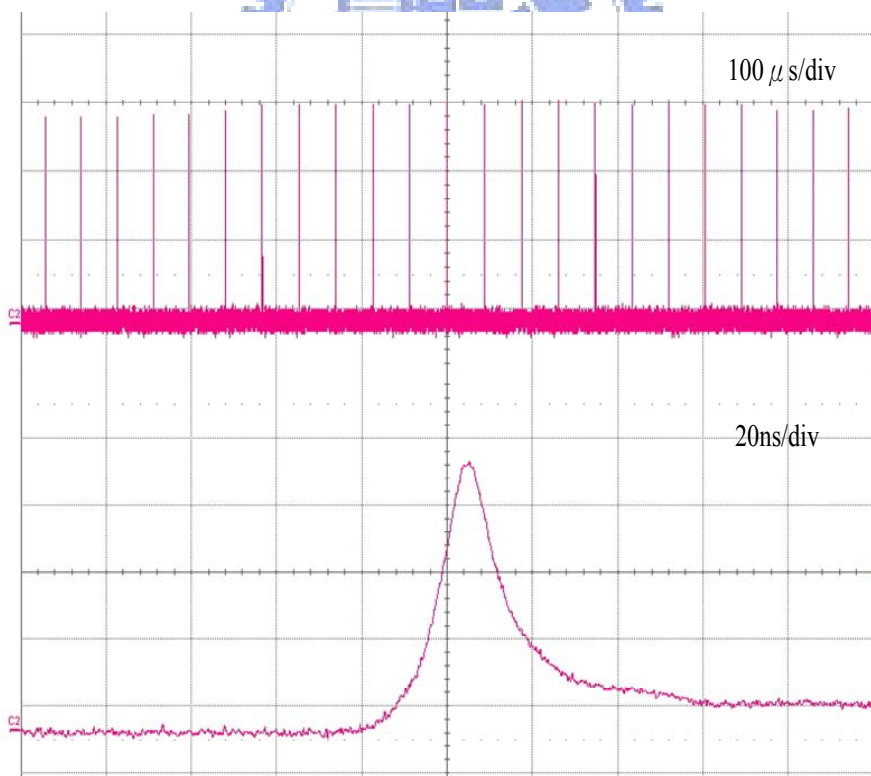
Fig.3.4.6 (a) Typical oscilloscope trace of a train of output pulses and (b) expanded shape of a

single pulse

3.4.3 Conclusion

The AlGaInAs QW/barrier structure grown on a Fe-doped substrate was used as a saturable absorber for the Q-switching of a diode-pumped Nd:YVO$_4$ laser operating at 1342 nm. An average output power of 1.53W was obtained at an incident pump power of 1.4W and Q-switching efficiency of 45% was higher than that of InGaAsP.   The present result indicates the temperature stability of AlGaInAs is better than InGaAsP such that AlGaInAs based SESA is promising candidate to develop high-performance Nd-doped 1.34μm passively Q-switched laser.

3.5. Summary

In this chapter, we have demonstrated a periodic AlGaInAs QW/barrier structure grown on a Fe-doped substrate was developed to be a saturable absorber with large absorption cross section, large modulation depth, and high damage threshold in diode-pumped Nd:YVO$_4$ laser operating at 1064 nm.   The barrier layers play a role not only to confine the carriers but also to locate the QW groups in the region of the nodes of the lasing standing wave to avoid damage.   Stable Q-switched pulses of 0.9 ns duration with an average output power of 3.5 W and a repetition rate of 110 kHz were obtained at an incident pump power of 13.5 W.

On the other hand, we also have demonstrated AlGaInAs QW/barrier structure grown on a Fe-doped substrate as a saturable absorber for the Q-switching of a diode-pumped Nd:YVO$_4$ laser operating at 1342 nm. Compared with InGaAsP, AlGaInAs have larger conduction band offset which can reduce carrier leakage and get higher temperature stability.   Therefore, AlGaInAs based SESA is promising candidate to develop high-performance Nd-doped 1.34μm passively Q-switched laser.
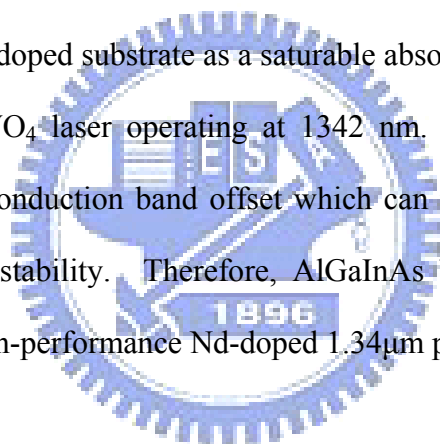
Chapter Four

Semiconductor saturable absorber (SESA) for mode-locked laser

4.1 Introduction

Ultra-short pulses are generated using mode-locked lasers and are defined as having a pulse duration of a few tens of picoseconds at the very most. De Maria *et al.* [1] produced the first ultrashort pulses just six years after Maiman's first laser was demonstrated.   Employing this technique, which phase-locks the longitudinal modes of the laser, the pulse width is inversely related to the bandwidth of the laser emission

Consider a laser cavity with many axial modes of distance $\delta\omega = c/2L$, where L is the cavity length and c is the speed of light. All the modes inside the gain-bandwidth of the laser material can oscillate, given that they reach the threshold. The emitted electrical field is a superposition of the contribution of each mode:

$$E(t) = \sum_{k=-(n-1)/2}^{+(n-1)/2} E_k(t)\, \exp\,\{i[2\pi(\omega_0 + k\delta\omega)t + \Phi_k]\} \tag{1}$$

Here, ω_0 denotes the center frequency (i.e., the frequency of the central axial mode), $E_k(t)$ and Φ_k refer to the amplitude and the phase of mode k, respectively. Generally, as each mode is subject to random fluctuations, its phase Φ_k is not correlated to that of the adjacent modes. Both the electrical field E(t) and the intensity I(t) are statistically varying functions of time, incoherent and without regular temporal structure. If it can be arranged that all the modes oscillate in phase, i.e., in the case of $\Phi_k - \Phi_{k-1} = \Delta\Phi =$ const., then the resulting electrical field becomes a temporally well-defined periodic function of time. When considering n oscillating axial modes with constant phase difference $\Delta\Phi$ and the same amplitude E_0, (1) yields

$$\frac{E(t)}{E_0} = \sum_{k=-(n+1)/2}^{+(n+1)/2} \exp(i \cdot \omega_0 \cdot t) \cdot \exp(i \cdot k \cdot \delta\omega \cdot t) = \exp(i \cdot \omega_0 \cdot t) \cdot \frac{\sin(\frac{n \cdot \delta\omega \cdot t}{2})}{\sin(\frac{\delta\omega \cdot t}{2})} \qquad (2)$$

It can be described by a train of short pulses, temporally spaced by the cavity roundtrip time $\tau_p = 1/\delta\omega = 2L/c$. In this way, the superposition of the electrical field of all the phase-locked axial cavity modes can be explained by a single optical pulse, circulating inside the cavity. After each roundtrip, i.e., after the time τ_p, a certain fraction of the circulating pulse is ejected from the cavity and a periodic signal with repetition rate $\nu_{rep} = 1/\tau_p$ can be detected. It can be seen from (2) that the pulse duration $\Delta\tau_p$ is getting shorter when the number of locked modes increases. From the same equation, $\Delta\tau_p$ can be estimated as

$$\Delta\tau_p = \frac{\tau_p}{n} = \frac{1}{\nu_{rep}} \cdot \frac{1}{n} \qquad (3)$$

Assuming that all axial modes inside a rectangular gain profile of the laser medium can be coupled together, the pulse duration can finally be approximated by

$$\Delta\tau_p \; ; \; \frac{1}{\Delta\omega} \qquad (4)$$

where $\Delta\omega$ is the line width of the laser transition, i.e., the width of the gain profile Therefore, a laser medium with a large gain-bandwidth is required for the generation of ultrashort laser pulses. In single axial mode operation, the laser can generate either continuous-wave (cw) or pulsed output, in the case when Q-switching is employed. Accordingly, phase locking of the axial modes can either lead to CW mode locking or Q-switched mode locking, where the train of mode-locked ultrashort pulses is additionally modulated by a superposed Q-switched process. For the generation of ultrashort pulses of high stability, the laser is typically operated in the regime of CW mode locking. However, depending on the actual method of mode locking applied,

the tendency for Q-switched mode locking cannot be eliminated completely.

The different techniques for mode locking are classified in two main categories, active and passive mode locking. Active mode locking generally refers to the case where the radiation in the laser cavity is actively modulated by an external signal with a repetition rate matched to the cavity roundtrip time. In the passively mode locking, the radiation itself in combination with an intra-cavity nonlinear device provides the necessary modulation.

Passive mode locking generally implies the insertion of a saturable absorption inside the cavity, which, in the most general case, is an element that generates high losses at low intensities and low losses at high intensities. Today, most commercial passive mode locked cw lasers is based on the saturable absorption in semiconductors. In these devices, multiple quantum-well (MQW) structures provide a resonant nonlinear absorption at the laser wavelength. The nonlinear element comprises a thin multilayer quantum well structure monolithically embedded between two reflective surfaces forming a Fabry–Perot resonator. Absorbed energy from the pulse causes carrier recombination in the quantum wells that leads eventually to absorption bleaching. The combination of the saturable absorber and mirror surfaces causes the reflectivity of the device to increase with increasing intensity.   The advantage of a SESAM lies in the inherent simplicity, the device essentially replaces the rear mirror of the laser resonator.

In this chapter, we demonstrate the continuous-mode-locked Nd:YVO$_4$ laser at 1342 nm by using AlGaInAs semiconductor saturable absorber.

4.2 Motivation and background

Diode-pumped solid-state lasers at 1.3μm have a wide variety of applications such as telecommunication, fiber sensing, ranging, and data storage. As a potentiality, numerous Nd-doped crystals have been employed for developing 1.3-μm lasers at continuous-wave (cw) or pulsed operation [1-6]. Passive mode locking with GaAs-based semiconductor saturable absorber mirrors (SESAM) has been extensively used for the generation of ultra-short pulses in the 0.8−1.1-μm spectral range [7,8]. However, it is rather difficult to design InGaAs SESAMs for 1.3-μm lasers because the required indium concentrations are beyond the critical strain-thickness limit. So far, two new schemes based on the GaAs substrate have been exploited to design SESAMs near 1.3 μm and 1.5 μm. One approach is the use of the quaternary alloy GaInNAs quantum wells (QWs) with low nitrogen concentrations in the active region [9-11]; the other technique is the use of the InAs/GaAs quantum-dot (QD) multilayer structures [12]. Nevertheless, the characteristic of the GaInNAs QWs is subject to drastic bandgap blue-shift when exposed to annealing. On the other hand, the epi-wafer of the InAs QDs usually suffers from the uniformity of optical characteristics. Therefore, it is highly desirable to develop a superior saturable absorber for passively mode-locked lasers in the 1.3−1.6-μm spectral range.

Since the quaternary alloys of InGaAsP and AlGaInAs can be grown epitaxially on an InP substrate without lattice mismatch in the 0.84-1.65μm spectral region, they have been confirmed to be promising materials for optoelectronic devices [13, 14]. The InGaAsP QWs have been used as saturable absorbers in Q-switched lasers at 1.34 μm [15, 16] and mode-locked lasers at 1.55 μm [17]. Compared with InGaAsP materials, the AlGaInAs quaternary alloy with a larger conduction band offset can provide a better electron confinement covering the same wavelength region [18, 19]. Although AlGaInAs/InP QWs have been designed to passively Q-switch lasers at

1.06-μm and 1.56-μm [20, 21], they have not yet been exploited to mode-lock a laser.

In this chapter, we design and fabricate AlGaInAs QWs to be a saturable absorber in a diode-pumped Nd:YVO$_4$ laser at 1.34 µm. With an incident pump power of 13.5W, we obtain an average output power of 1.05W with a stable continuous-mode-locked pulse train at a repetition rate of 152MHz. The pulse duration is found to be approximately 26.4 ps.

4.3. Diode-pumped 1342-nm NdYVO$_4$ passively mode-locked laser

4.3.1 Device fabrication and experiment setup

The AlGaInAs QWs, used as a saturable absorber in a mode-locked 1.34µm laser, was grown on Fe-doped InP substrate by metal organic chemical-vapor deposition (MOCVD). Instead of the conventional S-doped InP substrate, a Fe-doped InP substrate was used because it almost has no absorption for the light wavelength greater than 940 nm. Since the Fe-doped InP substrate is transparent at 1.34 µm, the function of the distributed Bragg reflector in the SESAMs device can be replaced by an external mirror. The saturable absorber is formed by two AlGaInAs QWs with the band-gap wavelength near 1.34 µm, spaced at quarter-wavelength intervals by AlGaInAs barrier layers. The backside of the substrate was mechanically polished after growth. The both sides of the SESA were coated for antireflection (AR) at 1.34 µm to reduce the couple cavity effects. Unlike for the saturable absorber based on InAs/GaAs QDs [12], the peak wavelength of the photoluminescence spectrum for AlGaInAs QWs almost does not vary with the position of the wafer. In other words, the uniformity of the optical property of AlGaInAs QWs is significantly superior to that of InAs/GaAs QDs. The initial transmission of the SESA device at the wavelength of 1.34 µm was measured to be approximately 97.5%. Figure 4.3.1

shows the transmittance spectrum at room temperature for the AR-coated AlGaInAs/InP saturable absorber. The total non-saturable loss introduced by the SESA was found to be less than 0.7%. According to the experimental results, the saturation fluence is estimated to be in the range of 20 $\mu J/cm^2$ and a modulation depth is about 1.8%.
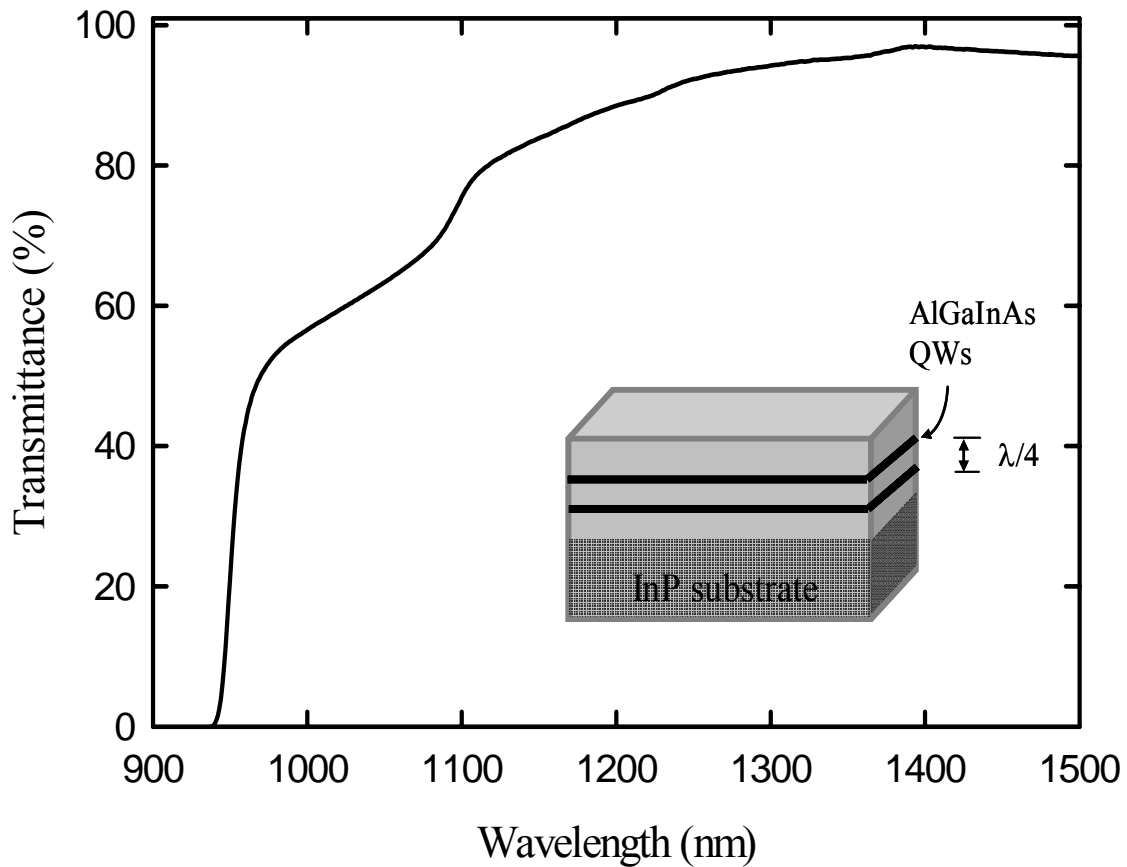
Fig.4.3.1. Transmittance spectrum at room temperature for the AR-coated AlGaInAs saturable absorber. Inset: schematic diagram of the AlGaInAs QW structure, where   is the value of lasing wavelength.

Figure 4.3.2 depicts the experimental configuration for a continuously mode-locked 1.34 μm Nd:YVO$_4$ laser with AlGaInAs QWs as a saturable absorber. The gain medium was a 0.3 at.% Nd:YVO$_4$ crystal with a length of 9 mm. Both sides of the laser crystal were coated for AR at 1.34 μm (R<0.2%) and a wedge-cut angle 0.5^o. The laser crystal was wrapped with indium foil and mounted in a

water-cooled copper block and the water temperature was maintained at 20°C.
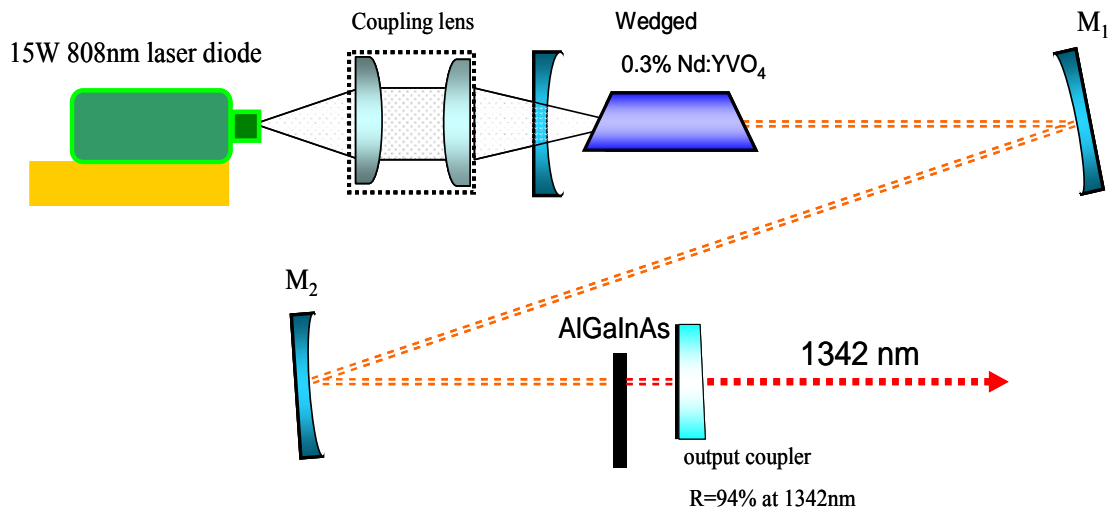
Fig. 4.3.2. Schematic of a diode-pumped self-starting continuous-mode-locked Nd:YVO$_4$ laser at 1342nm. LD, laser diode

The pump source was a 16-W fiber coupled laser diode at 808 nm with a core diameter of 800 μm and a numerical aperture (N.A.) of 0.16. Focusing lenses with 17.5-mm focal length and 85% coupling efficiency were used to reimage the pump beam into the laser crystal. The pump spot radius was approximately 350 μm. The laser cavity consisted of one input mirror; two high-reflection (HR) concave mirrors, M1 and M2, at lasing wavelength (R>99.8%); and an output coupler with reflectivity of 94% and a wedge-cut angle of 2°. The input mirror was a 500-mm radius of curvature concave mirror with an AR coating at 808 nm (R<0.2%) on the entrance face, a HR coating at the lasing wavelength (R>99.8%), and a high-transmission (HT) coating at 808nm (T>90%) on the other face. Note that the laser crystal as placed closed to the input mirror for spatial overlap of the transverse mode structure and radial pump power distribution. The radii of curvature of mirror M1 and M2 were 500 mm and 100 mm, respectively. M1 and M2 were separated by 600 mm; the overall cavity length was approximately 100 cm. The laser mode radii were 350 μm inside the laser crystal and 50 μm on the QW saturable absorber.

4.3.2 Experimental result and discussion

Prior to performing the mode-locked operation, we first studied the cw performance for the laser system with different reflectivity of 92%, 94%, 96%, and 98% at 1342 nm.   The optimum reflectivity of the output coupler was found to be 94%.   Figure 3.3.3 depicts the average output power at 1342 nm with respect to the incident pump power in cw operation and in cw mode-locked operation.
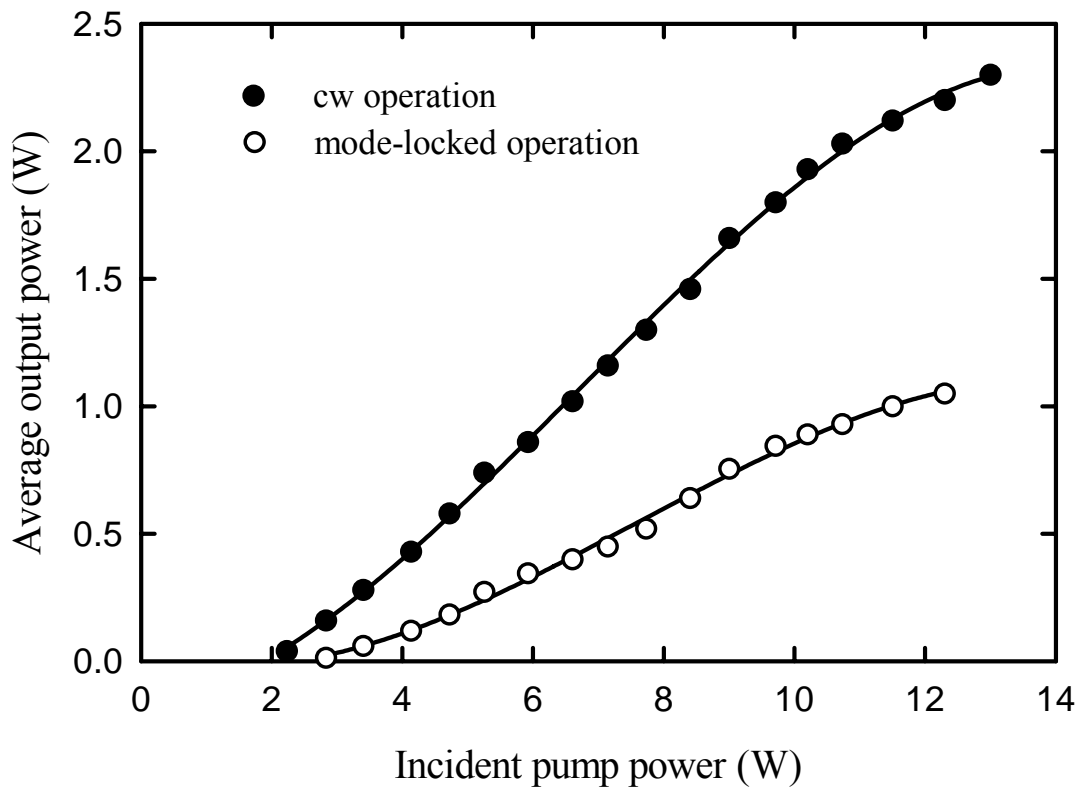
Fig. 4.3.3 Average output power at 1342nm versus incident pump power in cw and mode locked operations.

In the cw regime the laser had a slope efficiency of 21.4%; the output power reached 2.3W at an incident pump power of 13W.   With a AlGaInAs QWs saturable absorber, the laser self-started the cw mode-locked operation at pump powers greater than 4.5 W.   Experimental results revealed that the stable cw mode locking could be realized within the range of the pump power from 4.5 W to 12.3 W.   As shown in Fig. 4.3.3, the laser had a slope efficiency of 11%; the output power reached 1.05 W at an

incident pump power of 12.3 W.   If the pump power was increased beyond 12.3 W, the mode-locked pulse train exhibited unstable behavior because of the thermal effects. It is worth noting that we did not observe any optical damage in the AlGaInAs saturable absorber during the experiment.

The cw mode-locked pulse train was recorded by a LeCroy digital oscilloscope (Wavepro 7100; 10 G sample/s, 1 GHz bandwidth) with a fast p-i-n photo-diode. Figure 4.3.4(a) shows a typical pulse train of the cw mode-locked laser.   It can be seen that the pulse period of 6.6 ns is consistent with the round-trip time of the cavity length.

20ns/div
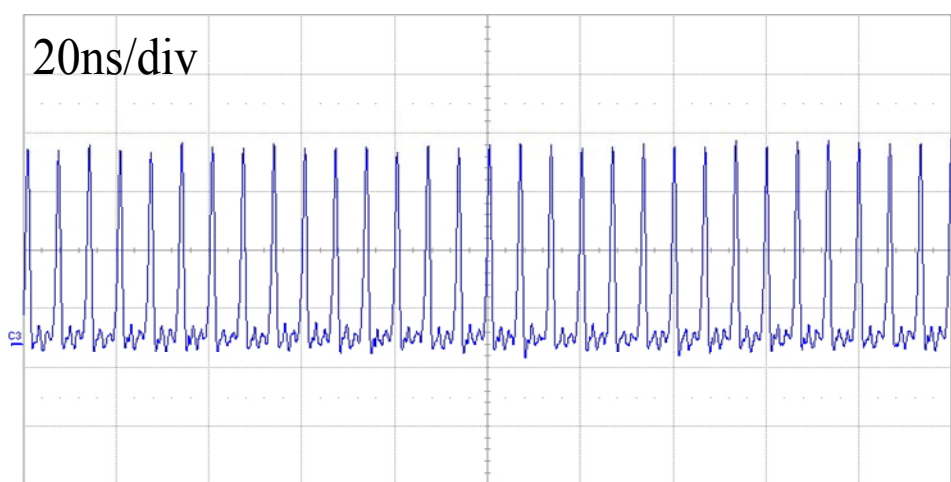
Fig. 4.3.4. (a) Typical oscilloscope trace of a train of mode-locked output pulses;

The pulse duration at the cw mode-locked operation was measured with an autocorrelator (APE pulse check, Angewandte physik & Elektronik GmbH).   With the Gaussian fitted profile, the pulse duration was found to be approximately 26.4 ps, as shown in Fig. 4.3.5.   The spectral properties of the laser were monitored by an optical spectrum analyzer (Advantest Q8347) with a resolution of 0.005 nm.   The spectral bandwidth (FWHM) was found to be 0.12 nm.   This result indicates a time-bandwidth product of 0.48.   The narrower bandwidth might arise from the etalon effect of the thin AlGaInAs QWs device.   It is expected that the etalon effect

can be effectively reduced by use of a high-quality AR coating on the both surface of the InP wafer.

pulse width ~26.4 ps

37 ps
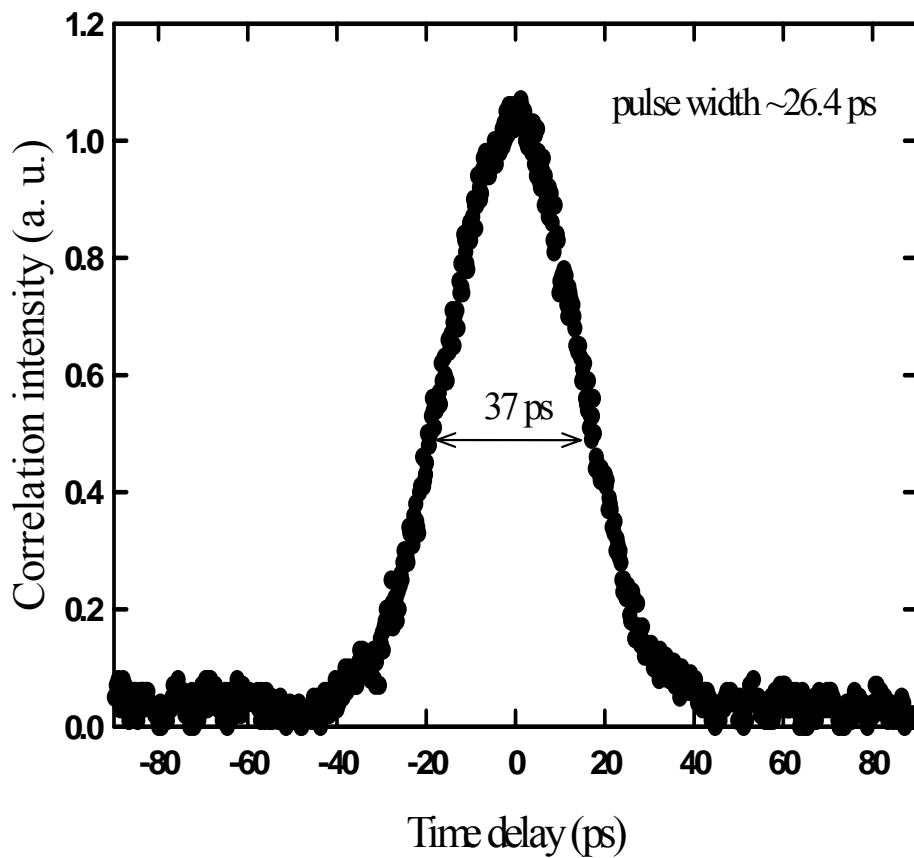
Fig. 4.3.5 Autocorrelation trace of the output pulses.

4.4. Summary and conclusion

We have designed AlGaInAs QWs grown on the Fe-doped InP substrate to be a saturable absorber for self-starting continuous-mode-locked Nd:YVO$_4$ laser at 1342 nm. Stable mode-locked pulses of 26.4 ps duration with a repetition rate of 152 MHz were generated within the range of incident pump power from 4.5 W to 12.3 W. The average output power for the cw mode-locked operation was 1.05 W at an incident pump power of 12.3 W. The present result confirms that the AlGaInAs QWs structures can be utilized to be saturable absorbers for the passively mode-locked lasers in the spectral region near 1.3 μm.

Chapter Five

Summary and future works

A periodic AlGaInAs QW/barrier structure grown on a Fe-doped substrate was used to not only be a saturable absorber for the 1064nm and 1342nm passively Q-switched and mode-locked lasers but also to be a gain medium for the 1360nm and 1570nm optically-pumped semiconductor lasers.

In passively Q-switched lasers, we have demonstrated that the AlGaInAs QWs based SESA is promising candidate to develop high-performance Nd-doped passively Q-switched laser. Compared with InGaAsP, AlGaInAs have larger conduction band offset which can reduce carrier leakage and get higher temperature stability. And the barrier layers play a role not only to confine the carriers but also to locate the QW groups in the region of the nodes of the lasing standing wave to avoid damage. Therefore, in 1.06μm PQS laser , stable Q-switched pulses of 0.9 ns duration with an average output power of 3.5 W and a repetition rate of 110 kHz were obtained at an incident pump power of 13.5 W. The remarkable performance confirms the prospect of using AlGaInAs QWs as saturable absorbers in solid-state lasers.

In passively mode-locked lasers, we have designed AlGaInAs QWs grown on the Fe-doped InP substrate to be a saturable absorber for self-starting continuous-mode-locked Nd:YVO$_4$ laser at 1342 nm. Stable mode-locked pulses of 26.4 ps duration with a repetition rate of 152 MHz were generated within the range of incident pump power from 4.5 W to 12.3 W. The average output power for the cw mode-locked operation was 1.05 W at an incident pump power of 12.3 W.

In optically-pumped semiconductor lasers, we have demonstrated the periodic AlGaInAs QW/barrier structure grown on an Fe-doped InP transparent substrate was

developed to be a gain medium in a room-temperature high-peak-power nanosecond laser at 1.36μm and 1.57μm. The quantum wells are separated by half-wavelength thick AlGaInAs barriers and designed to be located at the antinodes of the intra-cavity standing wave field to enhance the interaction between a standing wave optical field and an active medium. The maximum peak power was achieved 1.2kW and 290 W at 1.36μm and 1.57μm, respectively. For power scaling up, we also have demonstrated an optically pumped high-peak-power AlGaInAs/InP eye-safe laser by in-well pumping scheme. The conversion efficiency is enhanced over three times compared with barrier pumping scheme. Double gain chips were used to increase the absorption efficiency of pump laser and maximum output power and peak power was up to 300mW and 0.52kW. For optically-pumped semiconductor lasers, the performance of AlGaInAs quantum wells grown on InP substrate without DBR has been studied through many ways. We tried to analysis the effect of temperature, pumping spot size, different actively Q-switched frequency (or different duty cycle), different cavity setup (cavity length, output coupler) and improved the performance of AlGaInAs quantum well laser in the room-temperature.

In the future, we will try to deal with the thermal problems of optically-pumped semiconductor laser such that the OPSLs can be operated in the cw-mode. The ways to deal with the heat of OPSLs are substrate removal and bonding a heat-spreader to the semiconductor gain chip. Furthermore, we will also try to develop the 1.2μm and 660 nm (red) optically-pumped semiconductor laser.

In addition to be the saturable absorber and gain medium, many physical phenomena can be observed in semiconductor. Some topics like Rabi oscillation, slow light, PL spectrum, and exciton-polariton in semiconductor microcavity are interesting and important to understand the dynamic of the carrier in the semiconductor.

Reference

Reference (Chapter one)

[1]W. Koechner, "Solid-state laser engineering," 6th ISBN 0-387-29094-x, Springer-Verlag (1996)

[2]J.T. Verdeyen, "Laser Electronics," 3th ,ISBN:0-13-706666-X. ,Prentice Hall, (2000)

Reference (Chapter Two)

[1] M.Kuzetsov, F. Hakimi, R.Sprague, A. Mooradian,"Design and Characteristics of high-power(>0.5W CW) diode-pumped vertical-external-cavity surface-emitting semiconductor lasers with circular TEM$_{00}$ Beams." IEEE J.Sel. Top. Quanutm Electron, **5**, 561, (1999)

[2] M.Kuzetsov, F. Hakimi, R.Sprague, A. Mooradian, "High power(>0.5W CW) Diode pumped vertical external cavity surface emitting semiconductor laser with circular TEM00 Beam." IEEE Photonics Tech Lett, **9**,1064-1065 (1997)

[3] A.C. Tropper, H.D. Foreman, A.Granache, K.G. Wilcox and S. Hoogland, "Vertical-external-cavity semiconductor lasers." J Phys D, **37**, 75-85, (2004)

[4] U. Keller, A.C. Tropper, "Passively mode-locked surface-emitting semiconductor lasers." Phys. report **429** , 67-120 (2006)

[5] A.C. Tropper and Hoogland, "Extended cavity surface-emitting semiconductor lasers." Prog. Quantum. Electron **.30**, 1-43, (2006)

[6] M.Y.A. Raja, S.R.J Brueck, M Osinski, CF Schaus et al, "Resonant periodic gain surface-emitting semiconductor lasers"., IEEE J. Quantum Electron. **25**, 1500–1512 (1989)

[7] Li Fan, J Hader, M Schillgalies, M Fallahi, .R. Zakharian J.V. Moloney R. Bedford J.T. Murray S.W. Koch W. Stolz, "High-power optically pumped VECSEL using a double-well resonant periodic gain structure." IEEE Photo.Tech.

Let.**17**, 1764-1766 **,** (2005)

[8] A.Bousseksou, S. Bouchoule, M. Kurdi .etc "Fabrication and characterization of 1.55μm single tranverse mode large diameter electrically pumped VECSEL" Opt Quantum Electronic , **38** ,1269-1278(2006)

[9] A. Garnache, A. A. Kachanov, F. Stoeckel, and R. Houdré, "Diode-pumped broadband vertical-external-cavity surface-emitting semiconductor laser applied to high-sensitivity intracavity absorption spectroscopy," J. Opt. Soc. Am. B **17**, 1589-1598 (2000)

[10]G. B. Kim, J.Y. Kim, J. Lee, J. Yoo, K.S. Kim, S.M. Lee, S. Cho, S.J. Lim, T. Kim, and Y. Park, **"**End-pumped green and blue vertical external cavity surface emitting laser devices." Appl. Phys. Lett. **89**, 181106 (2006)

[11] J.E. Hastie, L.G. Morton, A.J. Kemp, and M.D. Dawson, A.B. Krysa and J.S. Roberts, **"**Tunable ultraviolet output from an intra-cavity frequency-doubled red vertical-external-cavity surface-emitting laser," Appl. Phys. Lett. **89**, 061114 (2006)

[12] J. Rautiainen, A. Härkönen, V.-M. Korpijärvi, P. Tuomisto, M. Guina, and O. G. Okhotnikov, "2.7 W tunable orange-red GaInNAs semiconductor disk laser," Opt. Express 15, 18345-18350 (2007)

[13] M. Fallahi, L. Fan, Y. Kaneda, C. J. Hader, H. Li, J. V. Moloney, B. Kunert, W. Stolz, S. Koch, J. Murray, R. Bedford, "5 W yellow laser by intra-cavity frequency doubling of high-power vertical external-cavity surface-emitting laser," IEEE Photon. Technol. Lett. *20,* pp. 1700-1702, (2008)

[14] Hans Lindberg, Anders Larsson, and Martin Strassner, "Single-frequency operation of a high-power, long-wavelength semiconductor disk laser," Opt. Lett. 30, 2260-2262 (2005)

[15] Peter Klopp, Florian Saas, Martin Zorn, Markus Weyers, and Uwe Griebner,

"290-fs pulses from a semiconductor disk laser," Opt. Express **16**, 5770-5775 (2008)

[16] A. Aschwanden, D. Lorenser, H. J. Unold, R. Paschotta, E. Gini, and U. Keller, "2.1-W picosecond passively mode-locked external-cavity semiconductor laser," Opt. Lett. **30**, 272-274 (2005)

[17] O. Casel, D. Woll, M.A. Tremont, H. Fuchs, R.Wallenstein, E. Gerster, P. Unger, M. Zorn and M. Weyers, "Blue 489-nm picosecond pulses generated by intra-cavity frequency doubling in a passively mode-locked optically pumped semiconductor disk laser" Appl. Phys. B **81**, 443–446 (2005)

[18] J. Lee , J. Kim , S. Lee , J. Yoo , K. S. Kim , S. Cho , S. J. Lim , G. B. Kim , S. Hwang , T. Kim and Y. Park, "9.1-W high-efficient continuous-wave end-pumped vertical-external-cavity surface-emitting semiconductor laser," IEEE Photon. Technol. Lett., **18**, pp. 2117, (2006).

[19] K. S. Kim, J. R. Yoo, S. H. Cho, S. M. Lee, S. J. Lim, J. Y. Kim, J. H. Lee, T. Kim, Y. J. Park, "1060 nm vertical-external-cavity surface-emitting lasers with an optical-to-optical efficiency of 44% at room temperature," Appl. Phys. Lett. 88, 091107 (2006)

[20] J. E. Hastie , J.-M. Hopkins , S. Calvez , C. W. Jeon , D. Burns , R. Abram , E. Riis , A. I. Ferguson and M. D. Dawson, "0.5-W single transverse-mode operation of an 850-nm diode-pumped surface-emitting semiconductor laser," IEEE Photon. Technol. Lett., **15**, pp. 894, (2004)

[21] S. Lutgen, T. Albrecht, P. Brick, W. Reill, J. Luft, and W. Spath, "8-W high-efficiency continuous-wave semiconductor disk laser at 1000 nm," Appl. Phys. Lett. **82**, 3620 (2003).

[22] H. Lindberg, M. Strassner, E. Gerster, and A. Larsson, "0.8 W optically pumped vertical external cavity surface emitting laser operating CW at 1550 nm,"

Electron. Lett., **40**, 601-602, (2004)

[23] H. Lindberg, M. Strassner, M. Bengtsson,and A. Larsson "High power optically pumped 1550nm VECSEL with a bonded silicon heat spreader", IEEE Photonics Technol. Lett, May 200

[24] J.M. Hopkins, N. Hempler, B. Rösener, N. Schulz, M. Rattunde, C. Manz, K. Köhler, J. Wagner, and D. Burns, "High-power, (AlGaIn)(AsSb) semiconductor disk laser at 2.0 μm," Opt. Lett. **33**, 201-203 (2008)

[25] J.-M. Hopkins, A. J. Maclean, D. Burns, E. Riis, N. Schulz, M. Rattunde, C. Manz, K. Köhler, and J. Wagner, "Tunable, Single-frequency, Diode-pumped 2.3μm VECSEL," Opt. Express **15**, 8212-8217 (2007)

[26] Nils Hempler, John-Mark Hopkins, Alan J. Kemp, Nico Schulz, Marcel Rattunde, Joachim Wagner, Martin D. Dawson, and David Burns, "Pulsed pumping of semiconductor disk lasers," Opt. Express **15**, 3247-3256 (2007)

[27] B. Rudin, A. Rutz, M. Hoffmann, D. J. H. C. Maas, A.-R. Bellancourt, E. Gini, T. Südmeyer, and U. Keller, "Highly efficient optically pumped vertical-emitting semiconductor laser with more than 20 W average output power in a fundamental transverse mode," Opt. Lett. **33**, 2719-2721 (2008)

[28] A.R. Zakharian, J. Hader, J.V. Moloney, S.W. Koch, and S. Lutgen, "Experimental and theoretical analysis of optically pumped semiconductor disk lases," Appl Phys Lett. **83**, pp.1313-1315,(2003)

[29] A. J. Kemp, G. J. Valentine, J.M. Hopkins, J. E. Hastie, S. A. Smith, S. Calvez, M. D. Dawson, and D. Burns, "Thermal managenemt in vertical-external-cavity surface-emitting lasers: Finite-element analysis of a heat-spreader approach," IEEE J. Quantum. Electron. **41**, 148-155 (2005).

[30] R. G. Bedforda, M. Kolesikb, J. L. A. Chillac, M. K. Reedc, T. R. Nelsona, J. V. Moloney, "Power-limiting mechanisms in VECSELs," Proc. of SPIE. **5814**

199-208, (2005)

[31] A. J. Kemp, A.J. Maclean, J. E. Hastie, S. A. Smith, J.M. Hopkins, S. Calvez, G. J. Valentine, M. D. Dawson and D. Burns, " Thermal lensing, thermal management and transverse mode control in microchip VECSELs." Appl. Phys. B **83**, 189–194 (2006)

[32] H. Lindberg, M.Strassner, J. Bengtsson and A. Larsson, "InP-based optically pumped VECSEL operating CW at 1550nm," IEEE Photon Technol. Lett, **16**, pp.362-364, (2004).

[33] H. Lindberg, M. Strassner, E. Gerster, J. Bengtsson, and A. Larsson, "Thermal management of optically pumped long-wavelength InP-based semiconductor disk lasers," IEEE J. Sel. Topics Quantum Electron.,**11**, 1126-1134 (2005)

[34]J. P. Tourrenc, S. Bouchoule, A. Khadour, J. Decobert, A. Miard, J. C. Harmand, and J. L. Oudar, "High-Power RT CW Operation of an OP-VECSEL at 1.56 μm with Hybrid Metallic-Metamorphic Mirrors," in *CLEO/Europe and IQEC 2007 Conference Digest*, , paper CB1_3. (Optical Society of America, 2007)

[35] Jussi Rautiainen, Jari Lyytikäinen, Alexei Sirbu, Alexandru Mereuta, Andrei Caliman, Eli Kapon, and Oleg G. Okhotnikov, "2.6 W optically-pumped semiconductor disk laser operating at 1.57-μm using wafer fusion," Opt. Express **16**, 21881-21886 (2008)

[36] Jari Lyytikäinen, Jussi Rautiainen, Lauri Toikkanen, Alexei Sirbu, Alexandru Mereuta, Andrei Caliman, Eli Kapon, and Oleg G. Okhotnikov, "1.3-μm optically-pumped semiconductor disk laser by wafer fusion," Opt. Express **17**, 9047-9052 (2009)

Reference (2.2)

[1] A.S. Grabtchikov, A.N. Kuzmin, V.A. Lisinetskii, V.A. Orlovich, A.A. Demidovich, K.V. Yumashev, N.V. Kuleshov, H.J. Eichler, and M.V. Danailov, "

Passively Q-switched 1.35 μm diode pumped Nd:KGW laser with V:YAG saturable absorber" Opt.Mater. **16**, 349 (2001).

[2]. R. Fluck, R. Häring, R. Paschotta, R. Gini, H. Melchior, and U. Keller,"Eyesafe pulsed microchip laser using semiconductor saturable absorber mirrors," Appl. Phys. Lett. **72**, 3273 (1998).

[3]. R.D. Stultz, V. Leyva, and K. Spariosu, "Short pulse, high-repetition rate, passively *Q*-switched Er:yttrium-aluminum-garnet laser at 1.6 microns," Appl. Phys. Lett. **87**, 241118 (2005).

[4]. V. G. Savitski, N. N. Posnov, P. V. Prokoshin, A. M. Malyarevich, K. V. Yumashev, M. I. Demchuk, and A.A. Lipovski," PbS-doped phosphate glasses saturable absorbers for 1.3-μm neodymium lasers," Appl. Phys. B **75**, 841 (2002).

[5]. D. L. Spies, "Highly efficient neodymium:yttrium aluminum garnet laser end pumped by a semiconductor laser array," Appl. Phys. Lett. **47**, 74 (1985).

[6]. M. Kuznetsov, F. Hakimi, R. Sprague, and A. Mooradian, "Design and characteristics of high-power(>0.5-W)diode-pumped vertical-external-cavity surface-emitting semiconductor lasers with circular TEM00 beams," IEEE J. Sel. Topics Quantum Electron. **5**, 561 (1999).

[7]. A. C. Tropper, H. D. Foreman, A. Garnache, K. G. Wilcox, and S. H. Hoogland, "Vertical-external-cavity semiconductor lasers," J. Phys. D **39**, R74 (2004).

[8]. M. Kondow, K. Uomi, A. Niwa, T. Kitatani, S.Watahiki, and Y. Yazawa," GaInNAs: a novel material for long-wavelength-range laser diodes with excellent high-temperature performance" Jpn. J. Appl. Phys. Part 1 **35**,1273 (1996).

[9]. J. M. Hopkins, S. A. Smith, C. W. Jeon, H. D. Sun, D. Burns, S. Calvez, M. D. Dawson, T. Jouhti, and M. Pessa, "0.6 W CW GaInNAs vertical external-cavity surface emitting laser operating at 1.32 μm," Electron. Lett. **4**, 30 (2004).

[10]. R. Fluck, R. Häring, R. Paschotta, R. Gini, H. Melchior, U. Keller, "Eyesafe pulsed microchip laser using semiconductor saturable absorber mirrors," Appl. Phys. Lett. **72**, 3273–3275 (1998)

[11]. R.D. Stultz, V. Leyva, K. Spariosu, "Short pulse, high-repetition rate, passively Q-switched Er:yttrium–aluminum–garnet laser at 1.6μm," Appl. Phys. Lett. **87**, 241118 (2005)

[12]. H.T. Huang, J.L. He, X.L. Dong, C.H. Zuo, B.T. Zhang, G. Qiu, Z.K. Liu, "High-repetition-rate eye-safe intracavity KTA OPO driven by a diode-end-pumped Q-switched Nd:YVO4 laser," Appl. Phys. B **90**, 43–45 (2008)

[13]. S. Kück, K. Petermann, U. Pohlmann, U. Schönhoff, G. Huber, "Tunable room-temperature laser action of Cr^{4+}-doped $Y_3Sc_xAl_{5-x}O12$," Appl. Phys. B **58**, 153–156 (1994)

[14]. N.V. Kuleshov, A.A. Lagatsky, A.V. Podlipensky, V.P. Mikhailov, A.A. Kornienko, E.B. Dunina, S. Hartung, G. Huber, "Fluorescence dynamics, excited-state absorption and stimulated emission of Er^{3+} in $KY(WO_4)_2$," J. Opt. Soc. Am. B **15**, 1205–1212 (1998)

[15]. I. Sokólska, E. Heumann, S. Kück, T. Łukasiewicz, "Laser oscillation of Er^{3+}:YVO_4 and Er^{3+}, Yb^{3+}:YVO_4 crystals in the spectral range around 1.6 μm. Appl. Phys. B **71**, 893–896 (2000)"

[16]. A. Sennaroglu, "Broadly tunable Cr^{4+}-doped solid-state lasers in the near infrared and visible," Prog. Quantum Electron. **26**, 287– 352 (2002)

[17]. P. ˇCerný, H. Jelínkova, P. Zverev, T.T. Basiev, "Solid state lasers with Raman frequency conversion," Prog. Quantum Electron. **28**, 113–143 (2004)

[18].Y.F. Chen, "Compact efficient all-solid-state eye-safe laser with self-frequency Raman conversion in a Nd:YVO_4 crystal." Opt. Lett. **29**, 2172–2174 (2004)

[19]. Y.F. Chen, "Efficient 1521-nm Nd :GdVO$_4$ Raman laser." Opt. Lett. **29**, 2632–2634 (2004)

[20]. J.T. Murray, R.C. Powell, D. Smith, W. Austin, R.A. Stolzenberger, "Generation of 1.5 μm radiation through intracavity solidstate Raman shifting in Ba(NO$_3$)$_2$ nonlinear crystals". Opt. Lett. **20**, 1017–1019 (1995)

[21]. A. Agnesi, S. Dell'Acqua, G. Reali, "Diode-pumped quasi-cw intracavity optical parametric oscillator at 1.57 μm with efficient pulse shortening." Appl. Phys. B **70**, 751–753 (2000)

[22]. Y.F. Chen, S.W. Chen, Y.C. Chen, Y.P. Lan, S.W. Tsai, "Compact efficient intracavity optical parametric oscillator with a passively Q-switched Nd:YVO$_4$/Cr^{4+}:YAG laser in a hemispherical cavity." Appl. Phys. B **77**, 493–495 (2003)

[23]. Y.F. Chen, L.Y. Tsai, "Comparison between shared and coupled resonators for passively Q-switched Nd:GdVO$_4$ intracavity optical parametric oscillators." Appl. Phys. B **82**, 403–406 (2006)

[24]. Y.F. Chen, "Design criteria for concentration optimization in scaling diode end-pumped lasers to high powers: influence of thermal fracture." IEEE J. Quantum Electron. **35**, 234–239 (1999)

[25]. H.J. Zhang, X.L. Meng, L. Zhu, H.Z. Zhang, P. Wang, J. Dawes, C.Q. Wang, Y.T. Chow, "Investigation on the growth and laser properties of Nd:GdVO$_4$ single crystal." Cryst. Res. Technol. **33**, 801–806 (1998)

[26]. T. Ogawa, Y. Urata, S. Wada, K. Onodera, H. Machida, H. Sagae, M. Higuchi, K. Kodaira, "Efficient laser performance of Nd:GdVO$_4$ crystals grown by the floating zone method." Opt. Lett.**28**, 2333–2335 (2003)

[27]. V. Lupei, N. Pavel, Y. Sato, T. Taira, "Highly efficient 1063-nm continuous-wave laser emission in Nd:GdVO$_4$." Opt. Lett. **28**, 2366–2368 (2003)

[28]. J. Minch, S.H. Park, T. Keating, S.L. Chuang, "Theory and experiment of $In_{1-x-y}Ga_xAs_yP_{1-y}$ and $In_{1-x-y}Ga_xAl_yAs$ long wavelength strained quantum-well lasers." J. IEEE. Quantum Electron. **35**, 771–782 (1999)

[29]. J.P. Donnelly, J.N.Walpole, S.H. Groves, R.J. Bailey, L.J.Missaggia, A. Napoleone, R.E. Reeder, C.C. Cook, "1.5-μm tapered-gainregion lasers with high-CW output powers." IEEE Photon. Technol. Lett. **10**, 1377–1379 (1998)

[30]. N. Nishiyama, C. Caneau, B. Hall, G. Guryanov, M.H. Hu, X.S. Liu, M.-J. Li, R. Bhat, C.E. Zah, "Long-wavelength verticalcavity surface-emitting lasers on InP with lattice matched AlGaInAs–InP DBR grown by MOCVD." IEEE J. Sel. Top. Quantum Electron **11**, 990–998 (2005)

[31]. S.R. Šelmi´c, G.A. Evans, T.M. Chou, J.B. Kirk, J.N. Walpole, J.P. Donnelly, C.T. Harris, L.J. Missaggia, "Single frequency 1550-nm AlGaInAs-InP tapered high-power laser with a distributed Bragg reflector." IEEE Photon. Technol. Lett. **14**, 890–892 (2002)

[32]. K.W. Su, S.C. Huang, A. Li, S.C. Liu, Y.F. Chen, K.F. Huang, "High-peak-power AlGaInAs quantum-well 1.3-mm laser pumped by a diode-pumped actively Q-switched solid-state laser." Opt. Lett. **31**, 2009–2011 (2003)

[33] M. Schmid, Sarah Benchabane, et al., "Optical in-well pumping of a vertical-external-cavity surface-emitting laser." Appl. Phys. Lett., **84,** No. 24, 4860-4862 (2004).

[34] S.-S. Beyertt, M. Zorn, et al., "Optical In-well Pumping of a Semiconductor Disk Laser With High Optical Efficiency." IEEE J. Quantum Electron. **41,** No. 12, 1439-1449 (2005).

[35] N. Schulz, M. Rattunde, C. Ritzenthaler, et al., " Resonant optical in-well pumping of an (AlGaIn)(AsSb)-based vertical-external-cavity surface-emitting

laser emitting at 2.35 μm." Appl. Phys. Lett., 91-091113 (2007).

[36] J.Wagner, N. Schulz, M. Rattunde, et al., "Barrier-and in-well pumped GaSb-based 2.3 μm VECSELs." Phys. Stat. Sol. (c) **4**, No. 5, 1597–1600 (2007).

[37] W. Zhang, T. Ackemann, S. McGinily, M. Schmid, E. Riis, and A. I. Ferguson, "Operation of an optical in-well-pumped vertical-external-cavity surface-emitting laser." Appl. Opts. **45,** No. 29, 7729-7735 (2006).

[38] N. Schu;z, M. Rattunde, C. Manz, K. Kohler, C. Wild, "GaSb-based VECSEL emitting around 2.35μm employing different optical pumping concepts." SPIE Vol.6184, (2006)

[39] T.Albrecht, W.Diehl, P. Brick, W. Reill, S. Lutgen, J. Luft, "Efficient quantum-well pumping of semiconductor disk lasers at 920nm." Conference on lasers& Electro-Optics(CLEO) **1**, pp.577-578 (2005)

[40] M. Ross, "YAG laser operation by semiconductor laser pumping." IEEE **56**, p. 196-197. ,(1968)

[41] A. Giesen, H. Hüge, A. Voss, K. Wittig, U. Brauch and H. Opower, "Scalable concept for diode-pumped high-power solid-state lasers." Appl. Phys. B **58**, 365–372, (1994)

[42] D. Dudley, N. Hodgson, H. Hoffman, and F. Kopper, "Direct 880 nm diode-pumping of vanadate lasers," in Conference on Lasers and Electro-Optics (CLEO), Vol. 73 of OSA (2002)

[43] Henry Plaessmann, Sean A. Re, Joseph J. Alonis, David L. Vecht, and William M. Grossman, "Multipass diode-pumped solid-state optical amplifier," Opt. Lett. **18**, 1420- (1993)

[44] N. Pavel, V. Lupei, and T. Taira, "1.34-μm efficient laser emission in highly-doped Nd:YAG under 885-nm diode pumping," Opt. Express **13**,

7948-7953 (2005)

[45] Zhiyun Huang, Yidong Huang, Yujin Chen, and Zundu Luo, "Theoretical study on the laser performances of Nd^{3+}:YAG and Nd^{3+}:YVO4 under indirect and direct pumping," J. Opt. Soc. Am. B **22**, 2564-2569 (2005)

[46] V. Lupei, G. Aka, and D. Vivien, "Highly efficient, 0.84 slope efficiency, 901 nm, quasi-two-level laser emission of Nd in strontium lanthanum aluminate," Opt. Lett. **31**, 1064-1066 (2006)

[47] N. Pavel, V. Lupei, J. Saikawa, T. Taira and H. Kan, "Neodymium concentration dependence of 0.94-, 1.06- and 1.34-µm laser emission and of heating effects under 809- and 885-nm diode laser pumping of Nd:YAG" Appl. Phys. B **82**, p. 599, (2006)

[48] N. Pavel, K. Lünstedt, K. Petermann, and G. Huber, "Multipass pumped Nd-based thin-disk lasers: continuous-wave laser operation at 1.06 and 0.9 µm with intracavity frequency doubling," Appl. Opt. **46**, 8256-8263 (2007)

[49] X. Li, X. Yu, J. Gao, F. Chen, J. Peng, J. Yu, and D. Chen, "Improvement in the laser performances of an A-O Q-switched Nd:GdVO$_4$ laser by direct-diode pumping into the emitting level." Laser Physics. **18**, No. 7, pp. 831–834. (2008)

[50] X. Ding, R. Wang, H. Zhang, X.Y. Yu, W.Q. Wen, P. Wang, J.Q. Yao "High-efficiency Nd:YVO4 laser emission under direct pumping at 880 nm" Optics Communications **282** ,981–984,(2009)

Reference (2.3)

[1]. C. E. Zah, R. Bhat, B.N. Pathak, F. Favire, W. Lin, M.C. Wang, N. C. Andreadakis, D.M. Hwang, M.A. Koza, T.P. Lee, Z. Wang, D. Darby, D. Flanders,"High-performance uncooled 1.3-µm $Al_xGa_yIn_{1-x-y}As$/InP strained-layer quantum-well lasers for subscriberloop applications." IEEE J. Quantum Electron. **30**, 511 (1994).

[2]. J. Minch, S. H. Park, T. Keating, and S. L. Chuang," Theory and experiment of $In_{1-x}Ga_xAs_yP_{1-y}$ and $In_{1-x-y}Ga_xAl_yAs$ long-wavelength strained quantum-well lasers." IEEE J. Quantum Electron. **35**, 771 (1999).

[3]. S.R. Selmic, T.M. Chou, J.P. Sih, J.B. Kirk, A. Mantie, J.K. Butler, D. Bour, and GA.Evans, "Design and characterization of 1.3-μm AlGaInAs-InP multiple-quantum-well lasers"IEEE J. Sel. Top. Quantum Electron. **7**, 340 (2001).

[4]. N. Nishiyama, C. Caneau, B. Hall, G. Guryanov, M. H. Hu, X. S. Liu, M.-J. Li, R. Bhat, and C. E. Zah,"Long-wavelength vertical-cavity surface-emitting lasers on InP with lattice matched AlGaInAs-InP DBR grown by MOCVD." IEEE J.Sel. Top. Quantum Electron. **11**, 990 (2005).

[5]. O. Hanaizumi, K. T. Jeong, S. Y. Kashiwada, I. Syuaib, K. Kawase, and S. Kawakami, "Observation of gain in an optically pumped surface-normal multiple-quantum-well optical amplifier." Opt. Lett. **21**, 269 (1996).

[6]. F. Sanchez, M. Brunel, and K. Aït-Ameur, "Pump-saturation effects in end-pumped solid-state lasers." J. Opt. Soc. Am. B **15**, 2390 (1998)

Reference (2.4)

[1]. J.J. Zayhowski, A. Mooradian, "Single-frequency microchip Nd lasers. Opt. Lett. **14**, 24–26 (1989)

[2]. G.J. Dixon, L.S. Lingvay, R.H. Jarman, "Properties of close coupled monolithic, lithium neodymium, tetraphosphate lasers." Proc.SPIE **1104**, 107 (1989)

Reference (2.5)

[1]. J.J. Zayhowski, A. Mooradian, "Single-frequency microchip Nd lasers. Opt. Lett. **14**, 24–26 (1989)

[2]. G.J. Dixon, L.S. Lingvay, R.H. Jarman, "Properties of close coupled monolithic, lithium neodymium, tetraphosphate lasers." Proc.SPIE **1104**, 107 (1989)

[3] L. Fan, M. Fallahi, J. Hader, A. R. Zakharian, J.V. Moloney, J. T. Murray, R. Bedford, W. Stolz, and S.W. Koch, "Multichip vertical-external-cavity surface-emitting lasers: a coherent power scaling scheme," Opt. Lett. **31**, 3612-3614 (2006)

[4] E.J. Saarinen, A. Härkönen, S. Suomalainen, and O.G. Okhotnikov, "Power scalable semiconductor disk laser using multiple gain cavity," Opt. Express **14**, 12868-12871 (2006)

[5] N. Hempler, J.M. Hopkins, A.J. Kemp, N. Schulz, M. Rattunde, J. Wagner, M. D. Dawson, and D. Burns, "Pulsed pumping of semiconductor disk lasers," Opt. Express **15**, 3247-3256 (2007)

[6] L. Fan, M. Fallahi, A. R. Zakharian, J. Hader, J. V. Moloney, R. Bedford, J.T. Murray, W. Stolz, and S.W. Koch, "Extended Tunability in a Two-Chip VECSEL" IEEE. Photo. Tech. Lett. **19**, No. 8, 544-546 (2007)

[7] S. C. Huang, H. L. Chang, K. W. Su, A. Li, S. C. Liu, Y. F. Chen, and K. F. Huang, "AlGaInAs/InP eye-safe laser pumped by a Q-switched Nd:GdVO$_4$ laser," Appl. Phys. B **94**, 483-487 (2009).

Reference (Chapter Three)

[1] Y. Kalisky, "Cr^{4+}-doped crystals: their use as lasers and passive Q switches," Prog. Quantum Electron. **28**, 249-303 (2004).

Reference (3.2)

[1] J. J. Zayhowski and C. Dill III, "Diode-pumped passively Q-switched picosecond microchip laser," Opt. Lett. **19**, 1427-1429 (1994).

[2] S. Forget, F. Druon, F. Balembois, P. Georges, N. Landru, J.-P. Fève, J. Lin, and Z. Weng, "Passively Q-switched diode-pumped Cr4+:YAG/Nd3+:GdVO4

monolithic microchip laser," Opt. Commun. **259**, 816-819 (2006).

[3] Y. F. Chen and S. W. Tsai, "Simultaneous Q-switching and mode-locking in a diode-pumped Nd:YVO$_4$/Cr^{4+}:YAG laser," IEEE J. Quantum Electron.**37**, 580-586 (2001).

[4] Y. Kalisky, "Cr^{4+}-doped crystals: their use as lasers and passive Q switches," Prog. Quantum Electron. **28**, 249-303 (2004).

[5] A. Sennaroglu, U. Demirbas, S. Ozharar, and F. Yaman, "Accurate determination of saturation parameters for Cr4+-dpoed solid-state saturable absorbers," J. Opt. Soc. Am. B **23**, 241-249 (2006).

[6] G. J. Spühler, R. Paschotta, R. Fluck, B. Braun, M. Moser, G. Zhang, E. Gini, and U. Keller, "Experimentally confirmed design guidelines for passively Q-switched microchip lasers using semiconductor saturable absorbers," J. Opt. Soc. Am. B **16**, 376-388 (1999).

[7] R. Häring, R. Paschotta, R. Fluck, E. Gini, H. Melchior, and U. Keller, "Passively Q-switched microchip laser at 1.5 μm," J. Opt. Soc. Am. B **18**, 1805-1812 (2001).

[8] J. J. Degnan, "Optimization of passively Q-switched lasers," IEEE J. Quantum Electron. **31**, 1890-1901 (1995).

[9] G. Xiao and M. Bass, "A generalized model Q-switched lasers including excited state absorption in the saturable absorber," IEEE J. Quantum Electron. **33**, 41-44 (1997).

[10] X. Zhang, S. Zhao, Q. Wang, Q. Zhang, L. Sun, and S. Zhang, "Optimization of Cr^{4+}-doped saturable-absorber Q-switched lasers," IEEE J. Quantum Electron. **33**, 2286-2294 (1997).

[11] R. E. Nahory, M. A. Pollack, W. D. Johnston, Jr., and R. L. Barns, "Band gap versus composition and demonstration of Vegard's law for In1-xGaxAsyP1-y

lattice matched to InP," Appl. Phys. Lett. **33**, 659-661 (1978).

[12] W. T. Tsang, F. K. Reinhart, and J. A. Ditzenberger, "1.3 μm wavelength GaInAsP/InP double-heterostructure lasers grown by molecular beam epitaxy," Appl. Phys. Lett. **41**, 1094-1096 (1982).

[13] H. Temkin, D. Coblentz, R. A. Logan, J. P. van der Ziel, T. Tanbun-Ek, R. D. Yadvish, and A. M. Sergent, "High temperature characteristics of InGaAsP/InP laser structures," Appl. Phys. Lett. **62**, 2402-2404 (1993).

[14] A. Li, S. C. Liu, K. W. Su, Y. L. Liao, S. C. Huang, Y. F. Chen, and K. F. Huang, "InGaAsP quantum-wells saturable absorber for diode-pumped passively Q-switched 1.3-μm lasers," Appl. Phys. B 84, 429-431 (2006).

[15] K. Alavi, H. Temkin, W. R. Wagner, and A. Y. Cho, "Optically pumped 1.55-μm double heterostructure $Ga_xAl_yIn_{1-x-y}As/Al_uIn_{1-u}As$ lasers grown by molecular beam epitaxy," Appl. Phys. Lett. **42**, 254-256 (1983).

[16] W. T. Tsang and N. A. Olsson, "New current injection 1.5-μm wavelength $Ga_xAl_yIn_{1-x-y}As/InP$ double-heterostructure laser grown by molecular beam epitaxy," Appl. Phys. Lett. **42**, 922-924 (1983).

[17] C. E. Zah, R. Bhat, B. N. Pathak, F. Favire, W. Lin, M. C. Wang, N. C. Andreadakis, D. M. Hwang, M. A. Koza, T. P. Lee, Z. Wang, D. Darby, D. Flanders, and J. J. Hsieh, "High-performance uncooled 1.3-μm $Al_xGa_yIn_{1-x-y}As/InP$ strained-layer quantum-well lasers for subscriber loop applications," IEEE J. Quantum Electron.,**30**, 511–521 (1994).

[18] N. Nishiyama, C. Caneau, B. Hall, G. Guryanov, M. H. Hu, X. S. Liu, M.-J. Li, R. Bhat, and C. E. Zah, "Long-wavelength vertical-cavity surface-emitting lasers on InP with lattice matched AlGaInAs–InP DBR grown by MOCVD," IEEE J. Sel. Topics Quantum Electron, vol. **11**, 990–998 (2005).

[19].Peng Li, Yufei Li, Yuming Sun, Xueyuan Hou, Huaijin Zhang, and Jiyang Wang.

"Passively Q-switched 1.34 μm $Nd:Y_xGd_{1-x}VO_4$ laser with $Co^{2+}:LaMgAl_{11}O_{19}$ saturable absorber" Optics Express, **14**, pp. 7730-7736 (2004)

[20].V.G. Savitski , A.M. Malyarevich, K.V. Yumashev, V.L. Kalashnikov, B.D. Sinclair, H. Raaben and A.A. Zhilin, "Experiment and modeling of a diode-pumped 1.3 μm $Nd:YVO_4$ laser passively Q-switched with PbS-doped glass." Appl. Phys. B **79**, 315–319 (2004)

[21]. V.G. Savitski, N.N. Posnov, P.V. Prokoshin , A.M. Malyarevich, K.V. Yumashev, M.I. Demchuk and A.A. Lipovskii, "PbS-doped phosphate glasses saturable absorbers for 1.3-μm neodymium lasers."   Appl. Phys. B **75**, 841–846 (2002)

[22]. A. Agnesi,A Guandalini, G. Reali, J.K.Jabczynski, K. Kopczynski and Z. Mierczyk, "Diode pumped $Nd:YVO_4$ laser at 1.34 μm Q-switched and mode locked by a $V^{3+}:YAG$ saturable absorber," Optics Comm **194**, 429-433, (2001)

[23].J.K Jabczynski, K.Kopczynski, Z. Mierczyk, A.Agnesi; A. Guandalini, G. Reali, "Application of $V^{3+}:YAG$ crystals for Q-switching and mode-locking of 1.3-um diode-pumped neodymium lasers,"   Opt. Eng., Vol. **40**, 2802 (2001)

[24].R. Fluck, G. Zhang, U. Keller, K.J. Weingarten, M.Moser, "Diode-pumped passively mode-locked 1.3-μm $Nd:YVO_4$ and Nd:YLF lasers by use of semiconductor saturable absorbers," Opt. Lett. **21**,1378 (1996)

[25]. H.D. Sun, G.J. Valentine, R. Macaluso, S. Calvez, D. Burns, M.D. Dawson, T. Jouhti, M. Pessa, "Low-loss 1.3-μm GaInNAs saturable Bragg reflector for high-power picosecond neodymium lasers," , Opt. Lett. **27**, 2124 (2002)

[26].V. Liverini, S. Schon, R. Grange, M. Haiml, S.C. Zeller, U. Keller, "Low-loss GaInNAs saturable absorber mode locking a 1.3-μm solid-state laser," Appl. Phys. Lett. **84**, 4002 (2004)

[27].H. C. Lai, A. Li, K. W. Su, M. L. Ku, Y. F. Chen, and K. F. Huang, "InAs GaAs quantum-dot saturable absorbers for diode-pumped passively Q-switched

Nd-doped 1.3-mm lasers," Opt. Lett. **30**, 480-482, (2005)

[28].K. W. Su, H. C. Lai, A. Li, Y. F. Chen, and K. F. Huang, "InAs/GaAs quantum-dot saturable absorber for a diode-pumped passively mode-locked Nd:YVO4 laser at 1342 nm," Opt. Lett. 30, pp. 1482-1484 (2005)

[29]. J. C. L. Yong, Judy M. Rorison, and Ian H. White, "1.3μm Quantum-Well InGaAsP, AlGaInAs, and InGaAsN Laser Material Gain: A Theoretical Study," IEEE J. Quantum Electronic, **38**, 1553-1564, (2002)

[30] Gerhard Boehm, Markus Ortsiefer, Robert Shau, Juergen Rosskopf, Christian Lauer, Markus Maute, Fabian Köhler, Felix Mederer, Ralf Meyer and Markus-Christian Amann, "InP-based VCSEL technology covering the wavelength range from 1.3 to 2.0 μm." J. Crystal Growth **251** , 748–753 (2003)

[31].Almuneau, G..Hall, E.Mukaihara, T.Nakagawa, S.Luo, C.Clarke, D.R.Coldren, "Improved electrical and thermal properties of InP-AlGaAsSb Bragg mirrors for long-wavelength vertical-cavity lasers," IEEE Photo.Tech. Lett, **12**, 1322-1324, (2000)

[32].N Nishiyama, C Caneau, B Hall, G Guryanov, MH Hu, "Long-wavelength vertical-cavity surface-emitting lasers on InP with lattice matched AlGaInAs-InP DBR grown by MOCVD," IEEE Quantum Electronic, **11**, 990-998,(2005)

[33].Y. Tsou, E. Garmire, W. Chen, M. Birnbaum, and R. Asthana, "Passive Q switching of Nd:YAG lasers by use of bulk semiconductors," Opt. Lett. **18**, 1514 (1993)

[34].R. Fluck, B. Braun, E. Gini, H. Melchior, and U. Kelle, "Passively Q-switched 1.34-μm Nd:YVO4 microchip laser with semiconductor saturable-absorber mirrors." Opt. Let. **22**, 991-993 (1997)

[35]. R. Häring, R. Paschotta, R. Fluck, E. Gini, H. Melchior, and U. Keller, "Passively *Q*-switched microchip laser at 1.5 *μ*m," J. Opt. Soc. Am. B **18**,

1805-1812 (2001)

[36].W. H. Loh, D. Atkinson, P. R. Morkel, M. Hopkinson, A. Rivers, A. J. Seeds, and D. N. Payne, "Passively mode-locked Er^{3+} fiber laser using a semiconductor nonlinear mirror." IEEE. Poto. Tech. Lett., **5**, 35-37, 1993

[37].Y-K Kuo , S-H Yen, M-W Yao, M-L Chen and B-T Liou, " Numerical study on gain and optical   properties of AlGaInAs, InGaNAs, and InGaAsP material systems for 1.3-μmsemiconductor lasers," Opt. Comm. **275**, 156–164 (2007)

[38].J.C.L.Yong, J.M. Rorison, R.V. Penty, I.H.White," Material gain comparison for InGaAsP, AlGaInAs and InGaAsN for 1.3micron laser diode." IEEE. Lasers and Electro-Optics,. CLEO '01. (2001)

[39]. S. C. Huang, S. C. Liu, A. Li, K. W. Su, Y. F. Chen, and K. F. Huang, "AlGaInAs quantum-well as a saturable absorber in a diode-pumped passively Q-switched solid-state laser," Opt. Lett. **32**, 1480-1482 (2007)

Reference (3.3)

[1]G. J. Spühler, R. Paschotta, R. Fluck, B. Braun, M. Moser, G. Zhang, E. Gini, and U. Keller, "Experimentally confirmed design guidelines for passively Q-switched microchip lasers using semiconductor saturable absorbers," J. Opt. Soc. Am. B 16, 376-388 (1999).

[2]S. Forget, F. Druon, F. Balembois, P. Georges, N. Landru, J.-P. Fève, J. Lin, and Z. Weng, "Passively Q-switched diode-pumped Cr^{4+}:YAG/Nd^{3+}:GdVO$_4$ monolithic microchip laser," Opt. Commun. 259, 816-819 (2006).

[3]A. Agnesi and S. Dell'acqua, "High-peak-power diode-pumped passively Q-switched Nd:YVO$_4$ laser," Appl. Phys. B 76, 351-354 (2003).

[4]Y. Feng, J. Lu, K. Takaichi, K. Ueda, H. Yagi, T. Yanagitani, and A. A. Kaminskii, "Passively Q-switched ceramic Nd^{3+}:YAG/Cr^{4+}:YAG lasers," Appl. Opt. 43, 2944-2947 (2004).

Reference (Chapter Four)

[1] W. Koechner, "Solid-state laser engineering," 6th ISBN 0-387-29094-x, Springer-Verlag (1996)

Reference (4.2)

[1] R. Fluck, G. Zhang, U. Keller, K. J. Weingarten, and M. Moser, "Diode-pumped passively mode-locked 1.3-μm Nd:YVO$_4$ and Nd:YLF lasers by use of semiconductor saturable absorbers," Opt. Lett. 21, 1378-1380 (1996).

[2] O. Musset and J. P. Boquillon, "Comparative laser study of Nd:KGW and Nd:YAG near 1.3 μm," Appl. Phys. B 64, 503-506 (1997).

[3] H. J. Zhang, J. H. Liu, J. Y. Wang, X. G. Xu, and M. H. Jiang, "Continuous-wave laser performance of Nd:LuVO4 crystal operating at 1,34 μm," Appl. Opt. 44, 7439-7441 (2005).

[4] H. T. Huang, J. L. He, C. H. Zuo, H. J. Zhang, J. Y. Wang, and H. T. Wang, "Co^{2+}:LMA crystal as saturable absorber for a diode-pumped passively Q-switched Nd:YVO4 laser at 1342 nm," Appl. Phys. B 89, 319-321 (2007).

[5] Y. F. Chen, L. J. Lee, T. M. Huang, and C. L. Wang, "Study of high-power diode-end-pumped Nd:YVO4 laser at 1.34 μm: influence of Auger upconversion," Opt. Commun. 163, 198-202 (1999).

[6] R. Zhou, S. C. Ruan, C. L. Du and J. Q. Yao, "High-power continuous-wave diode-end-pumped intracavity-frequency-doubled Nd:GdVO$_4$/LBO red laser," Opt. Commun. 282, 605-610 (2009).

[7] U. Keller, D. A. B. Miller, G. D. Boyd, T. H. Chiu, J. F. Ferguson, and M. T. Asom, "Solid-state low-loss intracavity saturable absorber for Nd:YLF lasers: an antiresonant semiconductor Fabry-Perot saturable absorber," Opt. Lett. 17, 505-507 (1992).

[8] U. Keller, K. J. Weingarten, F. X. Kärtner, D. Kopf, B. Braun, I. D. Jung, R. Fluck, C. Hönninger, N. Matuschek, and J. Aus Der Au, "Semiconductor saturable absorber mirrors (SESAM's) for femtosecondto nanosecond pulse generation in solid-state lasers," IEEE J. Sel. Top. Quantum Electron. 2. 435-453 (1996).

[9] M. Kondow, K. Uomi, A. Niwa, T. Kitatani, S. Watahiki, and Y. Yazawa, "GaInNAs: A novel material for long-wavelength-range laser diodes with excellent high-temperature performance," Japan. J. Appl. Phys. 35, 1273-1275 (1996).

[10] H. D. Sun, G. J. Valentine, R. Macaluso, S. Calvez, D. Burns, and M. D. Dawson, "Low-loss 1.3-μm GaInNAs saturable Bragg reflector for high-power picosecond neodymium lasers," Opt. Lett. 27, 2124-2126 (2002).

[11] G. J. Spühler, L. Krainer, V. Liverini, R. Grange, M. Haiml, S. Pawlik, B. Schmidt, S. Schön, and U. Keller, "Passively mode-locked 1.3-μm Multi-GHz Nd:YVO$_4$ lasers with low timing jitter," IEEE Photon. Technol. Lett. 17, 1319-1321 (2005).

[12] K. W. Su, H. C. Lai, A. Li, Y. F. Chen, and K. F. Huang ,"InAs/GaAs quantum-dot saturable absorber for a diode-pumped passively mode-locked Nd:YVO$_4$ laser at 1342 nm," Opt. Lett. 30, 1482-1484 (2005).

[13] H. Temkin, D. Coblentz, R. A. Logan, J. P. van der Ziel, T. Tanbun-Ek, R. D. Yadvish, and A. M. Sergent, "High temperature characteristics of InGaAsP/InP laser structures," Appl. Phys. Lett. 62, 2402-2404 (1993).

[14] N. Nishiyama, C. Caneau, B. Hall, G. Guryanov, M. H. Hu, X. S. Liu, M.-J. Li, R. Bhat, and C. E. Zah, "Long-wavelength vertical-cavity surface-emitting lasers on InP with lattice matched AlGaInAs–InP DBR grown by MOCVD," IEEE J. Sel. Topics Quantum Electron, vol. 11, 990–998 (2005).

[15] A. Li, S. C. Liu, K. W. Su, Y. L. Liao, S. C. Huang, Y. F. Chen, and K. F. Huang,

"InGaAsP quantum-wells saturable absorber for diode-pumped passively Q-switched 1.3-μm lasers," Appl. Phys. B 84, 429-431 (2006).

[16] R. Fluck, B. Braun, E. Gini, H. Melchior, and U. Keller, "Passively Q-switched 1.34- μm Nd:YVO$_4$ microchip laser with semiconductor saturable-absorber mirrors" Opt. Lett. 22, 991-993 (1997).

[17] B. C. Barnett, L. Rahman, M. N. Islam, Y. C. Chen, P. Bhattacharya, W. Riha, K. V. Reddy, A. T. Howe, K. A. Stair, H. Iwamura, S. R. Friberg, and T. Mukai, "High-power erbium-doped fiber laser mode locked by a semiconductor saturable absorber," Opt. Lett. 20, 471-473 (1995).

[18] K. Alavi, H. Temkin, W. R. Wagner, and A. Y. Cho, "Optically pumped 1.55-μm double heterostructure Ga$_x$Al$_y$In$_{1-x-y}$As/Al$_u$In$_{1-u}$As lasers grown by molecular beam epitaxy," Appl. Phys. Lett. 42, 254-256 (1983).

[19] W. T. Tsang and N. A. Olsson, "New current injection 1.5-μm wavelength Ga$_x$Al$_y$In$_{1-x-y}$As/InP double-heterostructure laser grown by molecular beam epitaxy," Appl. Phys. Lett. 42, 922-924 (1983).

[20] S. C. Huang, S. C. Liu, A. Li, K. W. Su, Y. F. Chen, and K. F. Huang, "AlGaInAs quantum-well as a saturable absorber in a diode-pumped passively Q-switched solid-state laser," Opt. Lett. 32, 1480-1482 (2007).

[21] J. Y. Huang, S. C. Huang, H. L. Chang, K. W. Su, Y. F. Chen, and K. F. Huang, "Passive Q switching of Er-Yb fiber laser with semiconductor saturable absorber," Opt. Express 16, 3002-3007 (2008).

List of published Journal papers

[1] A. Li, S.C. Liu, K.W. Su, Y.L. Liao, ***S.C. Huang***, Y.F. Chen, K.F. Huang
" InGaAsP quantum-wells saturable absorber for diode-pumped passively
Q-switched 1.3-μm lasers" Appl. phys B,B84, 429-431

[2] K. W. Su, ***S. C. Huang***, A. Li, S. C. Liu, Y. F. Chen, and K. F. Huang
"High-peak-power AlGaInAs quantum-well 1.3um laser pumped by a
diode-pumped actively *Q*-switched solid-state laser " Opt Lett Vol.31 No.13 2006

[3] ***S. C. Huang***, S. C. Liu, A. Li, K. W. Su, Y. F. Chen, and K. F. Huang "AlGaInAs
quantum-well as a saturable absorber in a diode-pumped passively
Q-switchedsolid-state laser" Opt Lett Vol.32, No.11 , 2007

[4] J. Y. Huang, ***S. C. Huang***, H. L. Chang, K. W. Su, Y. F. Chen*, and K. F. Huang
"Passive Q switching of Er-Yb fiber laser with semiconductor saturable absorber**"**
Vol. 16, No. 5 Opt Express 2008